Multicopper Oxidases and Oxygenases

Edward I. Solomon,* Uma M. Sundaram, and Timothy E. Machonkin

Department of Chemistry, Stanford University, Stanford, California 94305

Received August 6, 1996 (Revised Manuscript Received September 6, 1996)

Contents

I. Introduction

Copper is an essential trace element in living systems, present in the parts per million concentration range. It is a key cofactor in a diverse array of biological oxidation−reduction reactions. These involve either outer-sphere electron transfer, as in the blue copper proteins and the Cu_A site of cytochrome oxidase and nitrous oxide reductase, or inner-sphere electron transfer in the binding, activation, and reduction of dioxygen, superoxide, nitrite, and nitrous oxide. Copper sites have historically been divided into three classes based on their spectroscopic features, which reflect the geometric and electronic structure of the active site: type 1 (T1) or blue copper, type 2 (T2) or normal copper, and type 3 (T3) or coupled binuclear copper centers.[1−4] Over the last 10 years, this list has expanded to include the trinuclear copper clusters (comprised of a type 2 and a type 3 center),[5−7] the mixed-valent binuclear Cu_A site,[8−12] the Cu_B−$heme_A$ center of cytochrome *c* oxidase,[13] and the binuclear Cu_Z center of nitrous oxide reductase.[14]

These spectroscopic classifications are based upon the oxidized (i.e. cupric) state which has a d^9, open shell configuration and is thus amenable to study by a variety of spectroscopic methods.[15] Small-molecule copper(II) complexes are generally found to have a tetragonal geometry, due to the Jahn−Teller effect, with four tightly bound equatorial ligands and either none, one, or two weakly bound axial ligands (Figure 1A). This ligand field splits the d orbitals such that the $d_{x^2-y^2}$ is the highest energy half-occupied orbital. It has its lobes pointed at the four equatorial ligands and is thus involved in a strong antibonding interaction with these ligands. The unpaired electron in the $d_{x^2-y^2}$ orbital produces a characteristic $S = {}^1/_2$ EPR signal with $g_{\|} > g_{\perp} > 2.0023$ (Figure 1B). Note that the EPR spectrum presented is the first derivative of a powder or frozen solution of a copper(II) complex and has a peak present at a magnetic field associated with $g_{\|}$ ($=h\nu/\beta H = 0.71448\nu(\mathrm{MHz})/H(\mathrm{G})$) and an intense derivative shaped feature with its crossover point at a magnetic field associated with $g_{\perp}$ (the Zeeman splitting of the $S = {}^1/_2$ ground state for a magnetic field oriented perpendicular to the *z* axis, therefore in the equatorial plane). The two naturally occurring isotopes ^{63}Cu and ^{65}Cu (abundance of 69% and 31%, respectively) have a nuclear spin I of ${}^3/_2$ which couples to the electron spin to produce a $2I + 1$ or 4 line hyperfine splitting of the EPR signal. As shown in Figure 1B (bottom), the parallel hyperfine splitting, $A_{\|}$, observed for normal tetragonal Cu(II) complexes is generally large, in the range of 150−250 $\times 10^{-4}$ cm^{-1}, while the $A_{\perp}$ splitting is much smaller, $<35 \times 10^{-4}$ cm^{-1}.

The low-energy region of the absorption spectrum of a Cu(II) complex will be dominated by transitions from the filled d orbitals to the half-occupied $d_{x^2-y^2}$ orbital. Since these d orbitals are split in energy by the ligand field at the metal center (Figure 2A), the

S0009-2665(95)00046-X CCC: $25.00

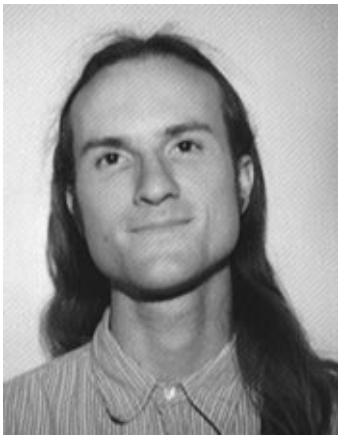

Tim Machonkin was born in Rochester, NY, in 1971 and grew up in Webster, NY. He attended the University of Michigan, where he did his undergraduate research under Prof. Vincent Pecoraro, studying the chlorination of alkenes by a manganese(IV) complex, and graduated in 1993 with a B.S. in chemistry and cellular/molecular biology. He then worked for one summer at Abbott Laboratories doing organic synthesis. Since then, he has been working toward his Ph.D. at Stanford University under the direction of Prof. Edward Solomon, with financial support from an NSF Predoctoral Fellowship and a Stanford University Leiberman Fellowship. His research is on the structure and reactivity of the copper sites in the multicopper oxidase ceruloplasmin. He is also a freshman advisor at Stanford and plays viola in the Stanford Symphony Orchestra.

Uma Maheswari Sundaram was born August 1967 in Madras, India. She received her B.Sc. in Chemistry from the Women's Christian College, Madras, and her M.Sc. in Chemistry from the Indian Institute of Technology (IIT), Madras. Her masters dissertation project was under the guidance of Prof. P. T. Manoharan of the Regional Sophisticated Instrumentation Center, IIT, Madras. She also worked on a summer project with Prof. S. Mitra of the Tata Institute of Fundamental Research, Bombay, India. She is currently working toward her Ph.D. in chemistry at Stanford University under the supervision of Prof. Edward I. Solomon. Her research interests are in the field of bioinorganic spectroscopy and she works on the spectroscopic study of oxygen intermediates of the multicopper oxidases. Her other interests include classical Indian music and tennis.

associated d → d transitions are sensitive probes of the ligand geometry. Tetragonal Cu(II) complexes exhibit d → d transitions in the ∼500 nm to 1 μm region (for example, in Cu/Zn superoxide dismutase,[16] Figure 2B), while copper(II) sites constrained by ligation to be close to tetrahedral exhibit d → d transitions in the 1−2 μm region. These transitions are electric dipole forbidden and thus generally appear as weak features in the absorption spectrum, $\epsilon < 200$ M^{-1} cm^{-1}. It should be noted that d → d transitions are often magnetic dipole allowed. Since this selection rule plays a key role in determining the rotational strength of features in the circular

Edward I. Solomon grew up in North Miami Beach, FL, received his Ph.D. from Princeton University (with D. S. McClure), and was a postdoctoral fellow at the H.C. Ørsted Institute (with C. J. Ballhausen) and then at Caltech (with H. B. Gray). He was a professor at the Massachusetts Institute of Technology until 1982, when he moved to Stanford University, where he is now the Monroe E. Spaght Professor of Humanities and Sciences. His research is in the fields of physical–inorganic and bioinorganic chemistry with emphasis on the application of a wide variety of spectroscopic methods to elucidate the electronic structure of transition metal complexes and its contribution to physical properties and reactivity.

dichroism (CD) spectrum of optically active sites (Figure 2C), d → d transitions can often have high CD intensities relative to absorption intensities (called the Kuhn anisotropy factor). Of higher energy in the absorption spectrum are the electric dipole allowed, hence intense, ligand-to-metal charge transfer (LMCT) transitions. The intensity of these transitions reflects the overlap of the ligand and metal orbitals involved in the charge transfer, and their energy splitting reflects differences in π and σ ligand−metal bonding interactions.[15] Therefore, the energy and intensity of charge transfer transitions are very useful probes of the bonding interactions of the ligand with the cupric center.

These EPR and absorption features are the basis for classifying active sites in copper proteins. The type 1 or blue copper centers exhibit an extremely intense absorption band, $\epsilon \sim 5000$ M^{-1} cm^{-1} at ∼600 nm, which is responsible for their deep blue color. This band is a cysteine sulfur to copper, LMCT transition. They also exhibit a very small Cu parallel hyperfine splitting in their EPR spectra (Figure 3A) due to the high covalency at the copper site (the unpaired electron is strongly delocalized onto the cysteine ligand, thus reducing its interaction with the nuclear spin on the copper). These sites are found in mononuclear copper proteins involved in intermolecular electron transfer (plastocyanins, azurins, stellacyanins, etc.) and the multicopper enzymes [laccase (Lc), ceruloplasmin (Cp), ascorbate oxidase (AO) (*vide infra*), and nitrite reductase], where it functions in intramolecular electron transfer. These sites and their properties are described in section IIIA of the review by Holm, Kennepohl, and Solomon (HKS) in this issue.[17] The type 2 or normal copper proteins exhibit EPR signals similar to those in Figure 1B for tetragonal Cu(II) complexes and often do not have observable ligand field transitions in their absorption spectra due to their low intensity. These sites are found in Cu/Zn superoxide dismutase (HKS, section IIIC) and in galactose oxidase, amine oxidase, dopam-

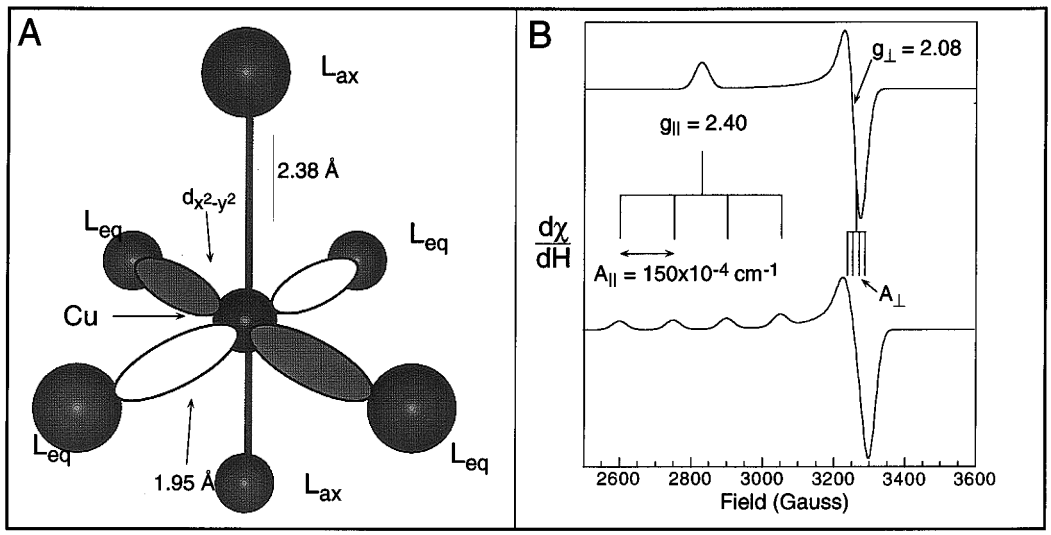

Figure 1. Geometry and EPR spectrum of a normal copper complex. (A) Geometry of the Jahn−Teller tetragonally distorted $Cu(H_2O)_6^{2+}$ ion with the $d_{x^2-y^2}$ orbital overlaid on the Cu(II) center. (B) Simulated EPR spectrum of $Cu(H_2O)_6^{2+}$ without (upper) and with (lower) the copper hyperfine splitting (at X-band, $\nu = 9.50$ GHz).

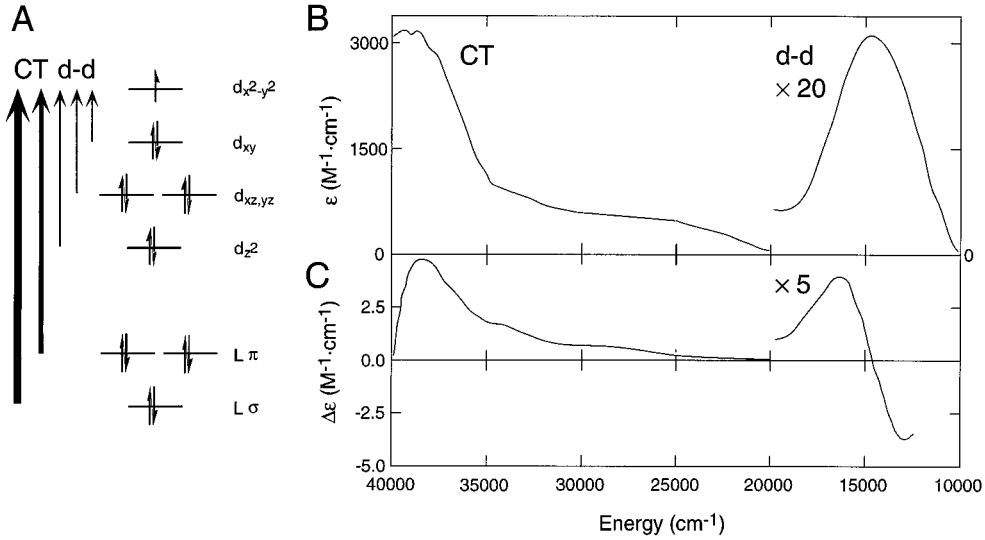

Figure 2. Electronic transitions of a normal copper complex. (A) Molecular orbital energy level diagram. The intense, electric dipole-allowed LMCT transitions are the bold arrows, the weak, electric dipole-forbidden d → d transitions are light arrows. (B) Absorption and (C) CD spectra of the normal copper protein Cu−Zn superoxide dismutase in the d → d and CT regions (adapted from ref 16).

ine β-hydroxylase (DβH), and peptidylglycine α-amidating monooxygenase (PAM) (see Klinman *et al.*,[18] Klinman's article in this issue,[19] and HKS[17]), where the reduced copper sites react with dioxygen to either reduce it to hydroperoxide or activate it for the hydroxylation of substrate. It is interesting to note that in DβH and PAM two copper ions are required for catalysis, yet the EPR signal of these enzymes is that of mononuclear tetragonal Cu(II) (Figure 3B). If two Cu(II)s are less than 6 Å apart, the $S = {}^1/_2$ magnetic dipole on each copper will couple to produce a broadening of the normal Cu(II) EPR signal or, for a distance of less than ~4 Å, a splitting of the spectroscopic features (i.e. zero field splitting of an $S_{TOT} = 1$ triplet; Figure 3C).[20−22] Thus the normal spectroscopic features of these enzymes indicate the two mononuclear Cu(II) centers are >6 Å apart.

The remaining known copper enzymes are the focus of this review. Hemocyanin and tyrosinase contain a coupled binuclear, type 3 copper center. These proteins contain two Cu(II)s but exhibit no EPR signal (Figure 3D) due to strong antiferromagnetic coupling (i.e. spin pairing) between the two $S = {}^1/_2$ metal ions due to their covalent overlap with a bridging ligand. Both enzymes bind dioxygen, and tyrosinase activates this ligand for hydroxylation of phenolic substrates. Laccase, ascorbate oxidase, and ceruloplasmin exhibit EPR features, indicating the presence of a combination of type 1 and type 2 centers, and have an additional EPR inactive, antiferromagnetically coupled type 3 center. The type 2 plus type 3 centers were originally shown from magnetic circular dichroism (MCD, *vide infra*)[5,6] and X-ray absorption spectroscopy (XAS, *vide infra*)[23] on laccase to form a trinuclear copper cluster, and this has now also been determined by crystallography for ascorbate oxidase[7] and ceruloplasmin.[24] This combination of four coppers (six in ceruloplasmin) couples four one-electron oxidations of substrate to the four electron reduction of dioxygen to water. The par-

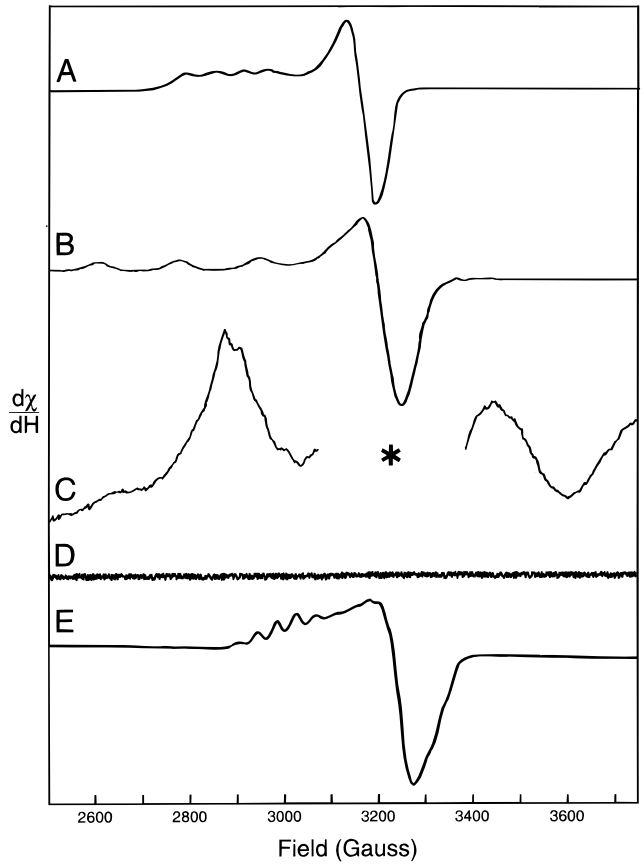

Figure 3. EPR spectra (X-band) of the different types of copper proteins. (A) The blue or type 1 copper protein plastocyanin. (B) The normal copper protein dopamine β-hydroxylase. (adapted from ref 18) (C) The uncoupled T3 coppers with a 4 Å Cu···Cu separation present in met-N_3^- T2D laccase (adapted from ref 22). *3100−3300 G region also includes overlapping spectral features from the T1 site which have been excluded for clarity. (D) The coupled binuclear copper protein oxyhemocyanin. (E) The Cu_A site in nitrous oxide reductase (adapted from ref 8).

ticulate form of methane monooxygenase (p-MMO) is thought to contain a different type of trinuclear copper cluster involved in the activation of dioxygen.[25]

Cytochrome *c* oxidase and nitrous oxide reductase contain a Cu_A center which has two coppers and exhibits the EPR signal in Figure 3E.[8,9] This has seven copper hyperfine lines, indicating that it involves an $S = {}^1/_2$ ground state delocalized over a mixed valent formally Cu(1.5)Cu(1.5) center (i.e. $2nI + 1 = 7$ with $I^{Cu} = {}^3/_2$ and the number of coppers $n = 2$). As with the blue copper center in the multicopper oxidases and nitrite reductase, the Cu_A site accepts electrons and is involved in long-range intramolecular electron transfer to the active site.

In addition to absorption and EPR, several other spectroscopic methods have proven to be extremely important in the study of copper sites in biology. Variable temperature MCD spectroscopy combines features of electronic absorption and EPR. As shown in Figure 4, both the ground and excited states split in the presence of a large magnetic field. The selection rules for circular polarization (CP) in a transverse magnetic field are $\Delta m = +1$ for left CP and $\Delta m = -1$ for right CP. Therefore, on going from the ground to a specific excited state, there will be

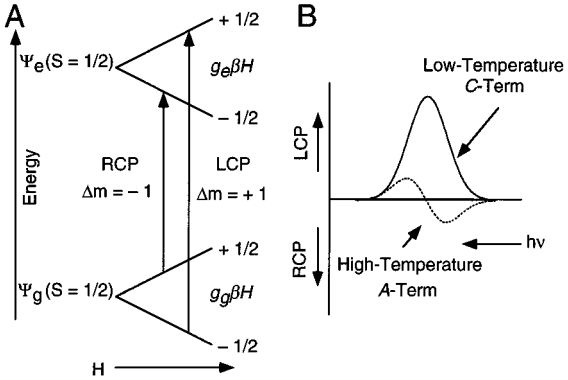

Figure 4. MCD A- and C-term mechanisms. (A) In the presence of a magnetic field, the degeneracy of the ground and excited states is split such that the RCP and LCP transitions will be at different energies. (B) When $kT \gg g\beta H$, the MCD transition in A will produce a derivative bandshape (A-term), while when $kT < g\beta H$, the two levels of the ground-state doublet are unequally populated, resulting in an MCD transition with an absorption bandshape (C-term).

two transitions of equal magnitude but opposite sign. Since the Zeeman splitting of the ground and excited state will be on the order of 10 cm^{-1} for experimental magnetic fields of ~7 T and absorption bands have widths of a few thousand inverse centimeters, these transitions will mostly cancel, producing a broad weak derivative-shaped MCD signal called an A term. This assumes equal population of the $M = {}^1/_2$ and $-{}^1/_2$ components of the ground state, therefore a high temperature. As the temperature is decreased, the population of the ${}^1/_2$ decreases and $-{}^1/_2$ increases, leading to a large (positive for the example in Figure 4) MCD feature at low temperature called a C term. This will be 2−3 orders of magnitude more intense than room temperature MCD features. Thus low-temperature MCD (LTMCD) is a sensitive probe of excited states associated with a copper center with a paramagnetic ground state.

In resonance Raman spectroscopy, the laser energy is tuned through a charge transfer absorption feature, and specific vibrational peaks in the Raman spectrum become enhanced. In the most generally observed A term resonance Raman effect[26] (the nomenclature is unfortunately the same as for MCD), the intensity of these vibrational features profile the bandshape of the electronic transition associated with the resonance effect (Figure 5). These vibrations reflect the change in geometry of the site on going from the ground to the charge transfer excited state. Thus, in addition to normal mode vibrational information on the active site, resonance Raman spectroscopy also probes the nature of the excited state.

All the above spectral methods are appropriate for the oxidized Cu(II) state but not the reduced Cu(I) closed shell, d^{10} site. However, Cu(I) complexes do exhibit a low-energy characteristic feature in their Cu K-edge X-ray absorption spectrum. The Cu(I) 1s → 4p transition, which is electric-dipole allowed and intense, occurs at ~8984 eV.[27,28] As shown in Figure 6, two-coordinate Cu(I) complexes will have two 4p orbitals at low energy (the $4p_z$ is shifted to higher energy due to antibonding interactions with the two axial ligands), producing an intense 1s → $4p_{x,y}$, 8984 eV feature, while three-coordinate Cu(I) complexes

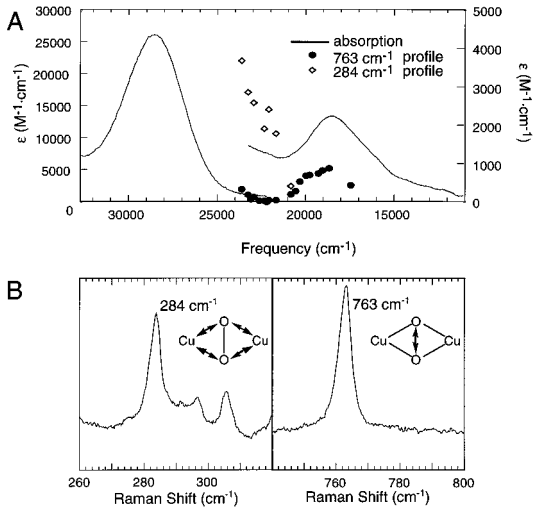

Figure 5. Resonance Raman effect, illustrated with the side-on μ-η^2:η^2-peroxo-bridged copper dimer.[77] (A) Absorption spectrum and resonance Raman profiles; i.e., intensity of a Raman peak is a function of the laser excitation energy. (B) Resonance Raman spectrum of the copper−copper stretch (284 cm^{-1}, left) and the intraperoxide stretch (763 cm^{-1}, right).

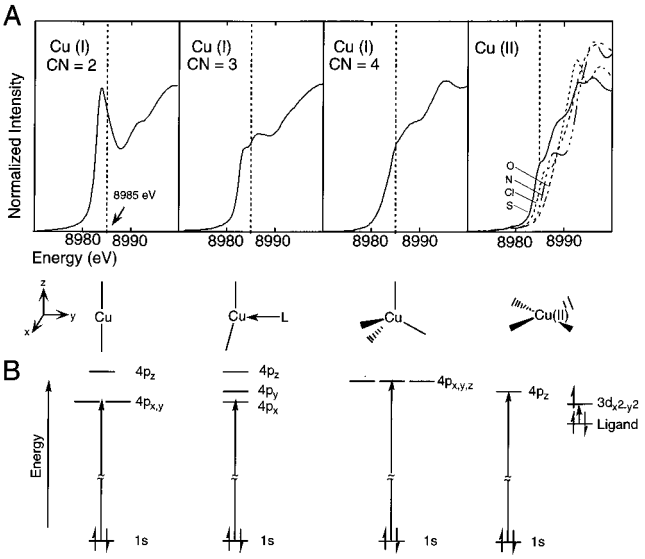

Figure 6. K-edge X-ray absorption spectra for Cu(I) and Cu(II) compounds (adapted from ref 28). (A) Representative XAS data for two-, three-, and four-coordinate Cu(I) and square-planar Cu(II) compounds. (B) Ligand field splitting diagrams for the corresponding Cu 1s → 4p transitions. Note that the edge spectra in Cu(II) has been assigned as a 1s → 4p + LMCT shakedown transition.

will have only one low energy 4p orbital and therefore exhibit an 8984 eV feature with lower intensity. Four-coordinate Cu(I) complexes have all 4p orbitals at higher energy and with reduced intensity due to covalency. Cu(II) complexes have a higher effective nuclear charge and thus their Cu K-edges are shifted out of this energy region. Thus the 8984 eV feature in the Cu K-edge provides a powerful probe of the reduced copper site and its coordination environment.

This review focuses on the multicopper enzymes involved in dioxygen activation and multielectron reduction. Recent reviews of the extensive and generally well-developed topic of copper/O_2 coordination chemistry and the electronic structure of copper−peroxy species are available.[29−33] Section II presents an overview of the coupled binuclear copper active site in the monooxygenase tyrosinase, its relation to the structurally defined site in hemocyanin, and a molecular level description of its catalytic mechanism. We also include a brief summary of other less well-defined related enzymes. In section III the focus is on the multicopper oxidases, which catalyze the four-electron reduction of dioxygen to water. Here the large body of spectroscopic and reactivity data available for the simplest of the multicopper oxidases, laccase, is correlated with the crystal structures now available for ascorbate oxidase[7] and, at lower resolution, ceruloplasmin.[24] These results generate a molecular mechanism for the reduction of dioxygen to water and insight into the electron transfer pathways. These are briefly correlated to the structural and spectroscopic data available for the equivalent reaction in cytochrome *c* oxidase. Concluding comments are presented in section IV.

II. Multicopper Oxygenases

A. Tyrosinase

1. Enzymology

By far the most well-studied multicopper oxygenase is tyrosinase [monophenol,dihydroxyphenylalanine (DOPA):dioxygen oxidoreductase, EC 1.14.18.1] which contains a coupled binuclear copper active site. This enzyme catalyzes both the orthohydroxylation of monophenols (cresolase activity, reaction 1) and the two-electron oxidation of *o*-diphenols to *o*-quinones (catecholase activity, reaction 2).

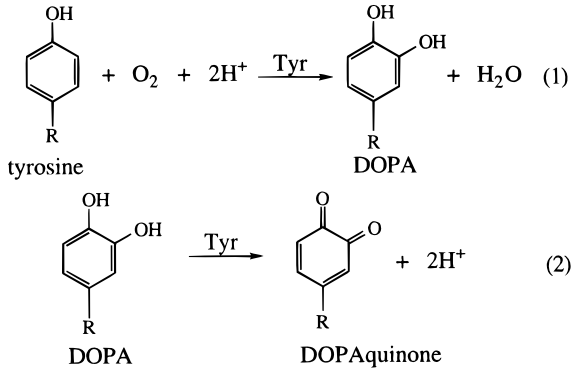

Early labeling studies by Mason demonstrated that the oxygen incorporated into the phenolic substrate derives from molecular O_2.[34] The two electrons required to reduce the second oxygen atom to H_2O are supplied by the substrate; thus, tyrosinase functions as an internal monooxygenase. The oxidase reaction is much more rapid than the oxygenation reaction ($k_{diphenolase} = 10^7\ s^{-1}$, $k_{monophenolase} = 10^3\ s^{-1}$).[35] Thus reaction 1, oxygenation of substrate to DOPA, is considered to be the rate-determining step, followed by the rapid two-electron oxidation of DOPA to the quinone. The DOPAquinone product then undergoes a series of nonenzymatic polymerization reactions to form the pigment melanin. While it is unfortunate that there is no crystal structure presently available for any tyrosinase, much insight into its active site and active site contributions to reactiv-

Table 1. Properties of Well-Characterized Tyrosinases[a]

source	no. subunits	MW/subunit (kDa)	spectroscopy of oxy form: absorption, nm ($10^{-3\times}$ M^{-1} cm^{-1})	spectroscopy of oxy form: CD, nm ($10^{-3\times}$ M^{-1} cm^{2} $dmol^{-1}$)	sequence	ref
			Eubacteria			
Streptomyces glaucescens	1	30.9	345 (17.4) 640 (1.5)	345 (−32.5) 470 (2.1) 575 (−1.7) 740 (5.0)	yes	39−41
			Fungi			
Neurospora crassa	1	46	345 (18) 425 (0.5) 600 (1.0)	345 (−27) 520 (0.6) 600 (1.0) 750 (+3)	yes	36,42−45
Mushroom (*Agaricus bisporus*)	2 2	13.4 43	345 (18) 600 (1.2)	353	no	46−50
			Plants			
Spinach-beet (*Beta vulgaris*)	1	40	345	ND	no	51−53
			Animals			
Human melanocyte	1	66.7	ND	ND	yes	54,55

[a] ND = no data available.

ity can be obtained from correlations to hemocyanins,[36] where crystal structures exist for both the deoxy[37] and oxy[38] forms of the active sites.

Tyrosinase is widely distributed among eukarya, and has also been identified in eubacteria of the *Streptomyces* genus. The best characterized preparations are from *Streptomyces glaucescens* and the fungi *Neurospora crassa* and *Agaricus bisporus* (see Table 1). The first two are monomeric proteins, while the last is a tetramer with two different subunits ("heavy" and "light") of the form H_2L_2. It has been isolated and at least partially purified from numerous plant and animal sources, but few of these have been well-characterized, and preparations often show a significant degree of heterogeneity. In addition, there has been a great deal of confusion as to whether many of the plant enzymes are tyrosinases, catechol oxidases, or possibly even laccases (*vide infra*). Unlike the fungal tyrosinases, human tyrosinase is a membrane-bound glycoprotein (13% carbohydrate).[54] Many of these enzymes have now been sequenced, including that from *N. crassa*[43−45] and human.[55] A variety of mutations in the human tyrosinase gene have been correlated with the pigment deficiency oculocutaneous albinism.[56] This nearly ubiquitous enzyme has been adapted to serve diverse physiological roles in different organisms.[57−59] In fungi and vertebrates, tyrosinase catalyzes the initial step in the formation of the pigment melanin from tyrosine. In plants, the physiological substrates are a variety of phenolics. Tyrosinase oxidizes these in the browning reaction observed when tissues are injured; however, the function of this reaction is not clear. One possible role is protection of the wound from pathogens or insects. In insects, tyrosinase is thought to be involved in wound healing and possibly sclerotization of the cuticle.

2. Similarities to Hemocyanins

Chemical and spectroscopic studies have been performed on a series of derivatives of five mollusk and five arthropod hemocyanins[60−67] and fungal tyrosinase,[36,47,48,68,69] which have demonstrated these proteins to have extremely similar active sites. The derivatives include the deoxy [Cu(I) Cu(I)], mixed-valent half-met [Cu(II) Cu(I)], EPR nondetectable met [Cu(II)−Cu(II)], EPR-detectable dimer [Cu(II)··· Cu(II)], and oxy [Cu(II) O_2^{2-} Cu(II)] sites, which are summarized in Figure 7.

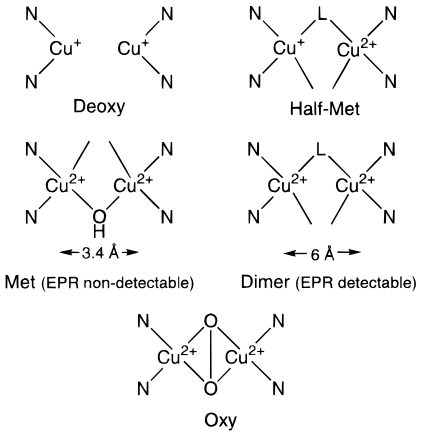

Figure 7. Derivatives of the coupled binuclear copper active site (L = exogenous ligand). Note that a third histidine is present on one or both of the coppers, but this is not shown for clarity.

The resting form of tyrosinase is the met derivative, which has two cupric centers but exhibits no EPR signal. While no crystal structure is available for met hemocyanin, the lack of an EPR signal has been shown to derive from antiferromagnetic coupling between the copper(II)s, which requires a superexchange pathway associated with a bridging ligand.[66] From the crystal structure of deoxy *Panulirus interruptus* hemocyanin, no protein residue in the vicinity of the copper site can bridge; thus, the bridging ligand must be hydroxide from water, and a similar situation is likely the case for met tyrosinase. EXAFS on met tyrosinase shows that the Cu−Cu distance is 3.4 Å, which is too large for two single-atom hydroxide bridges; thus, the met site would appear to have at least one H_2O-derived ligand bound terminally to the copper(II)s.[70] The met tyrosinase site is kinetically competent to oxidize diphenol but not monophenol substrates.[71]

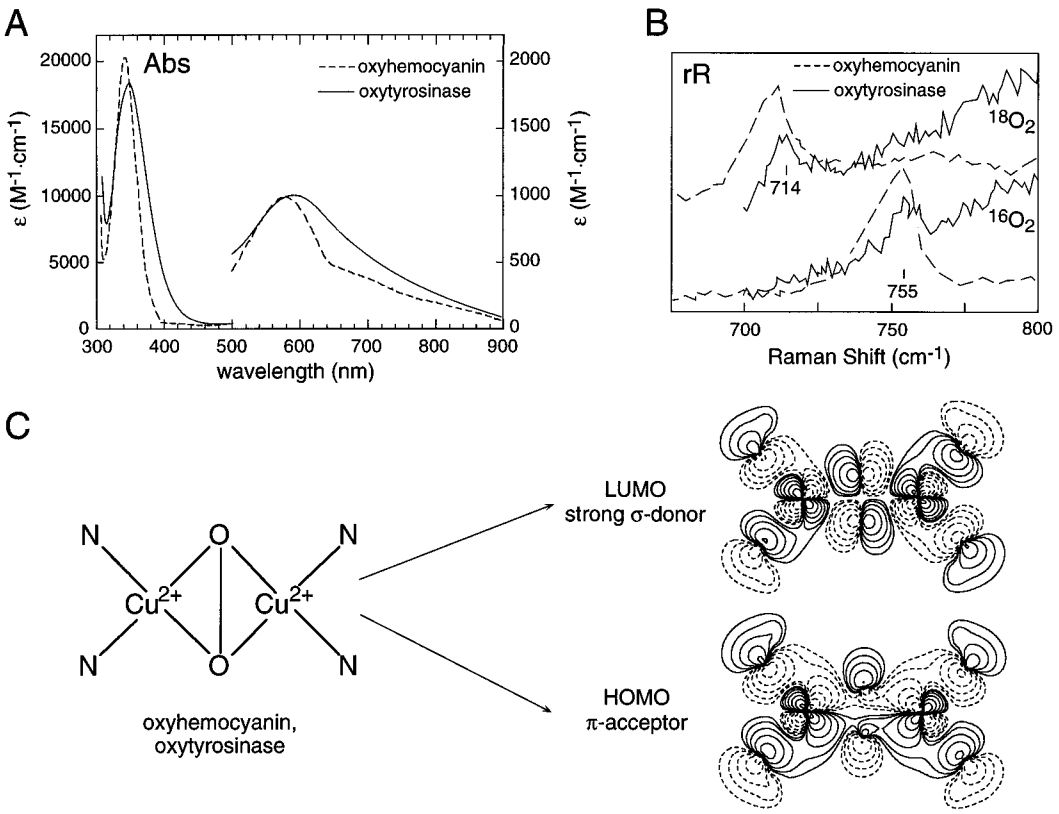

Figure 8. Similarities in the spectroscopic features of oxyhemocyanin and oxytyrosinase indicative of the side-on μ-η^2:η^2-peroxide bridging mode. (A) Absorption spectra of oxytyrosinase (solid line) and oxyhemocyanin (dashed line, adapted from ref 36). (B) Resonance Raman spectra of the intraperoxide stretch of oxytyrosinase (solid) and oxyhemocyanin (dashed) with $^{18}O_2$ (upper) and $^{16}O_2$ lower (adapted from refs 69 and 73). (C) Geometric and electronic structure of the side-on μ-η^2:η^2-peroxide model of the oxytyrosinase active site showing the contours of the HOMO and LUMO orbitals from broken-symmetry SCF-Xα-SW calculations.[76]

The oxytyrosinase site is produced from resting (i.e. met) tyrosinase by the addition of peroxide or by the two-electron reduction to the deoxy site followed by the reversible binding of dioxygen.[36,47,48] Oxytyrosinase reacts with monophenol as well as diphenol substrates,[71,72] and thus, its geometric and electronic structure are key to understanding the hydroxylation chemistry of this enzyme. Oxyhemocyanin exhibits unique spectroscopic features: an extremely intense absorption band at 350 nm with an $\epsilon \sim 20\,000$ M^{-1} cm^{-1},[62] an exceedingly low O−O stretching frequency of ~750 cm^{-1},[73] and a Cu−Cu distance of 3.6 Å by EXAFS[70] and X-ray crystallography.[38] These spectroscopic features are characteristic of the side-on μ-η^2:η^2 peroxide bridging mode, shown in Figure 8C, first observed in the copper model complex of Kitajima *et al.*[74] Oxytyrosinase exhibits essentially the same spectral features (see Figure 8A,B);[36,47,48,69,70] thus, a similar structure has been ascribed to the active site of oxytyrosinase. As described in detail in HKS,[17] these unique spectroscopic features are quite well-understood.[75−77] The intense absorption band (Figure 8A) indicates that the side-on peroxide is a very strong σ-donor ligand to the two copper(II)s (Figure 8C, LUMO), while the low O−O stretching frequency (Figure 8B) indicates an extremely weak O−O bond. This weak O−O bond derives from the ability of the peroxide to act as a π-acceptor ligand, wherein the π back-bonding shifts electron density into the σ^* orbital of the peroxide, which is highly antibonding with respect to the O−O bond, thus activating it for cleavage (Figure 8C, HOMO). Indeed, in the copper dimer of Tolman and co-workers, where the trispyrazolyl borate ligand of the Kitajima structure is replaced by triazacyclononane, the π back-bonding apparently contributes sufficient electron density into the peroxide σ^* orbital to cleave the O−O bond under certain conditions, thus generating a binuclear bis-μ-oxo structure.[78,79] This exhibits an intense absorption band at ~450 nm ($\epsilon \sim 13\,000$ M^{-1} cm^{-1}), a CuO_2Cu core vibration at ~610 cm^{-1} in the resonance Raman spectrum, and a Cu−Cu distance of 2.8 Å. However, no such intermediate is observed in tyrosinase.

3. Differences Relative to Hemocyanin

The coupled binuclear copper site in tyrosinase is capable of reacting with substrates, while that in hemocyanin is not. It has been of great importance to define the differences between these two similar proteins which could contribute to this difference in reactivity. One significant difference is accessibility to the active site. A large difference in the rate of displacement of the side-on bound peroxide in the oxy site by exogenous ligands is observed for tyrosinase relative to hemocyanin.[36,63,67] Azide displaces the peroxide in an associative reaction, which is similar to that observed for the equatorial ligands of square planar d^8 and tetragonal d^9 complexes.[80] These are thought to involve initial axial coordination of the incoming ligand, rearrangement through a trigonal bipyramidal intermediate and subsequent loss of the

displaced equatorial ligand. The rates of peroxide displacement by azide ($k_{hemocyanins} \leq 0.04\ h^{-1}$, $k_{tyrosinase} = 0.95\ h^{-1}$) show that the tyrosinase active site is considerably more accessible to exogenous ligands.

Insight into this difference in accessibility is available from sequence comparisons of tyrosinases to the structurally defined hemocyanins. Hemocyanins are larger proteins (molecular weight of arthropod hemocyanins $\approx$ 70 kDa) that have an additional domain which blocks access to the coupled binuclear copper site. Also, while the three His ligands of one of the coppers, designated Cu_B in *P. interruptus* hemocyanin, are conserved among the arthropod and mollusk hemocyanins and tyrosinases, the ligands of the second copper, designated Cu_A (but not to be confused with the binuclear Cu_A center in cytochrome *c* oxidase), may not be, which raises the possibility of a more exchangeable ligand position directly on at least one of the copper of tyrosinase.[81−83] Pfiffner and Lerch found that photooxidation of three histidines (His 188, 193, and 289) resulted in the loss of one copper and enzymatic inactivation.[84] One of these (His 289) is known to be a ligand at the Cu_B site, but the other two are not conserved in other tyrosinases. The tyrosinases and mollusk hemocyanins do share a possible Cu_A-binding region with high sequence homology, including two conserved histidines; however, the identity of the third ligand is not clear. In all of the tyrosinases and some of the hemocyanins, there is a third histidine in the same region of the sequence. Replacement of any one of these histidines in *S. glaucescens* tyrosinase leads to loss of one copper and enzyme inactivation, implying that these are the ligands to Cu_A in the tyrosinases,[41,85] although the third histidine is present in only some of the mollusk hemocyanins. There is also a conserved methionine in all of the mollusk hemocyanins two residues downstream from where the possible third Cu_A histidine ligand is found in the tyrosinases. Alternately, the third ligand could be water or another residue. In *N. crassa* tyrosinase, the putative third histidine ligand (His 96) is covalently linked to Cys 94 through a thioether bridge.[43,45] The CXH motif is found in some of the mollusk hemocyanins, and there is evidence for the presence of the covalent Cys-His unit in *Helix pomatia* hemocyanin.[86] A similar Cys-Tyr covalently linked unit is present as a ligand at the copper site in galactose oxidase.[87,88] This thioether linkage is thought to be a posttranslational modification induced by the copper center. In galactose oxidase, this 3′-cysteinyltyrosinase ligand becomes oxidized in the catalytically active form of the enzyme.[89] At present it is not clear how this Cys-His unit in tyrosinase relates to the coupled binuclear copper center and to its reactivity.

Mimosine, a substrate analogue (see insert, Figure 9A), displaces peroxide from oxytyrosinase ($k_{mimosine-tyrosinase} = 162\ h^{-1}$) but not oxyhemocyanin ($k_{mimosine-hemocyanins} \ll 10^{-4}\ h^{-1}$),[36,67] and it is found to bind directly to the coupled binuclear copper active site.[90] This is demonstrated by the appearance of a new absorption band at 425 nm, which is assigned as a mimosine-to-Cu(II) charge transfer transition (Figure 9A). Note that charge transfer intensity requires orbital overlap and thus direct coordination.

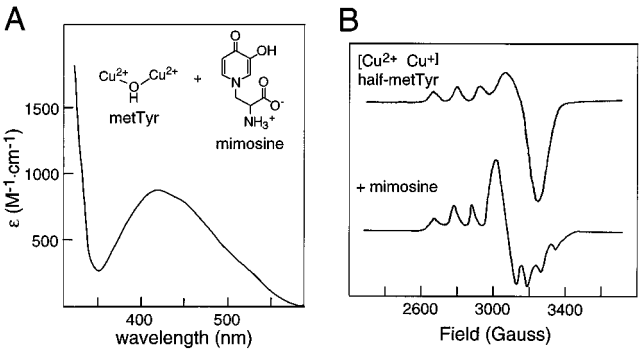

Figure 9. Spectroscopic features unique to tyrosinase (adapted from ref 90). (A) Absorption spectrum of met-mimosine tyrosinase (difference spectrum of met-mimosine minus met), showing the mimosine−Cu(II) charge transfer transition. (B) EPR spectrum of half-met-NO_2^- (upper) and half-met-mimosine (lower) tyrosinase.

The half-met derivative (see Figure 7), which has an $S = {}^1/_2$ ground state and is thus EPR active, has proved to be a particularly useful probe of this site. Addition of mimosine to half-met tyrosinase results in a new unusual EPR signal (Figure 9B) associated with the inhibitor bound form of the site. This unusual EPR signal is only observed when good inhibitors (*vide infra*) are bound to the half-met site. It has a large rhombic splitting and sizable Cu−hyperfine coupling in the $g_\perp$ region. These spectroscopic features require a significant amount of d_{z^2} mixing into the $d_{x^2-y^2}$ ground state which is associated with a large distortion of the EPR-active Cu(II) toward a trigonal bipyramidal structure. Thus, for tyrosinase, substrate analogs are capable of binding directly to at least one copper center and undergo a trigonal bipyramidal rearrangement which displaces the peroxide ligand from the oxytyrosinase active site.

Chemical and spectroscopic studies have been performed for the binding of a series of carboxylate competitive inhibitors to the oxy, met, and half-met derivatives of the coupled binuclear copper site in *N. crassa* tyrosinase.[72] The kinetic and thermodynamic parameters obtained are summarized in Table 2, where k_{on} refers to carboxylate binding, K_{disp} is the equilibrium constant for the displacement of peroxide from the oxy site, K is the binding constant of the carboxylate to met tyrosinase ($=K_{disp}/K_{O_2^{2-}}$, where $K_{O_2^{2-}}$, the binding constant for peroxide to met tyrosinase, is $\sim 2 \times 10^4$), $k_{off} = k_{on}/K_{disp}$, and K_I is the inhibition constant of the carboxylate for the oxidation of DOPA. These inhibitors divide into two groups: (1) poor inhibitors, which show equilibrium constants for binding to the enzyme site similar to those for binding to aqueous Cu(II) complexes ($K \sim 100\ M^{-1}$), and (2) good inhibitors, which bind with equilibrium constants higher by an order of magnitude relative to aqueous copper. Associated with the increased stability are unique spectroscopic features, similar to those observed for mimosine bound to half-met tyrosinase in Figure 9B, which indicate a trigonal bipyramidal rearrangement of the cupric center in the good inhibitor-bound forms. The good inhibitors are all substrate analogs in that the carboxylate is conjugated into an aromatic ring, providing a planar structure. This apparently has additional interactions with residues in the protein pocket which stabilize the trigonal bipyramidal geometry. Con-

Table 2. Kinetic and Thermodynamic Parameters for Carboxylate Binding to Met Tyrosinase (adapted from ref 72)

	k_{on}, M^{-1} h^{-1}	K_{disp}, M^{-1}	K, M^{-1}	k_{off}, h^{-1}	$1/K_I$, M^{-1}
o-toluic acid					<10
o-bromobenzoic acid					40
acetic acid	4	0.00360	180	1100	10
phenylacetic acid	5	0.00320	160	1400	110
naphthylacetic acid	5	0.00320	160	1400	90
cyclohexanecarboxylic acid	5	0.00300	150	1500	70
cyclopentanecarboxylic acid	4	0.00400	200	1000	70
m-toluic acid	8	0.00620	310	1300	450
m-bromobenzoic acid	17	0.0150	750	1150	700
benzoic acid	17	0.0160	800	1050	1400
p-toluic acid	24	0.0384	1920	650	2000
p-bromobenzoic acid	18	0.0282	1410	650	4100
p-ethylbenzoic acid	16	0.0150	750	1100	6800
picolinic acid	16	0.0152	760	1050	570
terephthalic acid	17	0.0156	780	1100	1200

verting the binding affinities of phenylacetic acid and *p*-toulic acid to tyrosinase to binding energies gives −2.9 kcal/mol for carboxylate binding to the binuclear cupric site and an additional −1.3 kcal/mol for the protein pocket interaction with the aromatic side chain of *p*-toulic acid.

In summary, while the CuO_2Cu unit of the oxytyrosinase site is very similar to that of oxyhemocyanin, the tyrosinase site is more accessible. Substrates and aromatic carboxylic acid inhibitors bind directly to the Cu(II) in a trigonal bipyramidal geometry, which is midway along the reaction coordinate for an axial to equatorial rearrangement. Furthermore, substrates and inhibitors have additional stabilizing interactions with the protein pocket.

4. Molecular Mechanism

The above considerations have led to the molecular mechanism for the monophenolase and diphenolase activity of tyrosinase based on the geometric and electronic structure of the oxyhemocyanin active site.[72] In the cresolase cycle, the monophenol binds to the axial position of one of the coppers of the oxy site, perhaps Cu_A, and undergoes a trigonal bipyramidal rearrangement toward the equatorial plane which orients its ortho-position for hydroxylation by peroxide. This generates a coordinated *o*-diphenolate, which is oxidized to the quinone, resulting in a deoxy site ready for further dioxygen binding. In the catecholase cycle, both the oxy and met sites react with *o*-diphenol, oxidizing it to the quinone. In comparing the kinetic constants for monophenolic versus diphenolic substrates, it is found that bulky substituents on the ring dramatically reduce the monophenolase but not diphenolase activity.[72] This suggests that while the monophenolic substrates require the axial to equatorial arrangement for ortho-hydroxylation, in Figure 10 the diphenolic substrates need not undergo rearrangement at the copper site for simple electron transfer. The fact that *o*-diphenol but not *m*- or *p*-diphenol (*o*- and *p*-diphenol have approximately the same potential) are oxidized by tyrosinase supports the bridged bidentate coordination mode indicated in Figure 10, although a bidentate mode bound to one copper is also a possibility.

While much of the earlier literature interpreted the complex kinetics of tyrosinase in terms of allosteric effects and two binding sites,[48,91,92] the molecular mechanism in Figure 10 accounts well for all the kinetics and inhibition patterns observed for this enzyme.[72] (1) The lag phase present for monophenolase but not diphenolase activity derives from the fact that the resting form of tyrosinase contains 10% to 15% oxy sites[48] and monophenolic substrates can react only with this oxy component (Figure 10). The final product of the four-electron oxidation is *o*-DOPAquinone, which rearranges internally to yield the diphenol leukoDOPAchrome, which in turn can react with additional *o*-DOPAquinone to yield DOPAchrome and DOPA.[93,94]

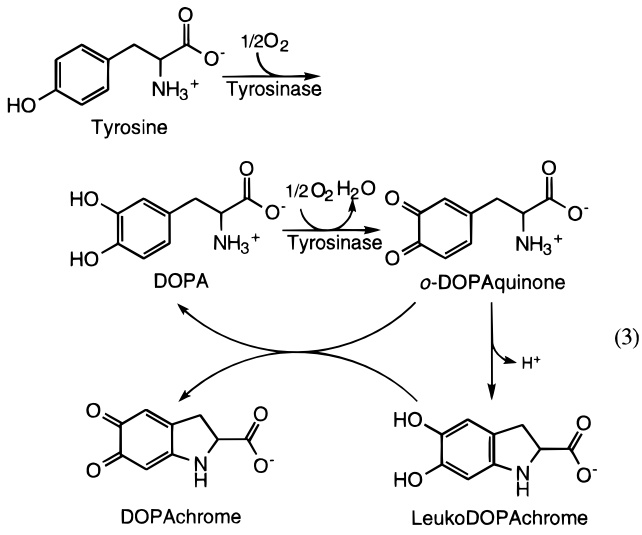

(3)

The diphenol can react with the met tyrosinase sites present, converting these to the deoxy form and bringing these into the monophenolase cycle (Figure 10). (2) Diphenol can react with both the met and oxy sites (Figure 10); however, monophenol can compete with diphenol for binding to the met tyrosinase site, inhibiting its reduction. (3) The inhibition pattern summarized in Table 3 results from the fact that benzoate binds to both the oxidized and reduced forms of the coupled binuclear copper site in tyrosinase, CN^- binds only to the reduced site, and azide binds to the oxidized met and oxy sites.

We have emphasized that the side-on, μ-η^2:η^2 peroxide has an unusual electronic structure which activates it for the hydroxylation reaction. Due to its strong σ donation to the coppers, the peroxide is

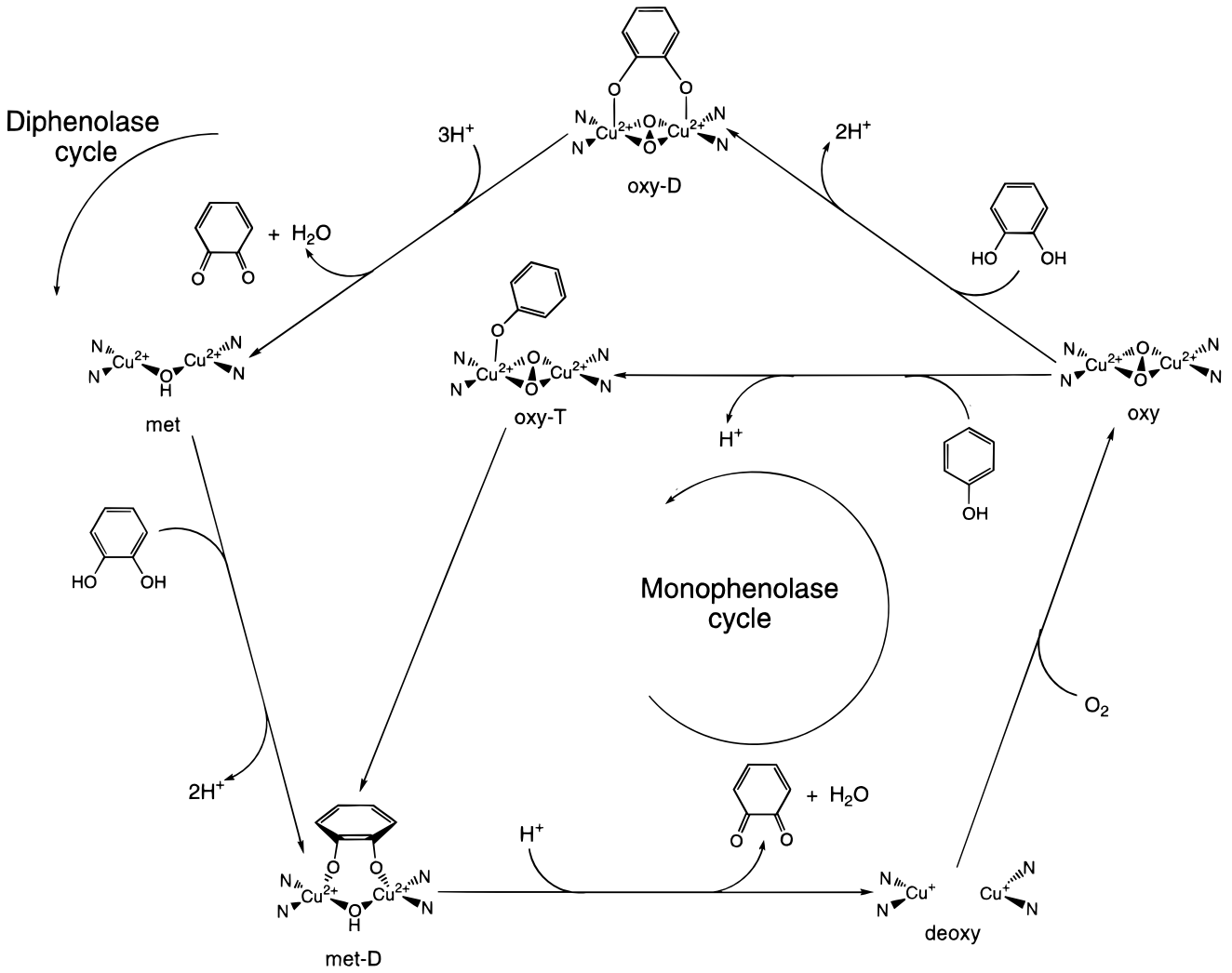

Figure 10. Catalytic cycle for the monooxygenation of monophenols and the oxidation of *o*-diphenols to *o*-quinones by tyrosinase (adapted from ref 72). Axial ligands at Cu not included for clarity. T = tyrosine and D = DOPA bound forms.

Table 3. Inhibition Patterns for Various Inhibitors of Tyrosinase (adapted from ref 72)

	cresolase activity with respect to		catecholase activity with respect to	
inhibitor	L-tyrosine	O_2	L-DOPA	O_2
carboxylate	competitive	noncompetitive	competitive	noncompetitive
CN^-	noncompetitive	ND[a]	noncompetitive	competitive
N_3^-	noncompetitive	noncompetitive	noncompetitive	noncompetitive

[a] ND = no data available.

more electrophilic than in end-on peroxycopper(II) complexes,[75−77] which are found to exhibit nucleophilic reactivity patterns.[95] Also, the participation of the peroxide σ^* orbital in back-bonding with the coppers leads to an extremely weak O−O bond, activating it for cleavage.[75−77] Coordination of the monophenolic substrate in the ternary intermediate in Figure 10 would donate additional electron density into this electrophilic center and initiate the hydroxylation reaction. It is an extremely interesting question as to whether the O−O bond cleaves prior to, concerted with, or subsequent to the attack on the ring (Figure 11). It is clear that in oxytyrosinase the O−O bond is still present, and in fact, oxytyrosinase is the most well-characterized of the oxygen intermediates involved in metalloenzyme hydroxylation reactions. However, since in tyrosinase the phenolic substrate coordinates directly to the metal center, it

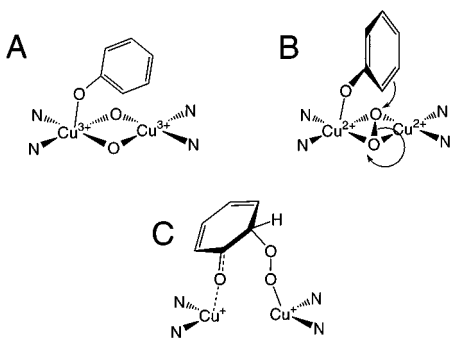

Figure 11. Three possible mechanistic scenarios for the monooxygenation of phenol by oxytyrosinase. (A) The O−O bond cleaves prior to attack on the ring, yielding a species which is formally binuclear Cu(III) bis μ-oxo. (B) O−O bond cleavage is concerted with attack on the ring. (C) The O−O bond is still present after attack on the ring, yielding an aryl peroxide intermediate.

can perturb the CuO_2Cu bonding by donating electron density and perhaps its acidic proton to the peroxide. The most well-defined model system in this regard is the $[Cu_2(m\text{-XYL})]^{2+}$ complex of Karlin *et al.*, where a noncoordinated xylyl ring is hydroxylated upon reaction with dioxygen.[96] This reaction is believed to occur via the formation of a μ-η^2:η^2 peroxide, on the basis of the observation of a transient increase in the absorption spectrum at 360 nm. Furthermore, the fluoro derivative of this compound is not hydroxylated but forms a stable oxygenation product with absorption bands at 360 ($\epsilon = 21\,400\ M^{-1}\ cm^{-1}$), 425 ($\epsilon = 3600\ M^{-1}\ cm^{-1}$), and 520 nm ($\epsilon = 1200\ M^{-1}\ cm^{-1}$), similar to that seen in known dicopper μ-η^2:η^2 peroxide complexes.[97] From the lack of a kinetic isotope effect,[98] the acceleration effects of electron-donor ring substituents on the reaction,[99,100] and the presence of a NIH shift,[101] $[Cu_2(m\text{-XYL})]^{2+}$ is well-characterized as undergoing an electrophilic addition reaction. Similar evidence has been observed in favor of an electrophilic reaction mechanism for tyrosinase.[72] A similar very small isotope effect is observed for tyrosinase,[102] and although an NIH shift has not been observed, its existence has not been ruled out.[101] Although careful quantitative studies on the effect of ring substituents on the rate of monophenol hydroxylation are not available, it has been noted that the phenols with electron-withdrawing substituents are not hydroxylated.[103] It is now important to define the nature of the oxygen intermediate in the Karlin hydroxylation model system,[96] learn more about electronic structure and reactivity of the bis μ-oxo complex of Tolman and co-workers,[78,79] and determine the effects of monophenolate coordination on the oxytyrosinase active site.[72]

B. Related Multicopper Enzymes

In addition to tyrosinase, there are two other copper-containing monooxygenases: a particulate form of methane monooxygense (pMMO) and ammonia monooxygenase (AMO). Monooxygenation of methane to methanol is the first step in the oxidation of methane by methanotrophic eubacteria, which use methane both as a carbon source and an energy source.[104]

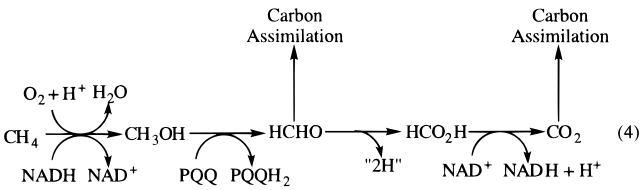

(4)

This first step is performed by the enzyme methane monooxygenase, which exists in two different forms, a soluble form found in the cytosol, sMMO, and a membrane-bound form, pMMO.[104] The predominant form, found in all methanotrophs, is pMMO. In contrast, sMMO is only found in certain species of methanotrophs and only under conditions of copper deficiency. Extensive characterization of sMMO has revealed that it consists of three components: a hydroxylase, a regulatory protein (protein B), and an NADH reductase. Spectroscopic and crystallographic studies of the sMMO hydroxylase component has defined the nature of the hydroxo-bridged binuclear iron site (for a review, see the article by Wallar and Lipscomb in this issue).[105] Although pMMO performs the same chemistry, it differs in several important regards. Copper is required for activity.[106,107] There is a correlation between copper concentration in the growth medium and *in vitro* and *in vivo* pMMO activity; furthermore, copper induces the expression of pMMO.[25,108−111] Copper leads to the expression of at least two new polypeptides with molecular weights of 41−47 and 21−27 kDa, and possibly a third.[25,108,109,111−113] The genes encoding the 47 and 27 kDa polypeptides have been cloned and sequenced.[114] Labeling of these polypeptides with [^{14}C]-acetylene, a suicide inhibitor which presumably binds at the active site, has further demonstrated that these polypeptides are constituents of the pMMO enzyme complex.[112,113,115] The two enzymes also have very different substrate, inhibitor, and stereochemical specificities. While sMMO can monooxygenate a wide variety of *n*-alkanes, *n*-alkenes, cycloalkanes, and aromatic compounds, pMMO can only monooxygenate *n*-alkanes or *n*-alkenes of five carbons or less.[106,116] For *n*-alkanes of three or more carbons, sMMO hydroxylates at both the 1- and 2-positions, while pMMO only hydroxylates at the 2-position.[106,116] Both enzymes are suicide-inhibited by acetylene, but only pMMO is strongly inhibited by typical metal-binding compounds such as cyanide and thiourea.[107] The hydroxylation of chiral alkanes indicates that sMMO reacts with 68% retention of configuration,[117] while pMMO shows 100% retention of configuration.[118] This argues against an alkyl radical or carbocation intermediate in the mechanism of pMMO; in contrast, the mechanism of sMMO has been considered to proceed via a short-lived radical.

pMMO has proven to be a difficult enzyme to study due to problems in obtaining pure enzyme that still retains activity. Recently, progress has been made in the determination of the active site structure of the pMMO from *Methylococcus capsulatus* (Bath). Working with membrane preparations, Chan and coworkers have proposed a ferromagnetically coupled trinuclear copper cluster as the active site of the enzyme, on the basis of EPR spectroscopy and magnetic susceptibility.[25,111,119] In addition to normal copper features, the EPR spectrum of highly oxidized membrane preparations of pMMO show a broad, nearly isotropic, and difficult to saturate EPR signal centered at $g \approx 2.0$ (Figure 12A, top). Magnetic saturation data obtained by SQUID magnetic susceptibility was best fit with an average spin of 1.4 ± 0.1, thus leading to an assignment of an $S = {}^3/_2$ ground state, which can be obtained by the ferromagnetic coupling of three Cu(II)s. A small zero-field splitting would then lead to the broad signal centered at $g \approx 2$. Partial reduction leads to the appearance of another axial signal centered around $g \approx 2$. The second derivative spectrum of this species shows an equally spaced, 10-line resolved hyperfine pattern ($A \approx 15$ G) with a 1:3:6:10:12:12:10:6:3:1 intensity pattern (Figure 12A, bottom). This intensity pattern is most consistent with a delocalized Cu(II)Cu(I)Cu(I) cluster with all coppers equivalent. An alternative explanation of the hyperfine pattern arising from four equivalent nitrogen nuclei is inconsistent with the

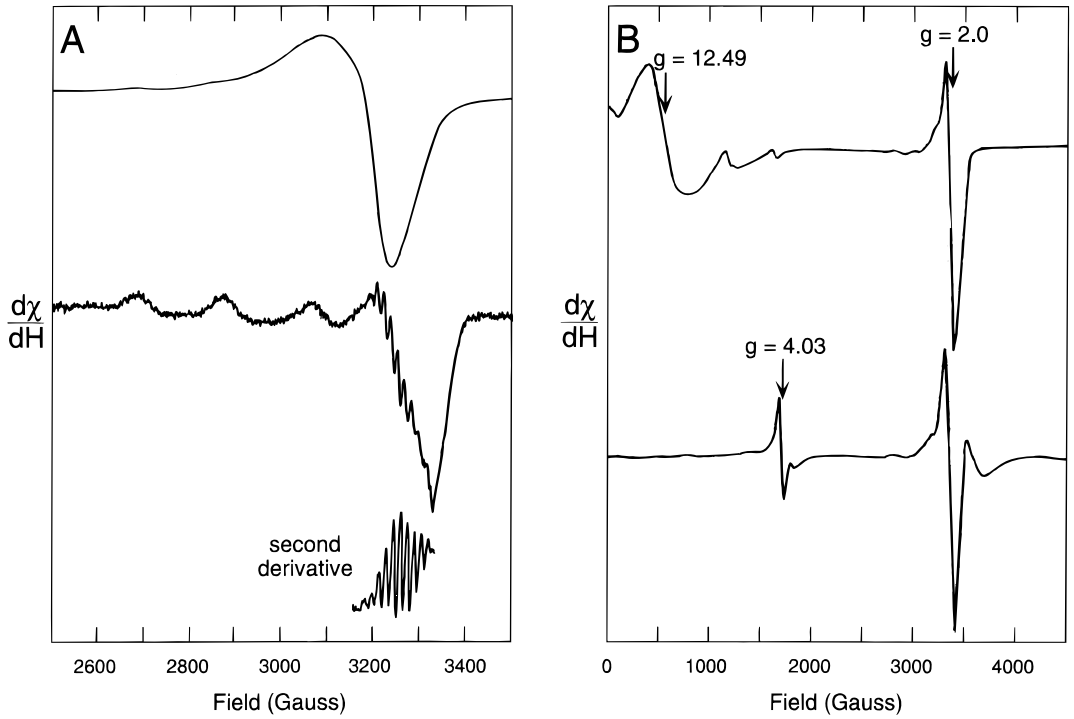

Figure 12. EPR spectra of pMMO. (A) EPR spectra reported by Chan and co-workers, showing the broad isotropic $g = 2.0$ signal obtained at high power (40 mW) and low temperature (7 K) and ascribed to a copper trimer (upper) and partial reduction of this species including the second derivative of the $g_{\perp}$ feature (lower). (Reprinted with permission from ref 25. Copyright 1994 American Society for Biochemistry and Molecular Biology.) (B) EPR spectra reported by Zahn and DiSpirito, showing the $g = 12.49$ signal (upper) and the $g = 4.03$ signal obtained upon reduction and addition of nitric oxide (lower). (Reprinted with permission from ref 113. Copyright 1996 American Society for Microbiology.)

intensity distribution. Ferromagnetically coupled copper clusters are relatively rare among small-molecule copper compounds, since this usually requires close to orthogonal bridging orbital pathways in non-mixed valent systems. The existence of such a structural motif would add another truly novel metal active site to the field of bioinorganic chemistry, and another challenge for the model chemist.

Recently, DiSpirito and co-workers were able to obtain active purified pMMO by solubilization with dodecyl-β-D-maltoside followed by anaerobic purification.[113] This group proposes that iron, in addition to copper, is required for enzyme activity. Although Chan and co-workers also observed an increase in the iron/protein ratio which follows the increase in the copper/protein ratio, they attributed this to an increase in membrane-bound cytochromes, while DiSpirito found that only 1.9% of the membrane-associated iron was in the form of heme. The purified pMMO enzyme complex consisted of 47, 27, and 25 kDa polypeptides and contained 2.5 irons and 14.5 coppers per complex. The EPR spectrum showed a normal copper signal at $g \approx 2$ and an unusual broad feature at $g = 12.5$ that disappeared upon reduction (Figure 12B, top). The unusual broad isotropic signal at $g \approx 2$ ascribed to a ferromagnetically coupled trinuclear copper site was not observed. Addition of nitric oxide to reduced pMMO yielded a signal at $g = 4.03$ (Figure 12B, bottom). This was assigned as an $S = {}^3/_2$ $\{Fe-NO\}^7$ species, as is observed in many mononuclear non-heme iron enzymes.[120] Further solubilization of purified pMMO yielded the selective isolation of the 47 and 27 kDa polypeptides, though it led to the elimination of activity. These peptides contained 0.9 irons, 0.6 coppers, and one acid-labile sulfur per complex. The EPR spectrum again showed normal copper; the presence of the $g = 12.5$ signal was preparation-dependent. In preparations lacking it, it could be regenerated by reduction followed by addition of acetylene. The rest of the copper that was present in the active purified pMMO was found associated with a low-molecular copper binding complex, a dimer with a molecular weight of 618 D, two to three coppers per subunit, and an EPR spectrum with unusually small hyperfine ($A_{||} < 150$ cm^{-1}) splitting that quantitates to only 30% of the total copper. In cells grown with copper, this copper-binding complex accounts for 75% of the total copper found in the membrane fraction. Because when pMMO is labeled with [^{14}C]acetylene (a suicide inhibitor which presumably acts at the active site) the label appears in the 47 and 27 kDa peptides, it was determined that the low molecular weight copper-binding complex does not contain the active site. On the basis of these data, a copper−iron binuclear center was proposed for the active site. The putative copper-binding complex needs to be further defined to determine its structure, how it binds copper, and what role it has in the pMMO activity.

Ammonia-oxidizing eubacteria, such as *Nitrosomonas europaea*, obtain energy from the oxidation of ammonia to nitrite.[121]

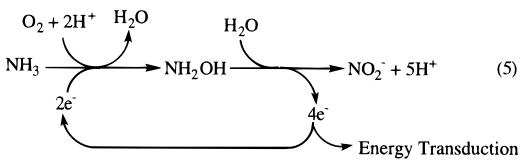

(5)

AMO catalyzes the first step of this reaction, the monooyxgenation of ammonia to hydroxylamine. Catalytically active AMO has not yet been purified, although active cell-free extracts have been prepared.[122] This membrane-bound protein shares many similarities with pMMO. In addition to ammonia, it can also oxidize a variety of hydrocarbons,[123] halogenated organics, carbon monoxide, and thioethers.[124] The hydroxylation of benzene derivatives was observed to occur with an NIH shift, suggesting that the reaction proceeds via electrophilic addition without the formation of an arene oxide intermediate.[125] As with pMMO, acetylene and other alkynes act as suicide inhibitors.[126,127] Isotopic labeling with [^{14}C]-acetylene has led to the identification of a 27−28 kDa polypeptide as a component of AMO containing the active site, and evidence exists for additional polypeptides with molecular weights of 55 and 65 kDa as components of AMO.[126,127] The gene for the 27−28 kDa acetylene-binding peptide (*amoA*) and a gene immediately downstream from *amoA* encoding for a 43 kDa polypeptide that copurified with the acetylene-binding peptide (*amoB*) have been identified and sequenced.[128,129] These polypeptides show a high degree of homology with those of pMMO. Evidence that AMO is a copper-containing enzyme comes from the fact that copper greatly increases the *in vitro* activity of AMO, and copper is required for acetylene inactivation and polypeptide-labeling.[130] Recently, addition of nitric oxide was used to generate a $g \approx 4$ EPR signal, similar to that seen in pMMO, which was assigned as an $S = {}^3/_2$ {Fe−NO}^{7} species.[131]

Many of the tyrosinase-like enzymes isolated from plants appear to lack monophenol monooxygenase (cresolase) activity (for a review, see ref 57). In all other respects, they are apparently the same as tyrosinase. On the basis of this, they have sometimes been given a separate designation as catechol oxidases (*o*-diphenol:dioxygen oxidoreductase, EC 1.10.3.1) Almost all are poorly characterized. They are known to contain copper,[132] and at least one is known to be inhibited by aryl carboxylic acids.[133] Part of the confusion stems from nomenclature. Often, the terms "phenol oxidases" and "polyphenol oxidases" are used to refer to both tyrosinases and laccases, and it can be difficult to distinguish between tyrosinase and laccase activity, since both can oxidize *o*-diphenols. It is also possible that some of these enzymes are in fact tyrosinases for which a cresolase activity has not yet been observed. Early studies on tyrosinase frequently report the loss of cresolase activity and isozymes or different oligomeric forms exhibiting vastly different catecholase/cresolase ratios or which completely lacked cresolase activity.[134,135] The cresolase activity of tyrosinase is dependent upon the presence of a small amount of oxy in the resting form. This accounts for the observed lag in cresolase activity, which can be eliminated by the addition of hydrogen peroxide or a reductant (*vide supra*). If there is very little or no oxy present in certain enzymes, then this might account for a lack of observed cresolase activity or with cresolase activity which has a much longer than normal lag phase. Nonetheless, there has recently been initial characterization of some enzymes designated as catechol oxidases isolated from *Populus nigra* and *Lycopus europaeus*.[132,136] The EXAFS of the resting met form shows an unusually short copper−copper distance of 2.9 Å. Addition of 6 equiv of hydrogen peroxide to *L. europaeus* enzyme and 80 equiv to *P. nigra* enzyme resulted in an absorbance band at 345 nm with $\epsilon = 3000-3500$ M^{-1} cm^{-1} which has been assigned as a peroxo to Cu(II) charge transfer band. However, this band is far weaker than the 345 nm band seen in oxytyrosinase ($\epsilon =$ 20 000 M^{-1} cm^{-1}; see Figure 8A) and which forms upon the addition of only a few equivalents of hydrogen peroxide to resting, met enzyme. For comparison, among the hemocyanins (Hcs), only mollusk Hcs can be converted from met to oxy by the addition of peroxide. A structural distortion of the copper site in arthropod Hc appears to interfere with peroxide binding and thus formation of oxyHc, which also prevents the catalase activity observed in the mollusk Hcs.[137] Thus, it is plausible that a similar phenomenon may explain the difficulty in formation of the oxy form in the plant enzymes and therefore their apparent lack of monooxygenase activity.

Hcs from *Octupus vularis* and *Sepioteuthis lessoniana* have been reported to possess cresolase and catecholase activity similar to tyrosinase, although at a much lower rate.[138,139] Little is known about this activity, particularly whether or not substrate oxidation occurs at the binuclear copper site. If it does, it may correlate with the limited accessibility that is present in Hc. Oxidation of phenolic substrates has been observed in mollusk Hcs but not in horseshoe crab Hc, the former of which are known to have greater accessibility to the binuclear copper active site.[63]

III. Multicopper Oxidases

A. Enzymology

The multicopper oxidases are a class of enzymes that can be defined by their spectroscopy, sequence homology, and reactivity. The currently well-defined multicopper oxidases are laccase (Lc), ascorbate oxidase (AO), and ceruloplasmin (Cp). Recently several new additional ones have been isolated and characterized: phenoxazinone synthase (PHS), bilirubin oxidase (BO), dihydrogeodin oxidase (DHGO), sulochrin oxidase (SO), and FET3. A combination of detailed spectroscopic studies and X-ray crystallography has revealed that all contain at least one blue copper or T1 site and a T2/T3 trinuclear cluster as the minimal functional unit. Cp is presently unique among the multicopper oxidases in that it possesses additional copper centers (*vide infra*). Functionally, all multicopper oxidases couple the four-electron reduction of dioxygen to water with the oxidation of substrate. In the well-characterized enzymes (Lc, AO, Cp), the substrate is oxidized by one electron. In the less well-characterized ones (PHS, BO, SO, DGHO), it has not been established whether substrate oxidation occurs by two electrons or by two sequential one-electron oxidations (*vide infra*).

The T1, or blue copper site (*vide supra*), has an absorption band at about 600 nm with $\epsilon \approx 5000$ M^{-1} cm^{-1} and an EPR spectrum with narrow parallel hyperfine splitting ($A_{\parallel} = 43-95 \times 10^{-4}$ cm^{-1}; see

Table 4). In *Rhus vernicifera* Lc, AO, and Cp, the potential of the T1 site is 344−580 mV *vs* NHE,[141,143,176,188] which is typical for a blue copper protein. Among the fungal Lcs, the potential can vary from approximately 465 mV *vs* NHE for *Myceliophthora thermophila*[162] to 775 mV for *Polyporus versicolor*.[155] This is despite the strong similarity of their T1 copper EPR parameters ($A_{\|} = 80-92 \times 10^{-4}$ cm^{-1}). Primary amino acid sequence homology shows that the conserved ligands for the T1 site are two histidine nitrogens and a cysteine thiolate sulfur. In addition, some multicopper oxidases, including AO, have a conserved methionine 10 residues from the cysteine, thus generating a first coordination sphere analogous to that in plastocyanin, while others have a noncoordinating residue, leucine or phenylalanine, at this position (see Figure 13). All of the fungal Lcs that have been sequenced to date, with the exception of *Aspergillus nidulans* Lc,[213] fall into this latter category. The reason for the very high reduction potentials, as well as the large range in reduction potentials among fungal Lcs, remains to be determined. Electronic structure studies on plastocyanin have demonstrated that a long, weak axial bond destabilizes the oxidized state more than the reduced site and is therefore a key factor in the high reduction potentials of blue copper sites in general, and that the strength of the copper-thioether bond inversely affects the strength of the copper-thiolate bond.[214] This trend is observed for a number of blue copper sites, including *Polyporus versicolor* Lc, wherein an increase in the potential has been correlated with an increase in the "local oscillator" $Cu-S_{Cys}$ stretching frequency, which implies a shorter $Cu-S_{Cys}$ bond.[215] Furthermore, in a series of Azurin mutants, replacement of the axial methionine with noncoordinating hydrophobic residues can raise the potential by as much as 138 mV.[216] Other possible factors influencing the reduction potentials of the fungal Lc T1 sites are electrostatic interactions between the metal site and the protein, water environment, and hydrogen-bonding interactions of the active site ligands (see the paper by Stephens in this issue).[217,218] The function of the T1 site within the enzyme is long-range intramolecular electron transfer, shuttling electrons from the substrate to the trinuclear cluster. The electrons are transferred from the T1 copper to the trinuclear cluster approximately 13 Å away along a cysteine-histidine pathway.[219]

The T2 copper exhibits EPR parameters typical for normal copper ($A_{\|} = 158-201 \times 10^{-4}$ cm^{-1}) and no intense features in the visible absorption spectrum. An archetypal feature of the T2 site in the multicopper oxidases is its ability to bind F^- with an unusually high affinity, a feature which can easily be identified by the 50×10^{-4} cm^{-1} superhyperfine splitting observed in the EPR spectrum (*vide infra*).[220−223] The potential of the T2 site has been reported only for *R. vernicifera* Lc, wherein it is 365 mV.[141] The T3 copper pair has an absorption band at around 330 nm ($\epsilon \approx 5000$ M^{-1} cm^{-1}) and is EPR-silent, indicative of a strongly antiferromagnetically coupled Cu(II) pair bridged by a hydroxide. The potential of the T3 pair ranges from slightly above 344 mV for *Cucurbita pepo medullosa* AO[176] to 782 mV for *Polyporus versicolor* Lc.[141] The reason for the high T3 copper reduction potential in *P. versicolor* Lc has not yet been addressed. The T2 and T3 sites form a trinuclear cluster, as first determined by spectroscopy[5,6,23] and later by X-ray crystallography.[7,24] A combination of X-ray crystallography and primary amino acid sequences indicate that the peptide ligands of the trinuclear cluster are eight histidines which occur in a highly conserved pattern of four HXH motifs (see Figure 13).[224] In one, X is the cysteine bound to the T1 copper and each of the histidines binds to one of the T3 coppers. About 35−75 residues upstream of this is another HXH motif. Close to the N-terminal end are two more HXHs separated by about 35−60 residues. The trinuclear cluster is the site of dioxygen binding and reduction (*vide infra*).

X-ray crystallography[7,24] and a comparison of the amino acid sequences[224,225] have also shown that the multicopper oxidases possess a distinctive subdomain structure. Lc and AO have three domains. The T1 site is in domain 3 and the trinuclear cluster is at the border between domains 1 and 3, possessing ligands from each domain (see Figure 14). Cp has a six domains arranged with approximate C_3 symmetry. The trinuclear site is between domains 1 and 6, again sharing ligands from each. Also, there are T1 or T1-like sites in domains 2, 4, and 6. In all three enzymes, there is a significant degree of internal homology among the subdomains, suggesting that they all arose from a common gene ancestor by gene duplication.

The interactions of the multicopper oxidases with substrates can be broadly divided into two categories: enzymes with low substrate specificity and enzymes with high specificity. The plant and fungal Lcs fall into the former category. They can oxidize diphenols, aryl diamines, and aminophenols. The K_m values are generally in the range of 1−10 mM, indicating that there is probably no binding pocket for substrate and that the oxidation is strictly outer-sphere.[146,162,226,227] In the Lcs, the oxidase activity (k_{cat}/K_m) correlates with the oxidation potential of the substrate (see Figure 15). These observations are consistent with Marcus theory when the rate-determining step is substrate reduction of the T1 site by an outer-sphere reaction in which the rate of electron transfer increases as the difference in the redox potentials of the substrate donor and T1 site acceptor increase, until the inverted region is reached.[228] The other multicopper oxidases possess a significant degree of substrate specificity (K_m < 1 mM), implying a substrate binding pocket. AO shows a high degree of specificity for L-ascorbate and analogs,[229,230] and Cp shows a high specificity for Fe(II).[231−235] SO and DHGO also have very high substrate specificities. The K_m of *Penecillium frequentans SO* is 6.5 μM for sulochrin, while for *p*-phenylenediamine it is 2 mM. In addition, the reactions these enzymes catalyze are stereospecific.

The following subsections briefly describe the enzymology and function of each of the multicopper oxidases.

Table 4. Properties of the Well-Characterized Multicopper Oxidases[a]

source	subunits	MW (kDa)	percent carbohydrate	EPR T1 $g_{\|\|}$	EPR T1 $A_{\|\|}$	EPR T2 $g_{\|\|}$	EPR T2 $A_{\|\|}$	potential (mV) T1	potential (mV) T3	sequence	ref
Plant Laccase											
Rhus vernicifera	1	110	45	2.300	39	2.24	182	394−434	434−483	no	140−144
Rhus succedanea	1	130	ND	2.204	76	2.217	184	ND	ND	no	142,144,145
Acer pseudoplatanus	1	97	40−45	ND	ND	ND	ND	ND	ND	yes	146−149
Pinus taeda	1	90	22	2.217	74.2	ND	ND	ND	ND	no	150
Fungal Laccase											
Polyporus versicolor	1	64.65	10.12	2.190	90	2.262	179	775−785	782	yes	141,151−155
Neurospora crassa	1	64−64.8	11−12	2.19	92	2.23	193	ND	ND	yes	156−158
Pleutrotus ostreatus	1	59−64	12.5	2.197	90	2.263	176	ND	ND	yes	159−161
Polyporus pinsitus 1	2	126	7	2.19	92	ND	ND	760−790	ND	yes	162−164
Rhizoctonia solani 4	2	132	10	2.21	85	ND	ND	680−730	ND	yes	162,165
Myceliophthora thermophila	2	160	14	ND	ND	ND	ND	450−480	ND	yes	162
Scytalidium therophilum	1	75−80	ND	2.20	90	ND	ND	480−530	ND	yes	162,166
Polyporus anisoporus	1	57.5	ND	ND	ND	ND	ND	775	ND	no	167
Phlebia radiata	1	64	11.8	2.19	90	2.25	170	ND	ND	yes	168,169
Podospora anserina				2.209	80	2.246	176	ND	ND	no	170−172
I	4	390	20−23.7								
II	1	70	22.7−24.9								
III	1	80	227.23.1								
Ascorbate Oxidase											
Cucurbita pepo medullosa	2	140	2.4	2.227	56	2.242	199	344	≥344	yes	173−176
Cucumis sativus	2	132	ND	2.22	50	ND	ND	350	ND	yes	177−179
Acremonium sp. HI-25	1	80	11.2	2.228	52	2.235	201	ND	ND	no	180,181
Ceruloplasmin											
Human I	1	132	9.0	2.215	95	2.247	189	490	ND	yes	182−189
				2.206	74			580	ND		
chicken	1	124−140	7.2	∼2.2	60−95	none		ND	ND	no	190,191
				∼2.2	60−95						
turtle *(Caretta caretta)*	1	145	ND	∼2.2	60−95	none		ND	ND	no	192
				∼2.2	60−95						
cow	1	126	14	2.22	76	2.26	158	370	ND	no	193,194
				2.25	67			390	ND		
sheep	1	125	ND	∼2.2	70	ND	ND	ND	ND	no	195,196
				∼2.2	60						
dolphin	1	140	ND	∼2.2	60−95	ND	ND	ND	ND	no	197
				∼2.2	60−95						
goose	1	121.3	6.65	2.239	63	2.239	189	ND	ND	no	198
Other Putative Multicopper Oxidases											
PHS (*Streptomyces antibioticus*)	6	540	ND	2.24	67	2.34	160	ND	ND	yes	199−202
	2	180									
BO (*Myrothecium verrucaria*)	1	64	6.3	ND	ND	ND	ND	480−490	ND	yes	162,203−206
BO (*Trachyderma tsunodae*)	1	64	ND	2.186	91.2	2.257	165.7	ND	ND	no	207
SO (*Penicillium frequentans*)	2	157	19.5	ND	ND	ND	ND	ND	ND	no	208
SO (*Oospora sulphurea-ochracea*)	2	128	ND	ND	ND	ND	ND	ND	ND	no	208
DHGO (*Aspirgillus terreus*)	2	153	8.9	2.217	71.9	ND	ND	ND	ND	yes	209,210
FET3 (*Saccharomyces cerevisiae*)	1	72.3	ND	ND	ND	ND	ND	ND	ND	yes	211,212

[a] ND = no data available.

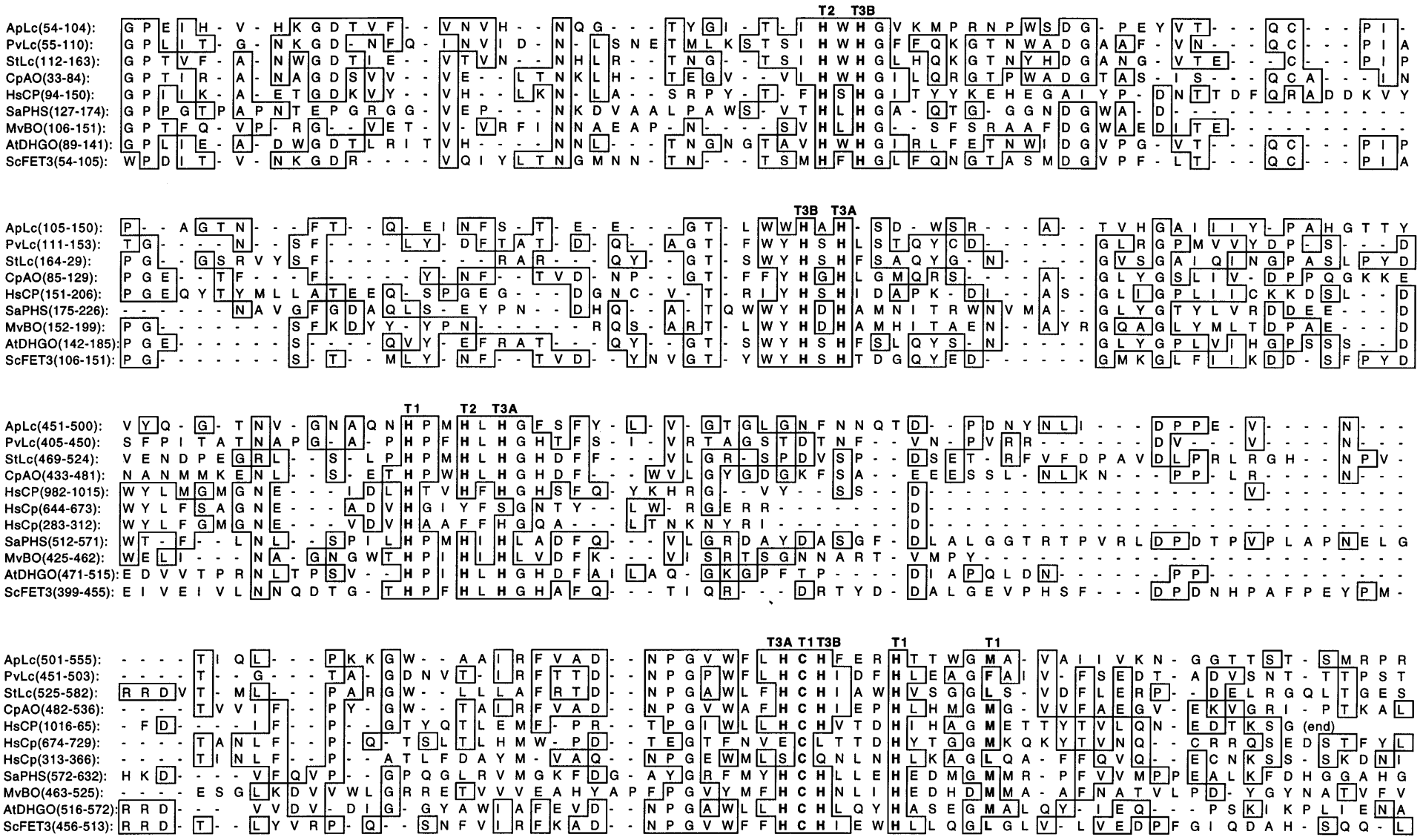

Figure 13. Selected portions of the amino acid sequences of a variety of multicopper oxidases, showing the high degree of homology at and around the copper binding regions. Identical residues are boxed. Numbering includes leader peptides. Abbreviations used for the different enzymes are as follows: ApLc, *Acer Pseudoplatanus* Lc (ref 147, GenBank/EMBL Data Bank accession number: U12757); PvLc, *Polyporus versicolor* Lc (ref 153, accession no. X84683); StLc, *Scyalidium thermophilum* Lc (ref 166); CpAO, *Cucurbita pepo medullosa* AO (ref 340, accession no. 442635); HsCP, Human Cp (ref 186, accession no. M13699); SaPHS, *Streptomyces antibioticus* PHS (ref 202, accession no. U04283); MvBO, *Myrothecium verrucaria* BO (ref 206, accession no. D12579); AtDHGO, *Aspirgillus terreus* DHGO (ref 210, accession no. D49538); ScFET3, *Saccharomyces cerevisiae* FET3 (ref 212, accession no. L25090).

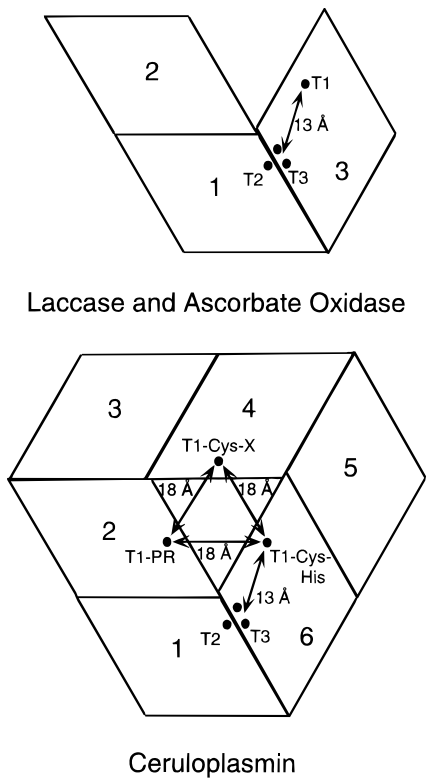

Figure 14. Schematic diagram of Lc, AO, and Cp, showing the domain structure and the geometric relationship among the various copper sites. (Reprinted with permission from ref 24. Copyright 1996 Springer-Verlag.)

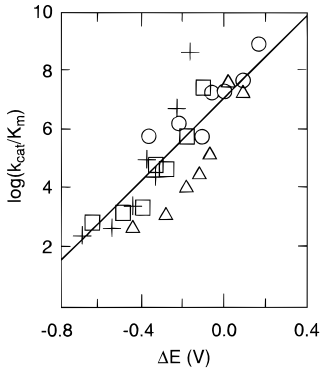

Figure 15. Correlation of $\log(k_{cat}/K_m)$ with ΔE ($=E_{LcT1\ site} - E_{substrate}$) at pH 5.0. The substrates used were guaiacol, 4-hydroxy-3-methoxybenzaldehyde, homovallinate, syringaldazine, ethyphenol, *o*-anisidine, and 2,2′-azinobis(3-benzthiazoline-6-sulfonic acid) (ABTS). The four fungal Lcs used and their T1 reduction potentials are *Polyporus pinsitus* (○, 780 mV), *Rhizoctonia solani* (△, 710 mV), *Myceliophthora thermophila* (+; 460 mV), and *Scytalidium thermophilum* (□, 510 mV). (Reprinted with permission from ref 227. Copyright 1996 American Chemical Society.)

1. Plant Laccase

The laccases (*p*-diphenol:dioxygen oxidoreductase, EC 1.10.3.2) can be divided into two categories, plant and fungal, although diphenol-oxidizing enzymes which are thought to be Lcs have also been identified in insects[58,236,237] and eubacteria.[238] By far the most studied plant Lc is from *Rhus vernicifera*, but it has also been purified to homogeneity and characterized from *Rhus succedanea* and two other sources (see Table 4). All of the plant Lcs are extracellular monomeric proteins with 22−45% glycosolation. The only plant Lc to have been sequenced is from *Acer pseudoplatanus*;[147] however, little spectroscopic or kinetic work has been done on this enzyme. Plant Lc has four coppers per molecule, one T1 copper and a T2/T3 trinuclear cluster. Two recent reviews of the enzymology and function of Lcs are refs 239 and 240.

Prior to 1992 it was thought by some that Lc was present in few plant species outside of *Rhus* and its immediate relatives (for a review, see ref 57); it has since been purified from other sources and has been detected in a variety of plants.[149,241−244] Although plant Lc was initially thought to catalyze lignin formation, peroxidase has long been considered the sole enzyme responsible for this function.[245−249] However, the potential role of Lc in lignin biosynthesis has recently been reexamined (for a review, see ref 243). Lc activity has been detected in the xylem cell walls of a wide variety of plant species,[149,150,241−244] even when catalase was added, thus eliminating the possible involvement of peroxidase. Most plant Lcs are capable of oxidatively coupling monolignols to dimers and trimers, while peroxidase has a much greater activity toward higher oligomers,[148,150,242,250,251] leading to the proposal that Lc catalyzes the initial polymerization of monolignols into oligolignols, while peroxidases then synthesize the extended polymeric lignin from oligolignols.[250] The physiological substrates which serve as the precursors to lignin formation are the monolignols *p*-coumaryl alcohol, coniferyl alcohol, and sinapyl alcohol. In products of the oxidation of coniferyl alcohol by crude *A. pseudoplatanus* Lc, two types of lignin dimer linkages were identified: β-5′ and β-β′.[250] Representative examples of such structures are shown in Table 5B. The proposed mechanism for the formation of oligomeric products involves coupling of the enzymatically generated substrate radicals.

R. vernicifera Lc is apparently not involved in lignin biosynthesis, since it cannot oxidize monolignols,[248] yet is present in large amounts in the tree's sap. It is known that Lc catalyzes polymerization of urushiol into lacquer, but the role of this process is unclear,[252,253] although a role in wound-healing has been proposed.[254] The dominant products of the partial oxidation of urushiol by *R. vernicifera* Lc are biphenyls and aryl side chain products, examples of which are shown in Table 5A.[253] The mechanism for the formation of the biphenyl products is believed to be radical substitution of the semiquinone formed by the one-electron oxidation of urushiol by Lc with another molecule of urushiol. Aryl side chain products are thought to be formed by the electrophilic substitution of a heptatrienyl cation on the urushiol ring. The heptatrienyl cation could be formed by the hydride abstraction of the heptatriene by a *o*-quinone, which in turn is formed by the disproportionation of the initially generated semiquinone.

2. Fungal Laccase

Fungal Lc has been detected and purified from many species, some of which produce multiple isozymes. The best characterized fungal Lcs are listed in Table 4. For many of these, the cDNA has been sequenced. All fungal Lcs are monomers or homodimers, with the exception of *Podospora anserina* isozyme I, which appears to be a homotetramer. Like the plant proteins, they are glycosylated, but

Table 5. The Physiologically Relevant Reactions Catalyzed by the Multicopper Oxidases

A. *Rhus* Laccase:

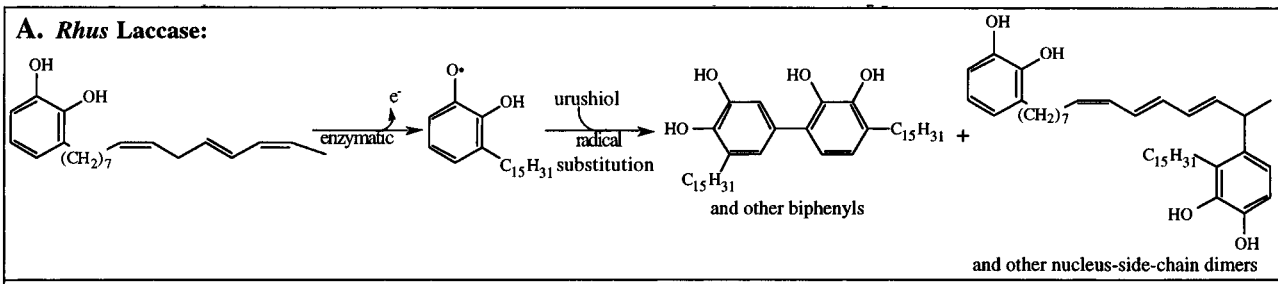

B. Other Plant Laccases:

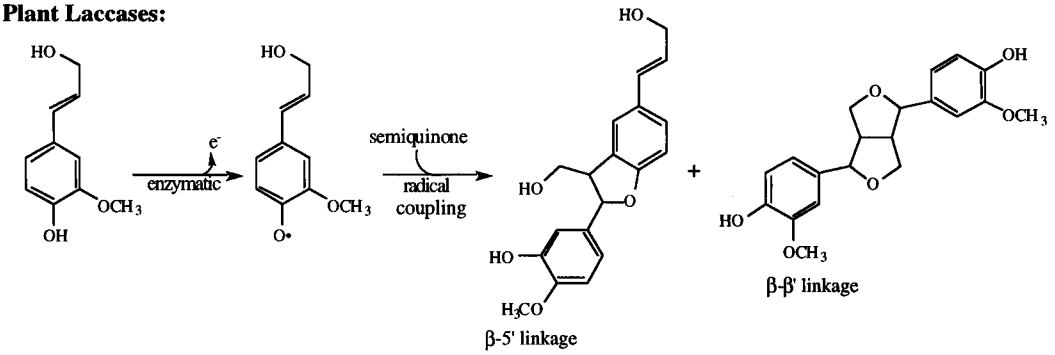

C. Fungal Laccase:

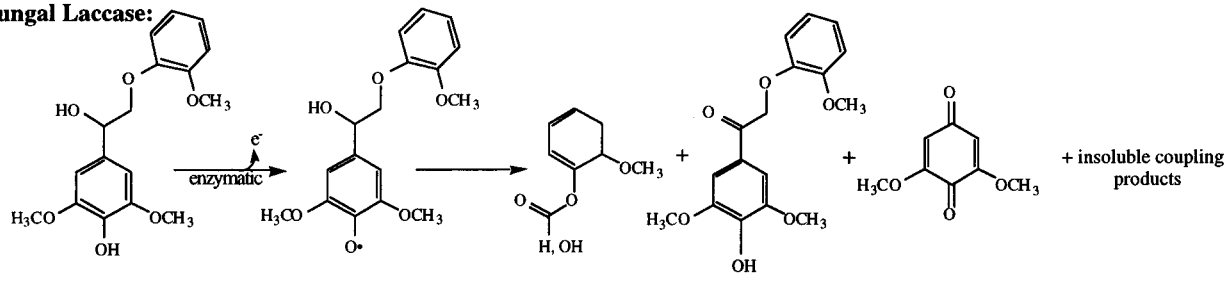

D. Ascorbate Oxidase:

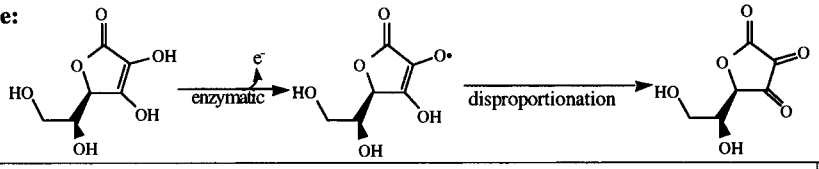

E. Ceruloplasmin and FET3

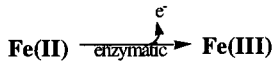

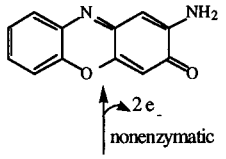

F. Phenoxazinone Synthase:

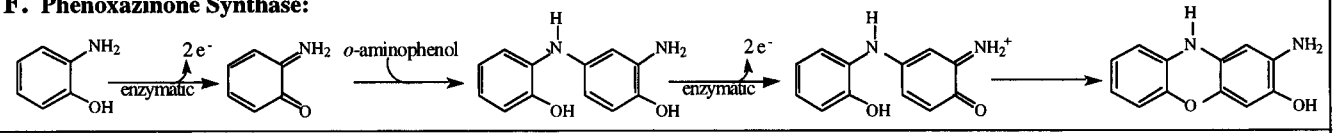

G. Bilirubin Oxidase:

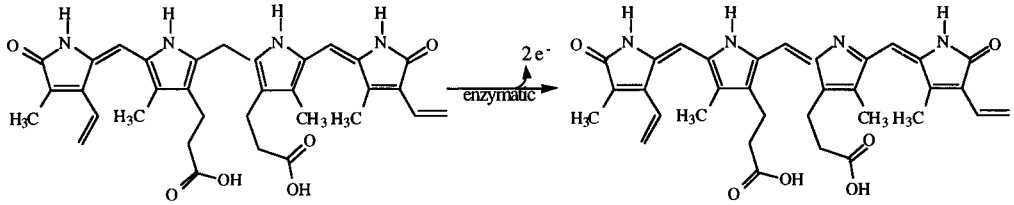

H. Sulochrin Oxidase (R = H):

Dihydrogeodin Oxidase (R = Cl):

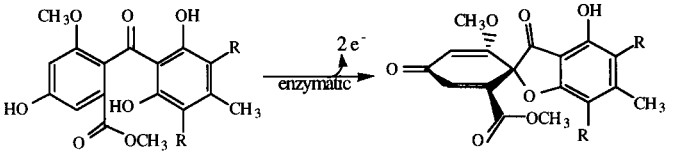

generally to a lesser extent (10−25%). The metal stoichiometry is, for all well-characterized enzymes, one T1 copper and a T2/T3 trinuclear cluster.

Lc is thought to be nearly ubiquitous among fungi. Most, but not all, are extracellular, and a given species may produce isozymes of both extra- and intracellular types. There are essentially three possible functions which have been ascribed to fungal Lcs: (1) pigment formation, (2) lignin degradation, and (3) detoxification. Pigment formation is the most-well established role for certain fungal Lcs. Lc-deficient mutants of *Aspergillus nidulans* produce yellow spores, instead of the wild-type green spores, unless partially purified Lc is added to the growth medium,[255] and pigmentation mutants of other fungi have been identified which produce atypical amounts of Lc isozymes[256] or no Lc.[257] The best evidence in support of a role in lignin degradation is that a Lc-deficient mutant of the white-rot fungus *Sporotrichum pulverulentum* is unable to degrade lignin, while Lc-plus revertants, or Lc-minus mutants for which purified Lc was added to the growth medium, are able to.[258] However, a putative role for Lc in lignin degradation is not unambiguous; peroxidase also plays a role, and some fungi apparently produce no Lc and yet are able to degrade lignin. Furthermore, although Lc can catalyze degradation of high-molecular weight lignin models *in vitro*, lower molecular weight compounds are repolymerized.[259] Dimer models can be cleaved[260,261] or oligomerized,[262] depending upon the compound. This problem can be overcome by pairing Lc with a mediator[263] or another lignolytic enzyme.[264−266] On this basis, it has been suggested that, *in vivo*, several different enzymes, including Lc, operate synergistically to degrade lignin. It has also been proposed that Lc is excreted by some fungi in order to remove potentially toxic phenols produced during lignin degradation and that Lc-deficient mutants might lack lignin-degradation ability because they were unable to remove these toxins, rather than because they could not catalyze lignin degradation.[240] Lc might also be excreted by fungi to detoxify phenols produced by other organisms.[267−269]

Like the plant Lcs, fungal Lcs have little substrate specificity. The physiological substrates of the fungal Lcs depend upon its role: in the case of Lc-catalyzed pigment formation, two fungal pigment precursors have been identified: 1,8-dihydroxynaphthalene[257] and parasperone A,[270] while in the case of lignin degradation and detoxification, these are necessarily highly variable and not well-defined. The *in vitro* reaction of lignin model compounds with fungal Lcs can lead to either degradation or oligomerization, depending upon the substrate. Both positions ortho to the phenol OH group must be blocked in order for degradation to predominate. For example, using syringylglycol-β-guaiacyl ether as the substrate, the cleavage products guaiacoxyacetaldehye, guaiacoxyacetic acid, and 2,6-dimethyl-*p*-benzoquinone were obtained (see Table 5C).[260] Dilignols with Hs ortho to the OH yield coupling products; no degradation is observed.[262] The proposed mechanism involves the radical coupling of two dilignol semiquinones, followed by cleavage of the benzyl-ring C−C bond. Dilignol semiquinone radical coupling, followed by loss of syringylglycol-β-guaiacyl ether, nucleophilic attack by water on the ring, and further oxidation, leads to the formation of 2,6-dimethyl-*p*-benzoquinone.

3. Ascorbate Oxidase

Well-characterized preparations of ascorbate oxidase (AO) (L-ascorbate:dioxygen oxidoreductase, EC 1.10.3.3) have been obtained from green zucchini squash (*Cucurbita pepo medullosa*), cucumber (*Cucumbis sativus*), and the bacterium *Acremonium* sp. HI-25. Their properties are listed in Table 4. The plant AOs are homodimers,[175] with each subunit containing one T1 copper and one T2/T3 trinuclear cluster. The carbohydrate content of *C. pepo medullosa* AO is 2.4%. *Acremonium* sp. HI-25 AO is a monomer with significantly greater degree of glycosolation (11.2%) and with the usual copper stoichiometry of one T1 site and a trinuclear cluster. Several AOs have been sequenced, including *C. pepo medullosa*. AO is one of two multicopper oxidases which has been crystallographically characterized (*vide infra*).[7]

AO is wide-spread among plants (for a review, see ref 271) and is also found in eubacteria[181,272] and possibly fungi.[273] Although AO has been known for decades, its function in plants has remained obscure. It is known to catalyze the oxidation of ascorbate to dehydroascorbate via the disproportionation of the semidehydroascorbate radical (Table 5D); however, the physiological role of this process is unclear. Most of the AO present in cells is associated with the cell wall,[274−279] and AO activity has been shown to be strongly correlated to the rate of plant growth via cell elongation.[274,275,278,280,281] Auxin (plant growth hormone) greatly stimulates *in vivo* oxidase activity[275] by induction of AO expression.[281] Auxin-induced cell enlargement can be inhibited by phenylthiourea, an AO inhibitor. Based on this, AO has been proposed to allow for cell expansion either by the reaction of dehydroascorbate with cell wall components to effect cell wall loosening[280] or by suppressing lignin formation.[282]

4. Ceruloplasmin

The most complex of the multicopper oxidases is ceruloplasmin (Cp) (ferroxidase, iron(II):dioxygen oxidoreductase, EC 1.16.3.1). Purified and well-characterized protein has been obtained from several sources, including human (see Table 4). All are monomers with a significant amount of glycosolation (9−14%). Human Cp has two forms, I and II, that differ only in their carbohydrate content and can be separated by hydroxyapatite chromatography.[283] The carbohydrate portion of human Cp has been sequenced and characterized,[284] as has the human Cp cDNA[186] and the protein itself.[185] Human Cp was recently crystallographically characterized at a resolution of 3.1 Å.[24] For a comprehensive review of much of the early literature on Cp, see ref 285.

Despite the large body of work that has been done on this protein, some of the basic properties remain to be defined. Ryden and Björk first proposed that human Cp contains six coppers per molecule, with an additional labile copper-binding site that does not

alter the oxidase activity.[182] Of these, two coppers are T1 sites with different EPR parameters,[189] reoxidation rates,[286,287] and reduction potentials.[188] Three of them correspond to the standard T2/T3 trinuclear cluster. The percent of copper that is paramagnetic by EPR[188,288,289] or magnetic susceptibility[290] is 40−50%. The identity of the sixth copper is unclear. Ortel *et al.*[291] and later Messerschimdt and Huber[224] examined the sequence homology among the various multicopper oxidases and plastocyanin and noted that there were three T1 sites, one with leucine in place of methionine, analogous to the high-potential T1 site of the fungal Lcs. The crystal structure shows six coppers: a trinuclear cluster and three coppers bound to the three T1-binding sites. Preliminary XAS data indicate that one of the T1 coppers stays permanently reduced.[292] Thus, the spectroscopic and crystallographic data on human Cp is consistent with the proposed stoichiometry of six coppers per molecule. Spectroscopic data on the other mammalian Cps also are also consistent with this copper stoichiometry.

Calabrese and co-workers have recently obtained and characterized Cp from two nonmammalian sources, chicken and turtle, that appear to contain only five coppers per molecule and still retain full activity.[191,192] EPR and absorption spectra show evidence for two different T1 coppers, but only 50% of the copper is EPR-detectable, and the spectrum shows no evidence for a T2 copper. This would imply a fifth copper that is only 50% EPR-detectable, the spectroscopic features of which are buried amid those of the T1 coppers. Calabrese *et al.* have ascribed this to a magnetically interacting T2/T3 trinuclear cluster; further work is needed to clarify this.

Cp appears to be ubiquitous among all vertebrates. Its function is not entirely resolved. Although Cp is capable of oxidizing aromatic diamines and other activated aromatics, its amine oxidase activity is far lower than that of *R. vernicifera* Lc,[226] and there is no direct biological evidence for a role in oxidation of organics. Both the biological and the kinetic data indicate that the physiologically relevant substrate of Cp is Fe(II) (Table 5E). Animals fed a diet high in iron but deficient in copper develop anemia,[293,294] which can be reversed by the intravenous administration of Cp but not $CuSO_4$.[294,295] Radiolabeled Fe(II) is cleared from the plasma far more slowly in copper-deficient than in normal pigs.[294] Perfusion of iron-loaded liver from copper-deficient pigs by Cp causes a rapid release of iron, while $CuSO_4$ and various other plasma constituents have no effect.[296] Extensive *in vitro* studies have demonstrated that Cp can efficiently catalyze the oxidation of Fe(II) to Fe(III), under close to physiological conditions.[231−234,297−299] Other serum components do not have such ability, and addition of azide, a Cp inhibitor,[300−302] eliminates the ability of serum to oxidize Fe(II) above the baseline nonenzymatic level.[298,299] Analysis of the kinetics of Cp ferroxidase activity demonstrates a high-affinity Fe(II)-binding site (K < 10 μM),[232−235] and equilibrium dialysis studies indicate that there are multiple binding sites for divalent metal ions (the average K_a for Fe(II) is 1.1×10^5 M^{-1}).[303] Lindley and co-workers have identified a pocket in the center of one side of the protein with a high concentration of aspartate, glutamate, and histidine residues which is within 10 Å of the T1 sites and could be a putative binding site for cations[24] (see also ref 304).

Oxidation of Fe(II) is important because iron enters the bloodstream from liver stores and the intestine as Fe(II), whereas it binds to transferrin as Fe(III), after which some eventually returns to blood as hemoglobin. Although Fe(II) is rapidly air-oxidized, plasma is actually a reducing environment. The partial pressure of O_2 is 80−100 Torr in arterial blood, but only about 1.5% is not bound to hemoglobin,[305] and plasma contains a significant concentration of ascorbate (34−91 μM),[306] which inhibits the nonenzymatic oxidation of Fe(II) but not the enzymatic oxidation.[231] Osaki *et al.* showed that while the nonenzymatic rate of Fe(II) oxidation under physiological conditions was insufficient to account for the observed rate of iron turnover in the body; the enzymatic rate was sufficient.[231] These data, combined with the biological results indicating that Cp plays a key role in iron metabolism, provide convincing evidence that the main role of Cp is oxidation of Fe(II) to facilitate its uptake by transferrin.

Nonetheless, the putative ferroxidase activity of Cp is still controversial. Anemia only occurs when Cp activity is less than 5% of normal,[294] leading some to argue that Cp is not a plasma ferroxidase. In addition, the concentration of Cp increases in response to acute infection or inflammation, a behavior seemingly inconsistent with a role in iron metabolism. This has been explained by the fact that inflammation or infection rapidly triggers removal of Fe−transferrin, a response which is believed to help fight off infection,[307] followed by an increase in the synthesis and plasma activity levels of transferrin and Cp, thus leading to a recovery of the normal Fe−transferrin level.[308,309] Recently, Gutteridge has shown that Cp can inhibit Fenton chemistry-induced oxidative damage to deoxyribose, lipids, and DNA.[310−316] This may also contribute to the role of Cp in inflammation, since inflammation increases the oxidative stress to surrounding tissues. By rapidly clearing both Fe(II) and O_2 from plasma without the production of the reactive oxygen species generated by the nonenzymatic oxidation of Fe(II), Cp protects cellular components from Fe(II)-catalyzed oxidative damage. This may explain the observed large excess of ferroxidase activity present in normal plasma.

Although the ferroxidase activity appears to be the primary function of Cp, there is strong evidence that a secondary function may be copper transport. Intravenously injected radiolabeled copper is first rapidly cleared from the plasma, then appears back in the plasma bound to Cp. Only after its concentration in plasma again decreases is there a slow, steady increase in the amount of radiolabeled copper in other organs.[317] Later studies confirmed that Cp, rather than labile copper in plasma, is the source for the copper bound to cytochrome *c* oxidase and CuZn−SOD in cells.[318−320] More recently, there have been a number of reports on the identification and partial characterization of specific Cp receptors from a number of different cell types.[321−326]

5. Other Putative Multicopper Oxidases

Recently, several possible new additions to the family of multicopper oxidases have been made (Table 4). One of these is phenoxazinone synthase (PHS). It has been purified from the bacterium *Streptomyces antibioticus* and identified in other strains of *Streptomyces*.[199,327,328] It exists predominantly as the hexamer and dimer of an 88 kDa polypeptide, as well as possibly other oligomers.[199,200] Its carbohydrate content is unknown, although the molecular weight as calculated from the sequence is only 70 kDa.[202] As isolated, it contains 0.8 coppers per molecule, but it can be reconstituted with a total of 4−5 coppers per molecule for full activity. It exhibits spectroscopic features indicative of one T1 site per monomer (absorption band at 598 nm, $\epsilon = 4000\ M^{-1}\ cm^{-1}$, EPR parameters of $g_{\|} = 2.24$ and $A_{\|} = 67 \times 10^{-4}\ cm^{-1}$).[201] Freeman *et al.* report that PHS lacks a T3 site, on the basis of the lack of a 330 nm band and that all of the copper is paramagnetic by EPR quantitation, and assign the remaining 3−4 coppers as T2 coppers. Anaerobic reduction of the enzyme with substrate results in a complete loss of T1 copper EPR features, but only a 50% reduction of the intensity of the $m_I = -^3/_2$ $A_{\|}$ T2 copper line, implying that only three coppers are reduced by substrate. If, however, two of the five coppers are indeed a T3 pair, then PHS would contain one T1 site and a T2/T3 trinuclear cluster, with the fifth copper being adventitiously bound and not involved in the activity. The sequence of PHS shows the same conserved copper binding domains present in all multicopper oxidases, including an axial T1 methionine (see Figure 13).[202] PHS catalyzes the oxidative condensation of 2 molecules of 4-methyl-3-hydroxyanthranilic acid to actinocin, the phenoxazinone chromophore of the drug actinomycin. It is also capable of catalyzing the oxidative condensation of other *o*-aminophenols as well as oxidation of *o*-diphenols and *p*-aminophenols, but at a lesser rate.[200,327−330] A mechanism for the reaction has been proposed (Table 5F) based upon trapping the reaction at various stages with substituted *o*-aminophenols.[200,329] According to this mechanism, the *o*-aminophenol is oxidized by two electrons to the quinone imine, which then conjugates to another molecule of *o*-aminophenol while still bound to the enzyme. This product is further oxidized by two electrons to give the *p*-quinonimine. The last two steps of the reaction, another conjugation to generate the tricyclic structure and another two-electron oxidation, are thought to be nonenzymatic.

Bilirubin oxidase (BO) (bilirubin:dioxygen oxidoreductase, EC 1.3.3.5) has been purified and characterized from two species of fungi: *Myrothecium verrucaria* and *Trachyderma tsudondae*. These enzymes both have a molecular weight of 64 kDa and are known to contain copper.[203−205,207] The former is also known to contain carbohydrate. Both exhibit the multicopper oxidase spectroscopic features of absorption bands at ∼600 and 330 nm. *M. verrucaria* BO was found to have two coppers per molecule,[205] but this is inconsistent with the spectroscopic and sequence data. *T. tsudondae* BO has four coppers per molecule, and the EPR spectrum shows both T1 and T2 coppers, with 50% of the total copper paramagnetic by EPR.[207] The sequence shows the usual consensus copper binding domains, including the axial methionine (see Figure 13).[206] Thus, it seems likely that the copper stoichiometry of BO is one T1 copper and a trinuclear cluster. BO oxidizes bilirubin as well as other tetrapyrroles (Table 5G), unlike Lc, but can also oxidize diphenols and aryl diamines.[204]

Sulochrin oxidase (SO) (sulochrin:O_2 oxidoreductase, EC 2.10.3.8) and dihydrogeodin oxidase (DHGO) are fungal enzymes involved in the synthesis of natural products called grisans. SO has been purified and characterized from *Penicillium frequentans* and *Oospora sulphurea-ochracea*.[208] DHGO has been purified and characterized from *Aspergillus terreus*.[209] They are homodimers with molecular weights of 128−157 kDa (see Table 4). The experimentally determined copper content is ∼6 for SO and 16 for DHGO, but the copper stoichiometry from spectroscopy and sequence data is 1 T1 copper and a trinuclear cluster per subunit. *P. frequentans* SO has an absorption band at 605 nm. The absorption spectrum of DHGO shows bands at 600 and 330 nm, indicative of T1 and T3 coppers, while the EPR spectrum shows the features of T1 and T2 coppers. The recently published sequence of DHGO shows the usual consensus multicopper oxidase copper binding domains, with a methionine T1 axial ligand (see Figure 13).[210] All are presumably glycoproteins, although the carbohydrate content of only the *P. frequentans* SO has been determined (19%). *P. frequentans* and *O. sulphurea-ochracea* SO catalyze the intramolecular stereoselective two-electron oxidative coupling of sulochrin to (+)- and (−)-bisdechlorogeodin, respectively, and DHGO catalyzes the formation of (+)-geodin (see Table 5H). SO is also capable of oxidizing a variety of substrates, including diphenols, aryl diamines, and ascorbate, but it binds sulochrin with a very high specificity.

FET3 is an extracellular membrane-bound protein found in *Saccharomyces cerevisae*.[211,212] Although its purification has not been reported, the amino acid sequence is known, and it possesses a high degree of homology with the other well-known multicopper oxidases, particularly in the copper-binding regions (see Figure 13). Like the fungal Lcs and one of the subdomains of human Cp, the residue 10 residues downstream of the conserved T1 cysteine is a leucine. Furthermore, it is known to possess copper-dependent ferroxidase activity (Table 5E). Copper depletion of *Saccharomyces cerevisea* results in the reversible reduction of Fe(II) transport activity, indicating that FET3 is a copper enzyme. Thus there is strong reason to believe that FET3 is a multicopper oxidase. FET3 functions in the high-affinity Fe(II) transport system in yeast. First, Fe(III) is reduced to Fe(II) by a plasma membrane ferrireductase, after which it is transported inside the cell by a high-affinity Fe(II) transport system.[304,331−333] Although the role of FET3 in this process is not yet known, Askwith *et al.* have proposed that FET3 may serve to reoxidize Fe(II) in order to release it from the Fe(II) transporter into the cytosol.[211]

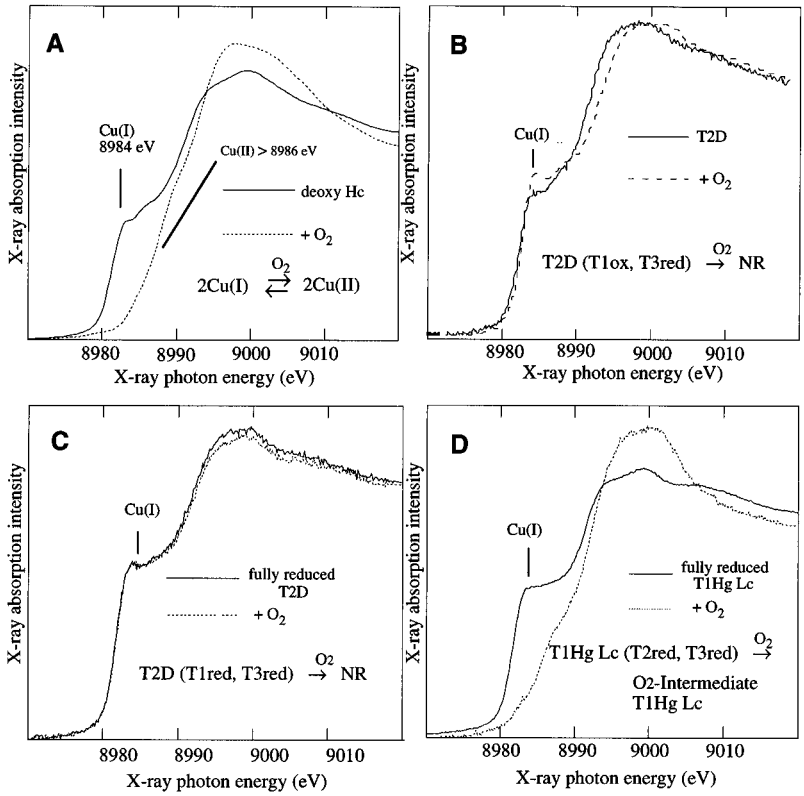

Figure 16. X-ray absorption spectra of Cu K-edges of Hc and Lc derivatives. Reaction of O_2 with (A) deoxyhemocyanin, (B) T2D Lc (T1 oxidized, T3 reduced), (C) reduced T2D Lc (T1 and T3 reduced), and (D) reduced T1Hg Lc (T2 and T3 reduced).

B. The Trinuclear Copper Cluster Site

1. Copper Centers Required for O_2 Reduction: Comparison to Hemocyanin and Tyrosinase

Laccase is the simplest of the multicopper oxidases, with one of each type of copper center for a total stoichiometry of four coppers. However, this is still a complex system which has been simplified through the study of a series of metal site derivatives. The type 2 depleted (T2D) derivative of laccase has the type 2 reversibly removed[334] while the type 1 mercury-substituted derivative (T1Hg) has the type 1 replaced by a spectroscopically innocent and redox-inactive mercuric ion.[335−337] Studies of these derivatives have demonstrated that the type 3 center is fundamentally different from the coupled binuclear copper site in hemocyanin and tyrosinase and have defined the copper centers required for the reduction of dioxygen. This is demonstrated by X-ray absorption spectroscopic studies at the copper K-edge.[28]

As illustrated for hemocyanin in Figure 16A, reduced copper has a characteristic XAS spectroscopic feature at 8984 eV which is not present for oxidized copper centers[28] (*vide supra*). Deoxyhemocyanin has two Cu(I)s which are oxidized to a binuclear cupric site upon binding O_2 to form oxyhemocyanin. The binuclear cupric site has no 8984 eV XAS feature. T2D laccase which has a reduced type 3 and an oxidized type 1 center also exhibits an 8984 eV feature associated with the reduced type 3 center (Figure 16B). However, exposure to dioxygen does not change this feature, indicating that, in contrast to hemocyanin, the reduced type 3 site in T2D laccase does not react with O_2.[28,338]

In a next set of experiments, the fully reduced T2D derivative of laccase (both the type 1 and type 3 centers are reduced) was reacted with O_2. This was an important experiment since many of the mechanistic considerations in the literature[339] have proposed that this combination of a reduced type 1 and reduced type 3 copper center was the structural unit required for O_2 reduction. It was believed that an oxygen intermediate could be formed in T2D Lc by reduction with ascorbate followed by oxygenation.[339] In this study, the T2D protein was incubated overnight with excess reductant, which could result in the migration of some reduced Cu to the type 2 center, generating native laccase (reduced) which would then react with dioxygen to form the native oxygen intermediate (*vide infra*). From Figure 16C, fully reduced T2D laccase clearly does not react with O_2 since it shows no change in the 8984 eV peak associated with Cu(I) over a time period of several hours, thus indicating that this combination of copper centers does not reduce O_2.[23]

Finally, the fully reduced T1Hg derivative was investigated with respect to its reactivity with dioxygen. From Figure 16D, the reduced site rapidly reacts with O_2 (i.e. the 8984 eV feature is eliminated).[23] This generates an oxygen intermediate which is discussed in section III.C.1. Importantly, these results demonstrate that the type 2 + type 3 centers are the minimum structural unit required for O_2 reduction. These results, combined with our MCD studies[6] on laccase, first demonstrated that the type 2 + type 3 copper centers form a trinuclear copper cluster site. This is strongly supported by the results of protein crystallography on ascorbate oxidase.[340]

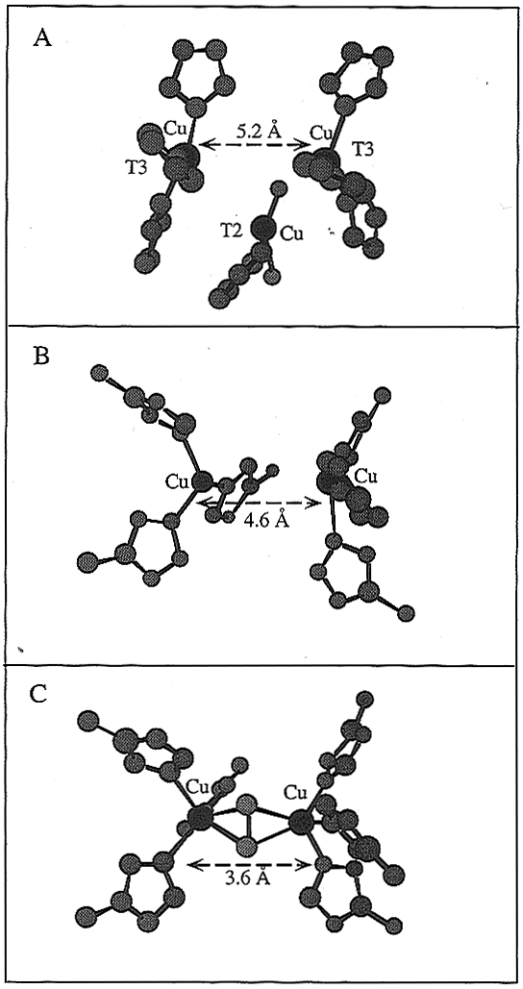

Figure 17. Crystal structures of (A) reduced AO,[38] (B) reduced Hc[341] (*Limulus polyphemus*), and (C) oxidized Hc.[342] The structures were generated using crystallographic coordinates.[7a] The accession numbers are 1ASO, 1LLA, and 1OXY, respectively.

2. Geometric and Electronic Structure of the Trinuclear Copper Cluster Site

The crystal structure of the reduced trinuclear copper cluster in ascorbate oxidase at 2.3 Å resolution is given in Figure 17A[341] and compared to the crystal structure at 2.18 Å resolution of the active site of deoxy hemocyanin from *Limulus polyphemus* in Figure 17B.[342] The two T3 Cu(I)s in both enzymes have three His in a trigonal planar geometry. The site in AO has the additional type 2 Cu of the trinuclear cluster, which is a three-coordinate T-shaped cuprous center with two His and one water ligand. Also there are several significant structural differences between the reduced type 3 center in ascorbate oxidase and the binuclear cuprous site in deoxyhemocyanin which should contribute to their differences in reactivity with O_2, i.e., the reduced type 3 site in the absence of the type 2 center does not react with O_2 (*vide supra*). The distance between the coppers in the type 3 center has increased from 4.6 Å in hemocyanin to 5.2 Å in ascorbate oxidase, and the His ligands of the type 3 are arranged in an eclipsed rather than the staggered configuration of hemocyanin. Calculations indicate that the staggered and eclipsed configurations are isoenergetic for a μ-η^2:η^2 bridging peroxide, when the Cu(II)s are in a square pyramidal geometry.[343] However, if the hydroxide bridge of the oxidized type 3 center in ascorbate oxidase (*vide infra*) is replaced by the μ-η^2:η^2 bridging peroxide of oxyhemocyanin, the geometry of both oxidized type 3 coppers would be close to trigonal bipyramidal and require a significant rearrangement of one of the axial histidine ligands to the equatorial position to achieve the square pyramidal structure of the oxyhemocyanin active site in Figure 17C.

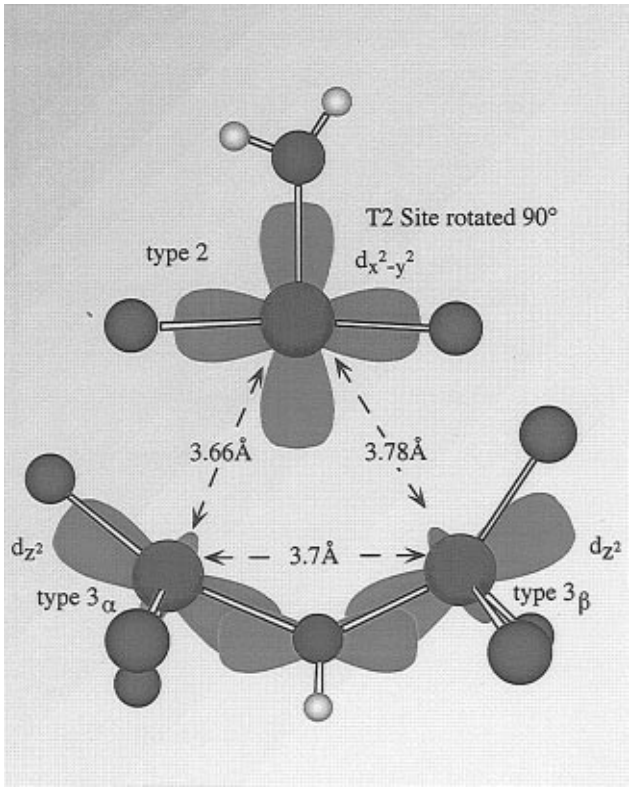

Figure 18. Geometric and electronic structure of the trinuclear copper cluster site. Oxidized trinuclear Copper cluster in AO,[7] generated using crystallographic coordinates[7a] (accession no. 1AOZ) with the half-occupied d orbitals of the ground state, obtained by ligand field calculations,[349] superimposed at each copper center. Note that the T2 copper center is rotated by 90° for clarity.

The crystal structure of the oxidized trinuclear site, shown in Figure 18,[7] is very much as predicted from spectroscopy[6] in that the two type 3 copper(II)s now have a hydroxide bridge responsible for antiferromagnetic coupling, the type 2 copper is unbridged but within 4 Å of both type 3 centers, and all three cupric centers have open coordination positions (*vide infra*). It is, however, surprising that the type 2 copper(II) is only three-coordinate as this geometry is not presently known in copper(II) coordination chemistry; also S-band EPR studies by McMillin and co-workers[344] suggested that three nitrogens were coordinated at the type 2 site, as well as a water-based ligand[345] with a pK_a of 6−7.[346]

The electronic spectroscopic features of the T1Hg derivative, which are not obscured by the dominant features of the type 1 center present in the native enzyme, enable one to define the ligand field at each copper center.[347] The LTMCD spectrum of T1Hg derivative directly probes the spectroscopic features of the paramagnetic, type 2 copper center. Its d → d

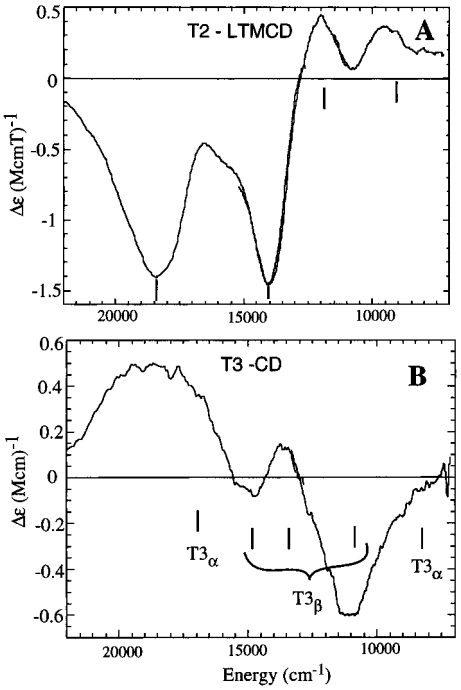

Figure 19. Spectroscopic features of the trinuclear Cu site in Lc: (A) LT MCD and (B) RT CD of oxidized T1Hg Lc. LT MCD gives T2 features and CD gives T3 d → d transitions (see the text). In both spectra, positions of the transitions are indicated; also, in the CD spectrum, the transitions are assigned to each of the two T3 coppers.

transitions are shown in Figure 19A. The type 3 coppers have more distorted geometric structures and, as a result, make the dominant contributions to the intensity in the absorption spectrum of T1Hg laccase.[22,346] Since CD intensity is proportional to the absorption intensity, the type 3 copper(II) d → d transitions also dominate the CD spectrum, wherein they are resolved. (This is demonstrated by the fact that the reduction of only the type 2 center in T1Hg laccase does not affect the CD features.[347]) Ligand-binding perturbations enable these d → d transitions to be distributed between the two type 3 coppers, which are inequivalent and are designated $T3_\alpha$ and $T3_\beta$.[347] These d → d transitions can be fit to a simple ligand field model (Companion−Komarynsky[348]) to obtain an initial description of their electronic structure[349] (superimposed in Figure 18). The type 2 copper has a $d_{x^2-y^2}$ ground state with a ligand field best described as square planar with a vacant equatorial position oriented toward the type 3 coppers. While both type 3 coppers have been described as tetrahedral,[7] their ligand fields are actually best described as trigonal bipyramidal with an open equatorial position on each copper oriented toward the type 2 center. This derives from the fact that the His N−Cu−OH angle of each type 3 center is much closer to linear than tetrahedral (~150°) and results in a d_{z^2} ground state oriented along this N−Cu−OH axial direction of the trigonal bipyramidal structure. This provides a very good superexchange pathway for antiferromagnetic coupling of the two type 3 Cu(II)s through the hydroxide bridge, as is experimentally observed ($-2J > 400$ cm^{-1} for the exchange spin-Hamiltonian, $H = -2JS_1 \cdot S_2$).[347]

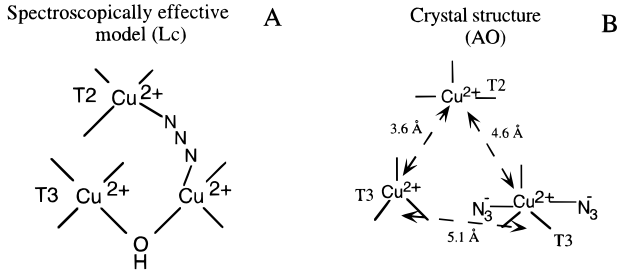

Figure 20. Azide binding to the trinuclear Cu cluster: (A) spectroscopically effective model from azide binding studies on Lc (from ref 6) and (B) crystal structure of azide-bound AO.[341] Generated using crystallographic coordinates[7a] (accession no. 1ASQ).

3. Exogenous Ligand Binding to the Trinuclear Copper Cluster Site

The fact that all three copper(II)s of the trinuclear copper cluster have open coordination positions oriented into the cluster relates well to our early MCD studies of azide binding.[6] These indicated that this exogenous ligand bridges between one type 3 and the type 2 copper center (Figure 20A), with the type 3 copper pair still antiferromagnetically coupled through the hydroxide bridge. However, the recent crystal structure of azide bound to the trinuclear copper cluster in ascorbate oxidase shown in Figure 20B[341] requires consideration. It shows two azides bound to one of the type 3 coppers, the hydroxide bridge is lost, and all coppers are unbridged at Cu−Cu distances between 3.6 and 5.2 Å. This large structural difference in azide derivatives is important to understand since it is relevant to possible structures of oxygen intermediates in the reaction mechanism (*vide infra*).

Indeed, when azide is added to the trinuclear copper cluster site in laccase, a new broad EPR signal is observed at liquid helium temperature,[5,347] shown in Figure 21A. This signal suggests more than one paramagnetic Cu(II) spin−spin dipolar interacting at a distance of ~4.5 Å, which would be consistent with the structure in Figure 20B. However, when the signal is quantitated under appropriate spectroscopic conditions, it corresponds to less than 10% of the azide-bound sites for laccase at a pH of 6.[22] Since broad EPR signals can be difficult to detect and quantitate, azide binding to laccase has also been probed by SQUID magnetic susceptibility (Figure 21B) studies to determine the total paramagnetism present.[350] The T1Hg derivative exhibits a slope in its Curie plot which quantitates to one $S = {}^1/_2$, corresponding to the type 2 copper(II). Addition of azide slightly increases the paramagnetic contribution, by an amount corresponding to ~10% of what would be observed if all the type 3 copper centers became paramagnetic, i.e. lost their bridging hydroxide ligand (fully uncoupled T3 line in Figure 21B). The pH and azide concentration dependence of the dipolar EPR signal in Figure 21A shows that this increases as the pH is lowered (Figure 21C). Under optimal uncoupling conditions (i.e., pH of 4.6), the signal still corresponds to only 13(±7)% of the type 3 sites.[22] Thus azide binding to the type 3 center increases the electron density on the bound copper, which lowers its inductive effect on the bridging

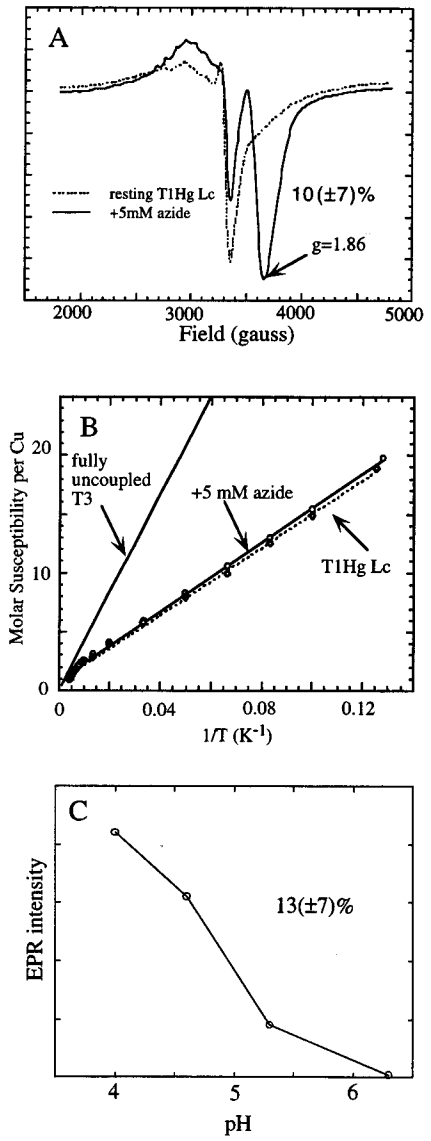

Figure 21. Spectroscopy on azide binding to Lc. (A) He EPR signal of azide bound to T1Hg Lc (resting T1Hg Lc included for reference) and (B) SQUID magnetic susceptibility studies on azide bound to T1Hg Lc (resting T1Hg Lc included for reference; also included is the theoretical slope if the T3 sites were 100% uncoupled); (C) pH dependence of the $g = 1.86$ He EPR signal of azide bound to T2D Lc.

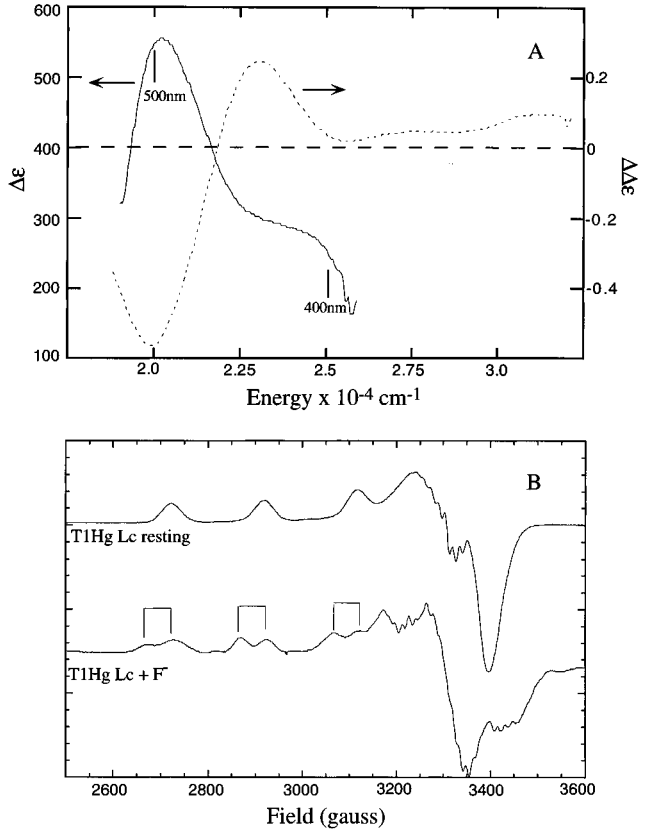

Figure 22. Ligand binding at the trinuclear cluster site. (A) high-affinity azide binding: (−) difference absorption at RT and (···) LT MCD. The appropriate *y*-axis scales for the two spectra are indicated by an arrow. (High-affinity azide binding occurs to the fraction (23%) of native Lc molecules with T2 ox, T3 red). (B) Fluoride binding to the fully oxidized trinuclear cluster. 77 K EPR spectrum of resting and fluoride-bound T1Hg Lc. (The F^- superhyperfine splitting is indicated.)

hydroxide and raises its effective pK_a, leading to some protonative uncoupling of the trinuclear copper cluster site below a pH of 7.[22] For laccase under physiological conditions, this corresponds to <10% of the azide-bound trinuclear copper cluster sites, while for crystals of ascorbate oxidase (under the conditions given in ref 341), the percentage of these uncoupled sites is apparently much higher. The pH of maximal activity for laccase is 7.5.[140]

It should also be noted that when the type 3 coppers are reduced and the type 2 center is oxidized, the azide affinity for the site markedly increases (from ~300 to ≥10^4 M^{-1}).[5,6] Azide clearly binds to the type 2 center, since this derivative exhibits azide to Cu(II) charge transfer transitions in the 20 000−25 000 cm^{-1} region which derive from a paramagnetic ground state, since they have corresponding features in LTMCD (Figure 22A, solid and dotted lines). Alternatively, fluoride does not bind to the type 3 reduced, type 2 oxidized derivative but does bind to the type 3 oxidized, type 2 oxidized form with a very high binding constant ($K \sim 10^4$ M^{-1}),[5] which is unusual for fluoride binding to aqueous Cu(II) ($K \sim 10$ M^{-1}). This exogenous ligand also binds to the type 2 Cu(II) center, since fluoride-bound T1Hg laccase exhibits ^{19}F ($I = {}^1/_2$) superhyperfine splitting in the EPR signal of the type 2 copper, while the oxidized type 3 copper remains antiferromagnetically coupled (Figure 22B). Both of the above observations indicate that exogenous ligands can bind to the type 2 center and that the oxidation state of the type 3 center greatly influences this binding. Finally, for the fully oxidized trinuclear copper cluster site, fluoride binding to the type 2 center competes with azide,[5,6] the latter ligand bound as described above. These results emphasize that both the type 2 and coupled type 3 copper(II) centers participate in exogenous ligand binding at the trinuclear copper cluster active site.[347]

A low-temperature annealing procedure for the preparation of ligand bound derivatives has been developed[337,351] wherein incubation of the protein and ligand at low temperatures (ca. −20 °C) promotes adduct formation at lower ligand concentrations. This procedure could be advantageous in adduct preparations where there are solubility or stability limitations. McMillin and co-workers also present evidence for temperature-dependent changes in the exchange

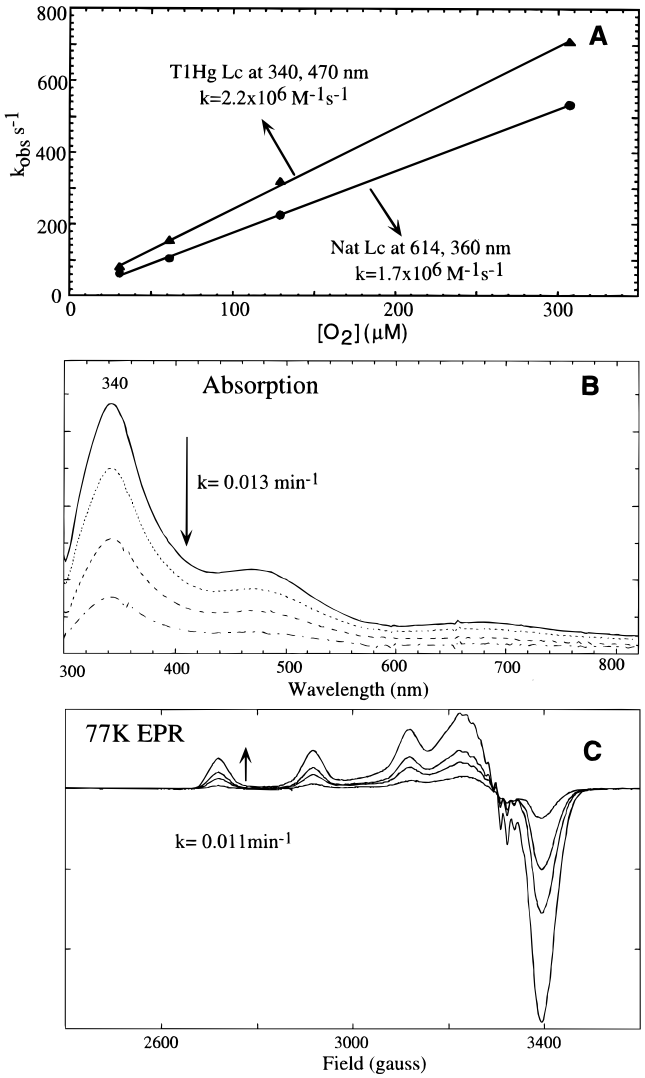

Figure 23. Oxygen intermediate of T1Hg Lc: (A) kinetics of formation, (B) decay of intermediate by absorption, and (C) decay of intermediate by EPR.

coupling within the type2/type3 cluster of Lc,[352] which needs further investigation.

C. Oxygen Intermediates and the Molecular Mechanism of O_2 Reduction to H_2O

1. The Oxygen Intermediate of T1Hg Laccase

When reduced native laccase is reacted with dioxygen, an intermediate is formed with absorption features at 360 and 600 nm,[353] the latter being associated with oxidation of the type 1 copper center (*vide infra*). Reaction of reduced T1Hg laccase with O_2 produces a new oxygen intermediate[23] with the absorption spectrum shown in Figure 23B. The kinetic rate for formation of both intermediates is linearly dependent on O_2 concentration and essentially the same, $\sim 2 \times 10^6\ M^{-1}\ s^{-1}$ (Figure 23A).[354] Since the native intermediate is at least one electron further reduced due to oxidation of the type 1 copper center which is not present in the T1Hg derivative, these results indicate that the T1Hg intermediate can be a precursor of the native intermediate and the rate-determining step in its formation. Thus, the rate of the type 1 to trinuclear copper electron transfer is fast, $>10^3\ s^{-1}$. The T1Hg oxygen intermediate exhibits no EPR signal, but its decay to the EPR signal associated with the oxidized type 2 copper center occurs at the same rate as the disappearance of the absorption feature associated with the intermediate (Figure 23C and B). The rate is slow, particularly at high pH and low temperature (pH 7.4, temperature 4 °C), and this has enabled the stabilization of this intermediate for detailed spectroscopic study as summarized below.[355]

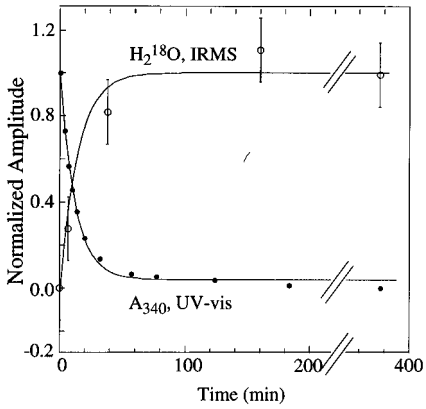

Figure 24. IRMS of the decay of the oxygen intermediate of T1Hg Lc. Also included is the decay of the intermediate under the same conditions monitored by absorption as in Figure 23B.

First, the number of oxygen atoms contained in the T1Hg oxygen intermediate was determined by isotope ratio mass spectrometry (IRMS). The reduced T1Hg derivative was reacted with $^{18}O_2$, and the time dependence of the appearance of ^{18}O isotope label in the solvent H_2O was determined by IRMS. As shown in Figure 24, the kinetics for the appearance of $H_2{}^{18}O$ parallels the decay of the oxygen intermediate as monitored by absorption and EPR. Quantitation of the $H_2{}^{18}O$ in water during the time course of the reaction demonstrates that no oxygen is released on formation of the intermediate, but both oxygen atoms appear upon its decay. Thus the T1Hg oxygen intermediate contains both atoms of oxygen, consistent with a superoxide, peroxide, or perhaps bis-μ-oxo species; however, the latter would require oxidation to the Cu(III) level.

The coppers involved in the reduction of O_2 to form the T1Hg intermediate were monitored by CD and LTMCD spectroscopy in the ligand field region. From Figure 25A, the CD spectrum of the oxidized intermediate is very similar to that of the oxidized trinuclear copper cluster. Since the CD spectrum probes the type 3 coppers (*vide supra*) both appear to be oxidized, with shifts in their energies and intensities associated with coordination of the exogenous oxygen intermediate. Alternatively, the LTMCD spectrum of the T1Hg oxygen intermediate exhibits no signal (Figure 25B). This is consistent with the EPR results and indicates that the type 2 center is reduced in the intermediate. Thus, two electrons appear to have been transferred to dioxygen from the type 3 coppers to generate a peroxide-level intermediate.

Both of the type 3 coppers are oxidized, yet there is no EPR or LTMCD signal associated with the T1Hg intermediate, hence the possibility of its paramagnetism was explored through SQUID magnetic

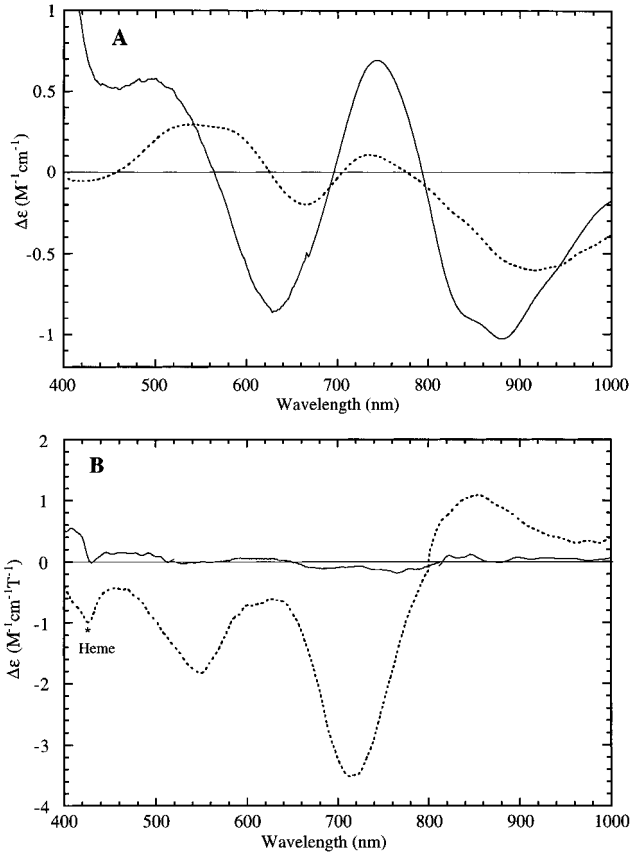

Figure 25. Ligand field spectral features of the oxygen intermediate of T1Hg Lc monitored by (A) RT CD for the T3 centers and (B) LT MCD for the T2 centers. Also included are spectra of resting T1Hg Lc (···) as references.

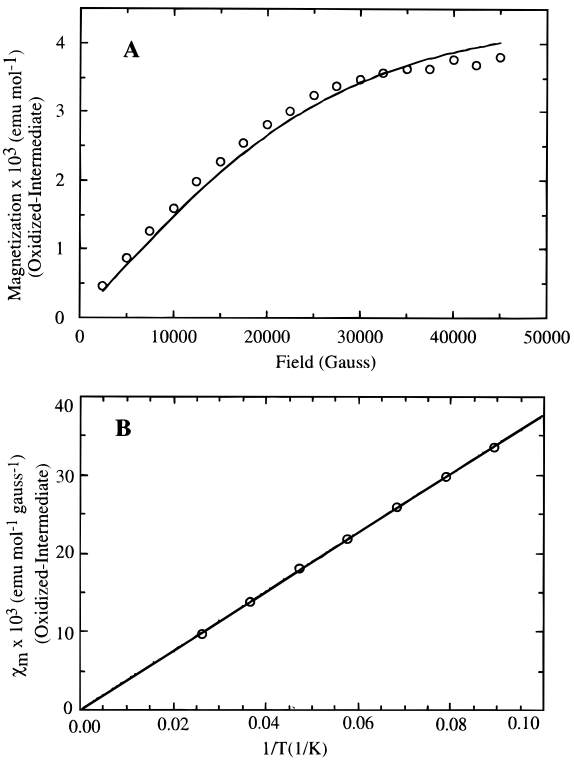

Figure 26. SQUID magnetic susceptibility of the oxygen intermediate of T1Hg Lc: (A) saturation behavior at 2 K and (B) Curie slope from 10 to 100 K at 4 T. Note that the data are plotted as the difference (fully oxidized protein − intermediate) to account for protein diamagnetism and dissolved O_2.

susceptibility studies. Parts A and B of Figure 26 show the saturation magnetization and Curie, $\chi \propto 1/T$, dependence of the T1Hg intermediate, respectively. Note that the data presented are the fully oxidized T1Hg minus the intermediate, where the oxidized form is used as a reference to account for diamagnetism of the protein solution and dissolved dioxygen. From Figure 26A,B, the magnetism is positive, indicating that the oxidized T1Hg derivative is more paramagnetic than the T1Hg oxygen intermediate. Quantitatively, the magnetism accounts for one more paramagnetic copper in oxidized T1Hg laccase than in the oxygen intermediate. Since the oxidized trinuclear copper cluster contains one paramagnetic type 2 Cu(II) center, this indicates that the oxygen intermediate is diamagnetic. Thus, the two type 3 Cu(II)s must be antiferromagnetically coupled, and from the error bars in the data points, the lower limit of this coupling is $-2J > 200$ cm^{-1}. This coupling could be associated with a peroxide bridge, OH^- bridge, or both. Insight into these possibilities could be obtained through XAS spectroscopy.

Figure 27 gives the Fourier transforms of the EXAFS spectra of the reduced and oxidized trinuclear copper cluster sites and that of the T1Hg oxygen intermediate. The key feature to note in these data is that a new strong peak is present at $R \sim 3$ Å only in the oxygen intermediate. When phase-shift corrected, this corresponds to two coppers being tightly bridged at a Cu−Cu distance of 3.4 Å. Since this feature is not present in the oxidized trinuclear copper site, it is not associated with the hydroxide bridge. The distance of 3.4 Å also excludes the possibility of two single atom bridges (i.e., a μ-η^1:η^1 peroxy, μ-hydroxy species). Thus the peroxide appears to bridge two coppers at a distance of 3.4 Å and these can either be the oxidized type 3 pair or the oxidized T3−reduced T2 unit, where we prefer the latter possibility on the basis of exogenous ligand binding and the requirement of the presence of the type 2 center for dioxygen reduction (*vide supra*). The type 3 would then be antiferromagnetically coupled through a hydroxide bridge as in the fully oxidized trinuclear copper cluster site.

Finally, the charge transfer absorption spectrum of the T1Hg oxygen intermediate in Figure 28A provides insight into the nature of the bound peroxide species. It is significantly different from the charge transfer spectrum of oxyhemocyanin and oxytyrosinase[62] (Figure 28B); the intensity is reduced by a factor of 5. Since the charge transfer spectrum reflects both the geometric and electronic structure of the bound peroxide species, this clearly demonstrates that a different structure is involved in the reversible binding and activation of peroxide (i.e., the μ-η^2:η^2 peroxy binuclear cupric structure) as compared to promoting its further reduction to water at the trinuclear copper cluster site. The charge transfer spectrum is also very different from that of the end-on peroxide-bound copper(II) structures of Karlin *et al.*[356,357] in that the charge transfer band of the T1Hg oxygen intermediate is at a much higher energy (340 *vs* ~500 nm, see Figure 29C,D). These features of the T1Hg oxygen intermediate charge transfer spectrum indicate that the peroxide has a

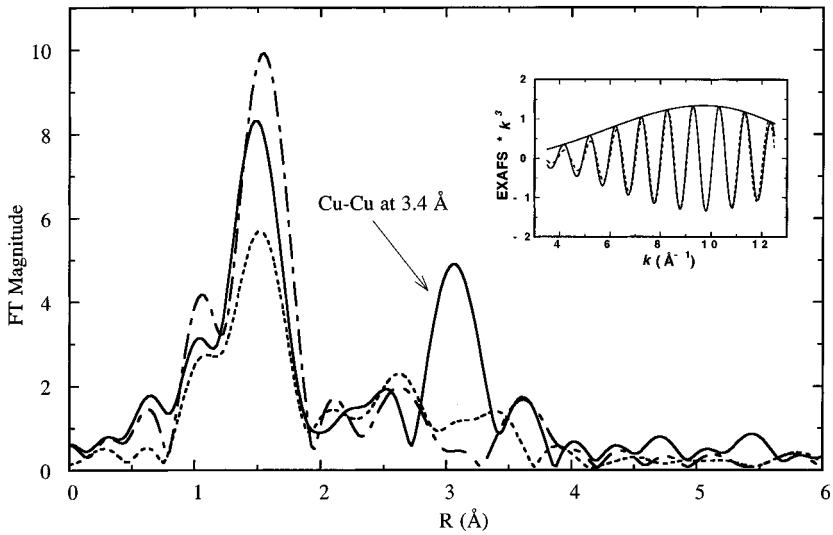

Figure 27. Fourier transforms (FT) of the EXAFS data for the intermediate (−), reduced (- - -), and oxidized (− - −) forms of T1Hg laccase. The FT peak positions are offset to lower R by an atom-dependent phase shift of ~0.4 Å. Inset: Fourier back-transform of the 3.0 Å peak (*R* window of 2.7−3.4 Å) for the T1Hg Lc intermediate (−), and the fit to the data with (···) the *k* dependence of amplitude indicating that it is associated with a Cu−Cu interaction.

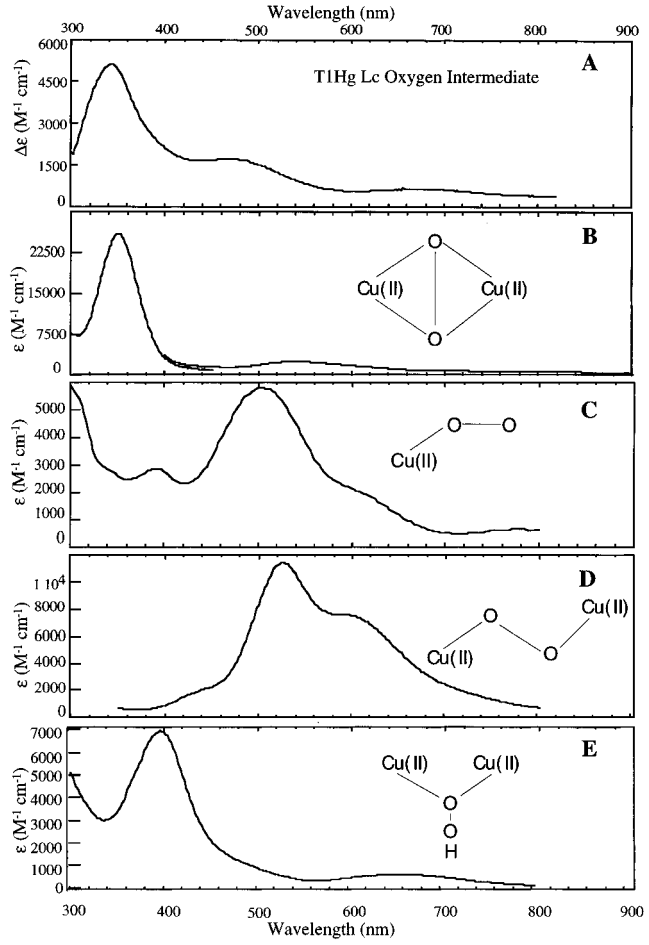

Figure 28. Absorption spectrum of the T1Hg Lc oxygen intermediate compared to spectra of peroxo−Cu(II) model complexes: (A) CT absorption spectrum of T1Hg Lc intermediate[355] and (B−E) spectra of model complexes,[74,356−358] with structural types indicated.

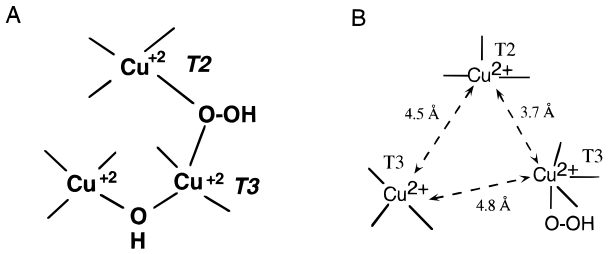

Figure 29. Geometric structure of the T1Hg Lc peroxide adduct. (A) Spectroscopically effective model from peroxide binding studies in Lc[349] and (B) crystal structure of peroxide-bound AO.[341] Generated using crystallographic coordinates[7a] (accession no. 1ASP).

very limited donor interaction with copper(II) but has an additional strong bonding interaction. On the basis of a comparison to data on peroxide−Cu(II) model complexes (for example, Figure 28E[358]), this is reasonably associated with protonation of the peroxide intermediate at the trinuclear copper cluster site.

Support for the peroxide bridging to the type 2 copper is provided by spectroscopic studies on the peroxide adduct of the fully oxidized trinuclear copper cluster site.[349] The EXAFS spectrum of the peroxide adduct shows the same 3.4 Å Cu−Cu interaction as in the intermediate, indicating a similar peroxide bridging structure (Figure 29A). Detailed spectroscopic studies on this adduct[349] support the spectroscopically effective model of hydroperoxide bridging the type 2 and coupled type 3 copper centers proposed for the intermediate Figure 29A. Note that this model differs from the crystal structure of the peroxide adduct of ascorbate oxidase[341] where hydroperoxide binds to one type 3 copper and all bridging interactions are eliminated. It should be emphasized that this structure (Figure 29B) cannot be appropriate for the peroxide adduct or intermediate of laccase since these show no EPR or magnetism associated with the type 3 coppers and exhibit a strong bridging interaction at 3.4 Å in XAS. It is possible that the two structures in Figure 29 are related by a protonative equilibrium as with azide binding (*vide supra*), and this is under investigation.[349]

Some confusion which exists in the literature concerning a "high-affinity" peroxide-bound form of

both native (with a binding constant of $K_B > 10^8$)[359] and T2D Lc ($K_B > 10^4$)[360] should be addressed. The spectroscopic changes observed upon stoichiometric addition of peroxide in both cases were interpreted by these researchers as indicating new peroxide derivatives. However, these spectroscopic changes have been shown by XAS edge studies to be due to oxidation of reduced Cu sites (~23% reduced T3 copper in the native enzyme[28] and ~100% reduced T3 copper in the T2D protein[338]). Alternatively, the low-affinity peroxide adduct of T1Hg Lc discussed above (which is formed on addition of ~200-fold excess H_2O_2) is clearly a peroxide-bound form and is structurally similar to the peroxide-level intermediate of T1Hg Lc.

Insight into possible electronic structure contributions to the reactivity of the hydroperoxide−Cu(II) structure is now becoming available from detailed spectroscopic studies on model complexes.[361] Karlin *et al.*[358] have prepared a series of hydroperoxide and acyl peroxide bridged binuclear cupric complexes. The μ-1,1 hydroperoxide−binuclear cupric complex exhibits an absorption band at 400 nm, $\epsilon \sim 7000$ M^{-1} cm^{-1} (Figure 28E). This band is assigned as a peroxide π^*_σ to Cu(II) charge transfer transition based on the rR profile of an O−O stretch at 892 cm^{-1}.[361] From our past analyses of peroxide−Cu(II) model complexes, charge transfer intensity quantitates the σ donor strength of the peroxide ligand.[77] On the basis of the relatively low charge transfer intensity in Figure 28E, the hydroperoxide model complex has an extremely weak donor interaction with the Cu(II)s despite having two Cu(II)−peroxide interactions. The O−O stretching frequency of 892 cm^{-1} is unusually high compared to other peroxo−copper complexes. A normal coordinate analysis indicates that this 892 cm^{-1} vibration reflects an unusually strong O−O bond in the hydroperoxo−copper complex. These data together with density functional calculations are being used to define the nature of the hydroperoxo−Cu bond and its contributions to reactivity[361] (i.e., promoting further reduction to water in the hydroperoxide versus activation for hydroxylation in the side-on bridged peroxy structure).

2. The Oxygen Intermediate of Native Laccase

Reaction of fully reduced native laccase (i.e. type 1 reduced−type 2 reduced−type 3 reduced) with dioxygen produces a native Lc oxygen intermediate. This species is at least one electron further reduced than the T1Hg Lc oxygen intermediate, since the type 1 copper is also oxidized upon formation of the native intermediate. The native intermediate exhibits an absorption feature at 360 nm,[353] and an unusual EPR signal which is present only below 20K[362] (i.e., fast relaxation) has an unusually low *g*-value centered at 1.94 and broadens when prepared with $^{17}O_2$ (Figure 30).[363] This, combined with the absence of a type 2 EPR signal at liquid nitrogen temperatures, led researchers to assign the native intermediate as an oxyl or hydroxyl radical bound to a Cu(I) site. Studies on the proton uptake indicated that two protons were taken up during formation and two protons released on decay.[364] The intermediate decays to generate the resting enzyme with a rate dependent on temperature and pH. This has also enabled the generation of this intermediate in a glass form suitable for variable-temperature variable-field MCD spectroscopy.[365] As shown in Figure 31A, the native intermediate exhibits two intense MCD fea-

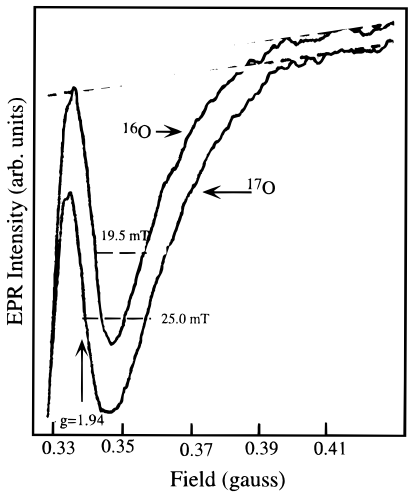

Figure 30. EPR signal of the oxygen intermediate of native Lc. (A) X-band at 16 K which shows broadening of the low *g* value signal with labeled oxygen ($^{17}O_2$, $I_{^{17}O} = 5/2$). (Reprinted with permission from ref 363. Copyright 1976 Academic.)

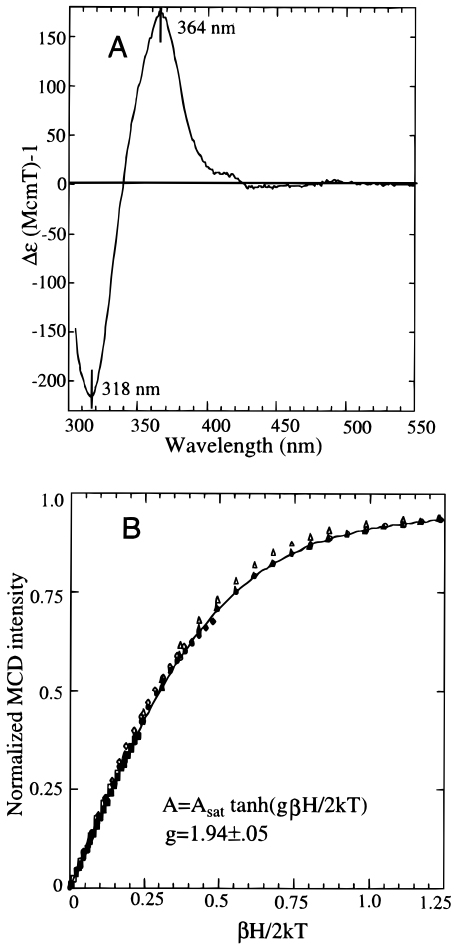

Figure 31. MCD spectra of the native Lc oxygen intermediate. (A) LT MCD in the charge transfer region and (B) saturation magnetization data for the 364 and 318 nm MCD bands. The solid line shows the fit to these data with a $g = 1.94$ ground state.

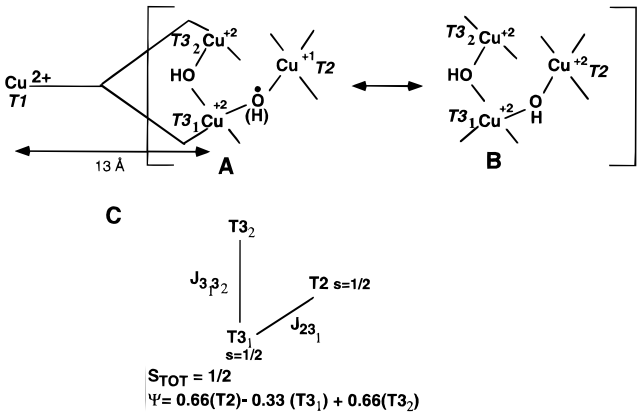

Figure 32. Geometric and electronic structure description of the native Lc oxygen intermediate. A and B are two limiting descriptions of the "native intermediate", B being supported by MCD spectroscopy. (C) exchange (*J*) coupling scheme for the trinuclear Cu cluster relevant for the "native intermediate".

tures at 364 and 318 nm. The saturation magnetization behavior (MCD amplitude as a function of temperature and magnetic field) of these features shown in Figure 31B gives a *g*-value of 1.94, which correlates these excited state features with the ground state feature in the EPR spectrum of the intermediate. Importantly, the high intensity of these LTMCD, C-term features requires that these be associated with a paramagnetic center having a high spin−orbit coupling constant, which is the case for Cu(II) but not for an oxygen-centered radical. Thus, a significant amount of electron density from the reduced type 2 center is, in fact, shifted to the oxygen in the intermediate, indicating that it is best described as a four-electron reduced hydroxide product (with all coppers oxidized) rather than a three-electron reduced oxyl or hydroxyl species (Figure 32B *vs* 32A).[365] The results of the proton uptake study are consistent with this description of the native intermediate, taking into account the proton associated with the formation of the hydroxide bridge (between the type 3 coppers) from solvent water. It should be noted that this putative all-hydroxide bridged trinuclear copper cluster would have a significant exchange coupling between both pairs of coppers (T2−T3, $T3_1$−$T3_2$) and thus an $S_{total} = {}^1/_2$ wave function delocalized over all three copper centers (Figure 32C).[3] This should exhibit a very different EPR signal (i.e., the $g \sim 1.94$ signal in Figure 30) from that of the resting enzyme where the type 2 is not bridged to the coupled type 3 coppers. This will be the subject of further spectroscopic study.

3. Molecular Mechanism for the Four-Electron Reduction of O_2 to H_2O

Spectroscopic studies combined with crystallography have provided significant insight into the mechanism of reduction of dioxygen by the multicopper oxidases (Figure 33).[355] The fully reduced site reacts with O_2 to generate a peroxide-level intermediate, best described as a bridged hydroperoxide species. This is activated for further reduction (as compared to reaction of the peroxide or reversible O_2 binding) to generate the native "intermediate" which is more appropriately described as a hydroxide product (one

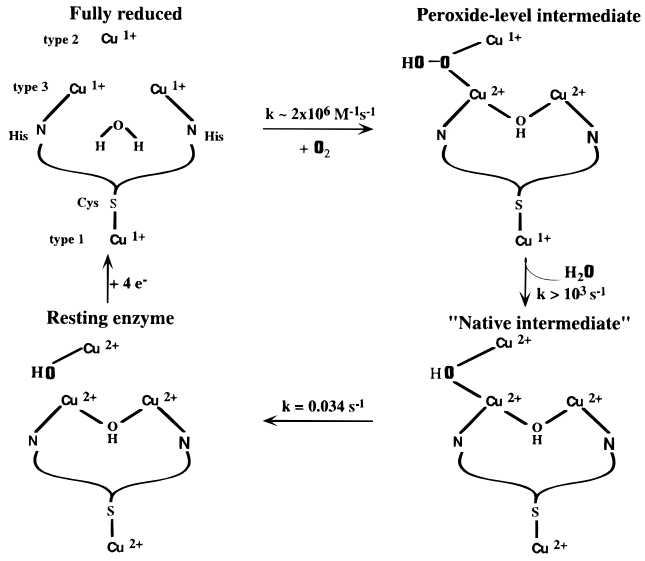

Figure 33. Mechanism proposed for the four-electron reduction of O_2 to H_2O by the multicopper oxidases.

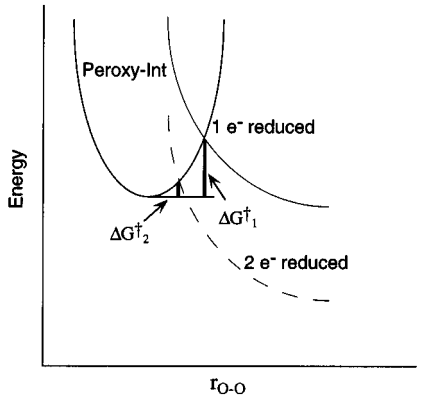

Figure 34. Potential energy diagram for reduction of the peroxide intermediate of laccase. (−) one-electron reduction. (- - -) two-electron reduction. $\Delta G^{\ddagger}_1$ and $\Delta G^{\ddagger}_2$ are the activation energy (Franck−Condon) barriers for one- and two-electron reduction, respectively.

additional electron from the type 1 and another from the type 2) bridging the T2 and one of the T3 coppers in the trinuclear copper cluster. Thus, the reduction of O_2 by the fully reduced enzyme occurs in two, two-electron steps. The first is rate-determining [not to be confused with the rate-determining step for the overall catalytic cycle, which is substrate oxidation (*vide supra*)] and the second is fast. It is important to recognize that there is a large Franck−Condon barrier to reduction of peroxide associated with O−O bond rupture (Figure 34) (particularly for the hydroperoxide which has a strong O−O bond, *vide supra*). The large thermodynamic driving force associated with the two-electron rather than one-electron reduction is required to overcome this barrier for a high electron transfer rate, as is observed in the native enzyme.

Finally, this form is reduced for further turnover or relaxes to the resting state. From kinetics results, tree Lc has a maximal turnover with DMPD substrate corresponding to a $t_{1/2}$ of ~2 ms for conversion of the enzyme form in the rate limiting step.[366] The decay of the native intermediate to the resting enzyme ($t_{1/2}$ of 13 s)[367] therefore cannot be relevant during enzyme turnover which likely occurs by

reduction of the "native intermediate" (*vide infra*). Note that on decay of the "native intermediate" in Figure 33, the H_2O resulting from dioxygen reduction ends up on the type 2 Cu, as is observed from EPR studies using ^{17}O-labeled dioxygen.[368]

In summary, the type 3 center is fundamentally different from the coupled binuclear copper site in hemocyanin and tyrosinase. It is part of a type 2/type 3 trinuclear copper cluster which is required for O_2 reduction. This reaction generates a peroxide-level oxygen intermediate which is different from that of oxyhemocyanin and oxytyrosinase, thus indicating that differences in geometric and electronic structure are required for the differences in reactivity of peroxide activation versus promotion of its further reduction to water. Finally, the four-electron reduction of dioxygen occurs in two two-electron steps. The first is rate-limiting and the second is fast, consistent with the large driving force associated with the two-electron reduction of peroxide, as is required to overcome the significant Franck−Condon barrier for O−O bond cleavage.

D. Type 1–Trinuclear Interactions

1. Reduction Kinetics

The mechanism of reduction of oxidized Lc is complex, but in order to be consistent with the turnover kinetics, the T1 to trinuclear electron transfer rate must be fast. Several attempts have been made to elucidate this mechanism. As discussed in section III.A, the rate of oxidation of substrate is dependent upon its reduction potential. This implies that electron transfer from the substrate to the type 1 site (the initial electron acceptor from substrate) is the rate-determining step in turnover. Analysis of the steady-state kinetics by Petersen and Degn yielded second-order rate constants (at pH of 7.5 and 25 °C) of 1.17×10^3 M^{-1} s^{-1} and 259 M^{-1} s^{-1} for hydroquinone and ascorbate, respectively.[366] The maximal turnover rate for the substrates studied was 560 s^{-1}, implying that the rate of electron transfer from the T1 to the trinuclear cluster must significantly exceed this value.

Reinhammar and co-workers examined the transient kinetics of reduction of resting fully oxidized Lc and found complex, multiphasic kinetics.[345,367,369] With hydroquinone at pH 7.4, reduction of the T1 copper showed an initial phase and a final phase with bimolecular rates of 1.58×10^3 and 800 M^{-1} s^{-1}, respectively. Reduction of the T3 pair showed an initial rate of 1.45×10^3 M^{-1} s^{-1} and a final, substrate-independent rate of 0.40 s^{-1}. Although initial and final rates of reduction of the T2 copper were not reported, the rate of reduction of the T2 site was slower than that of the T3 pair, and at 2.5 s, 30% was still Cu(II). Several groups have attempted to measure the rate of electron transfer from the T1 site to the trinuclear cluster following reduction of the T1 site in resting fully oxidized Lc or AO by either pulsed radiolysis or laser flash photolysis.[370−372] Again, multiphasic kinetics were observed in some cases, but the fast rate was in the range of 150−200 s^{-1}. Thus, the rates of electron transfer from the T1 site to the trinuclear cluster in resting fully oxidized Lc are too slow to be consistent with turnover.

The transient kinetics of reoxidation of fully reduced Lc has a similar problem. Formation of the "native intermediate" is very fast, occurring at a rate of 5×10^6 M^{-1} s^{-1} (*vide supra*), again implying fast T1−trinuclear electron transfer, but decay of the "native intermediate" to the resting fully oxidized is very slow ($t_{1/2}$ of 13 s).[367] This indicates that the decay of the "native intermediate" to the resting fully oxidized cannot occur under turnover conditions. Furthermore, under turnover conditions, a substantial concentration of native intermediate is observed.[367] Spectroscopic studies have now defined the structure of the "native intermediate" of Lc to be a fully oxidized enzyme with the hydroxide product still bridging the T2 and T3 coppers.[365] These results imply that the fully oxidized resting form of the enzyme is not catalytically relevant; the "native intermediate" is the catalytically active four-electron oxidized form, which is rereduced rapidly during turnover. Some work has been reported on the transient reduction kinetics of the "native intermediate" which indicates that it exhibits very different reduction behavior than the resting fully oxidized enzyme.[373] With ascorbate at pH 7.4 and 25 °C, rates obtained were 0.11 s^{-1} for reduction of the T1 site and 0.177 s^{-1} for reduction of the T3 pair in the "native intermediate", while the steady-state rate under these conditions was approximately 0.13 s^{-1}. The final phase in reduction of the T1 and T3 sites was not observed. This indicates that the transient reduction kinetics of the "native intermediate" are consistent with turnover and, most importantly, that the T1 site to trinuclear cluster electron transfer rate in the "native intermediate" is fast.

A working model of the mechanism for the catalytic cycle of laccase which is consistent with the available kinetic and spectroscopic data (*vide supra*) is summarized in Figure 35. The major question remaining in the reductive part of the cycle is the mechanism by which the trinuclear cluster is reduced. Starting from the "native intermediate", substrate reduces the T1 site. From this point, two possible mechanisms may be envisioned: (A) The T1 transfers its electron to the T2 and then is rereduced; the T1 and T2 transfer two electrons to the T3; the T1 is rereduced; the T1 transfers its electron to the T2 and gets rereduced, ultimately resulting in the fully reduced form of the enzyme.[369] This possible mechanism would be consistent with the fact that in resting fully oxidized Lc the T3 center acts as a strictly two-electron acceptor, i.e., no "half-met" T3 pair has been observed. (B) The trinuclear cluster is sequentially reduced by three one-electron transfer steps from the T1 site. Since reduction of the "native intermediate" has not been systematically studied, the possibility remains that additional interactions between the T2 and T3 centers in the "native intermediate" allow the T3 coppers to act as one-electron acceptors (note that the order in which the three coppers are reduced is not known). Indeed, Reinhammar has reported the appearance of a new EPR feature (different from that of the T1 and T2 centers) upon formation of the "native intermediate" in the presence of excess reductant, presumably due to rapid rereduction of the "native intermediate", giving support for this latter mechanism.[374]

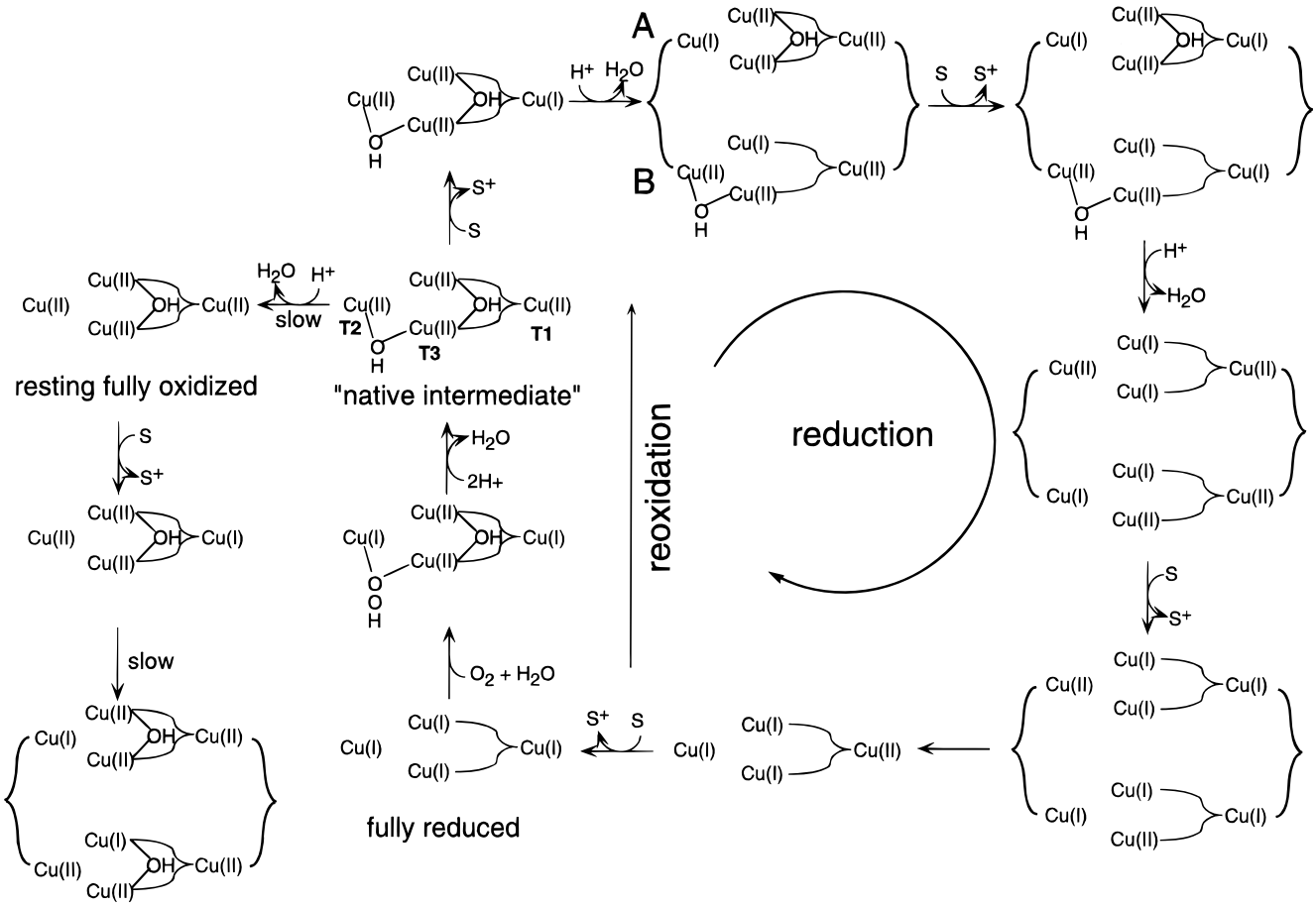

Figure 35. The catalytic cycle of Lc, showing the proposed mechanisms for the reduction and reoxidation of the copper sites. (Center) Starting from the "native intermediate", substrate reduces the T1 site, which then transfers the electron to the trinuclear cluster. Two possible mechanisms for the reduction of the trinuclear cluster are shown: (A) the T1 and T2 sites together reduce the T3 pair and (B) each copper in the trinuclear cluster is sequentially reduced by electron transfer from the T1 site, in which case the T3 site no longer acts as a two-electron acceptor (for further details, see the text). (Left) Slow decay of the "native intermediate" leads to the resting fully oxidized form. In this form, the T1 site can still be reduced by substrate, but electron transfer to the trinuclear site is too slow to be catalytically relevant.

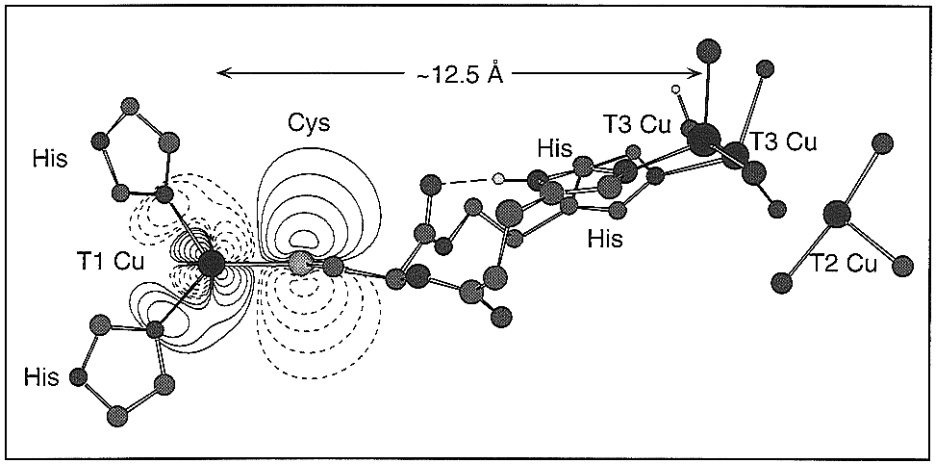

Figure 36. T1 to trinuclear electron transfer pathway in AO. The HOMO wave function of the blue copper center has been superimposed on the T1 copper, showing substantial electron delocalization onto the cysteine S pπ orbital that activates electron transfer to the trinuclear cluster across 12.5 Å.

2. The Type 1–Trinuclear Pathway and Allosteric Interactions

From the above discussion, the T1 to trinuclear electron transfer rate is fast under turnover conditions, and it is clear from the crystal structure of AO that there is an efficient pathway for this electron transfer. The cysteine bound to the T1 copper is flanked on either side by histidines that are ligated to each of the T3 coppers (see Figure 36). This provides a ~13 Å pathway for electron transfer from the T1 to the trinuclear cluster, consisting of nine covalent bonds (or seven covalent and one hydrogen bond).[372,375] The electronic structure of the blue copper site is optimized for efficient long-range

electron transfer to the trinuclear cluster by providing a large electron coupling matrix element into the pathway through the $Cu-S_{Cys}$ bond (see HKS).[17] Studies on the blue copper protein plastocyanin have shown that this unusually short, strong $Cu-S_{Cys}$ bond is highly covalent. SCF-Xα-SW calculations indicate that the HOMO wave function of plastocyanin has 42% Cu $d_{x^2-y^2}$ and 38% S_{Cys} character, but only 2.3% N_{His} character.[219,376,377] The large overlap between the Cu $d_{x^2-y^2}$ and the S_{Cys} $p\pi$ orbitals is also revealed by the intense, low-energy charge-transfer transition and the unusually small $A_{\|}$ hyperfine of the T1 copper. Cu L-edge[378] and S K-edge XAS[379] have provided direct confirmation of the high degree of covalency of the $Cu-S_{Cys}$ bond. The HOMO wave function is directed through the cysteine to the histidines bound to the T3 coppers, thus providing the large electronic coupling and leading to fast intramolecular electron transfer.

Given the close mechanical coupling between the T1 site and the trinuclear cluster via the Cys-His pathway, it is possible that perturbations in the geometry at the trinuclear cluster, either from changes in the redox state of the coppers or exogenous ligand binding, may alter the geometry at the T1 site. Such changes have indeed been spectroscopically observed in T2D Lc.[33822,380] In deoxy T2D Lc (T3 pair is reduced), the resonance Raman spectrum of the T1 site shows vibrations at 383 and 375 cm^{-1}. Upon oxidation of the T3 site to the met T2D derivative, these two bands coalesce to a single peak at 383 cm^{-1}, very similar to that observed in oxidized native Lc (see Figure 37A).[338,380] Oxidation also increases the $A_{\|}$ in the EPR spectrum from 38 to 44 $\times$ 10^{-4} cm^{-1} and decreases the intensity of the 614 nm band by ≥ -600 M^{-1} cm^{-1}.[22,338,380] These changes imply that the $Cu-S_{Cys}$ bond of the T1 site is more covalent when the T3 pair is reduced than when it is oxidized. Binding of exogenous ligands to the T3 site when it is oxidized or reduced in T2D Lc also perturbs the EPR parameters of the T1 copper (see Figure 37B).[22,380]

It is possible to consider how the structural perturbations induced by reduction of the trinuclear cluster might affect the ligand field at the T1 site by comparison of the crystal structures of reduced and oxidized AO. In going from the oxidized to the reduced state, the main geometric perturbations associated with the His-Cys-His linkage occurs at the T3 site. The T3 Cu−Cu distance increases from 3.69 to 5.13 Å. Associated with this, the histidines move ~0.3 Å apart and shift orientation from being angled inward toward the coppers to being nearly parallel (see Figure 38A). Furthermore, the whole His-Cys-His linkages moves out of the plane defined by the T3 and T1 coppers (see Figure 38B). This may alter the $S_{Cys}-Cu_{T1}-N_{His}$ bond angles, which would be consistent with the spectroscopic changes, indicating that the $Cu-S_{Cys}$ bond is more covalent when the T3 site is reduced.

The functional significance of alterations of the electronic and geometric structure of the T1 site upon changes in the redox state of the trinuclear cluster or upon exogenous ligand binding has yet to be determined. Such changes could alter the potential

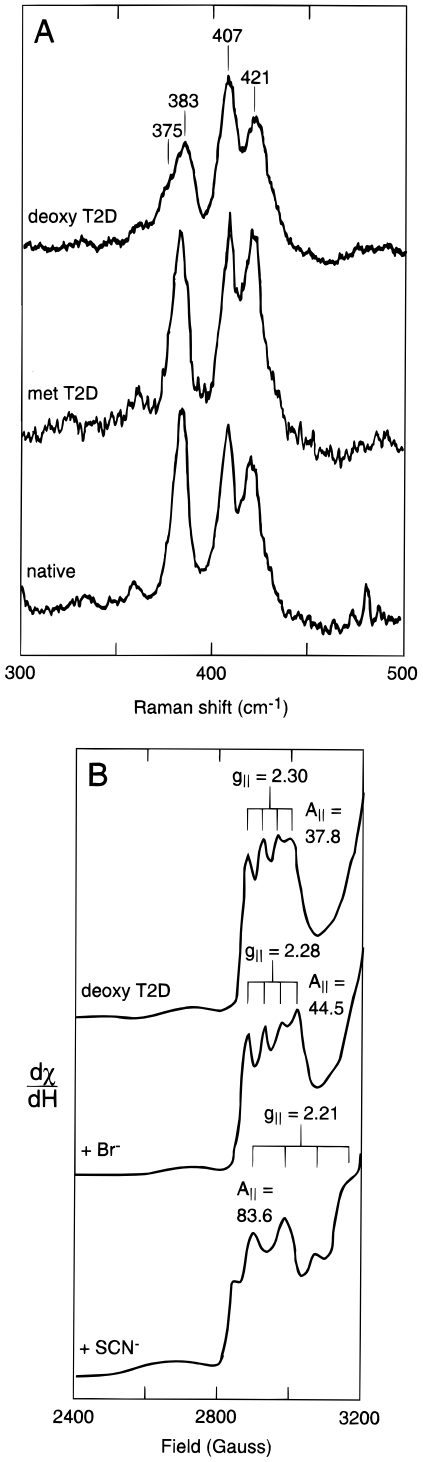

Figure 37. Perturbations of the spectroscopic features of the T1 site upon alterations at the T3 site (adapted from ref 380). (A) Resonance Raman spectra of deoxy T2D ($T1_{ox}$, $T3_{red}$), met T2D ($T1_{ox}$, $T3_{ox}$), and native Lc ($T1_{ox}$, $T2/T3_{ox}$), showing that the two bands at 375 and 383 cm^{-1} coalesce into one upon oxidation of the T3 coppers. (B) EPR spectra of the $g_{\|}$ region of deoxy T2D and deoxy T2D with Br^- and SCN^- bound to the T3 coppers.

of the T1 site and the electronic coupling to the trinuclear copper cluster. Several possibilities can be envisioned. One is that as the trinuclear cluster is reduced, and the potential of the T1 copper increases, thus making it easier to reduce; i.e., reduction (or reoxidation) of the enzyme occurs cooperatively. Under conditions of limiting substrate, this would avoid accumulation of a large concentra-

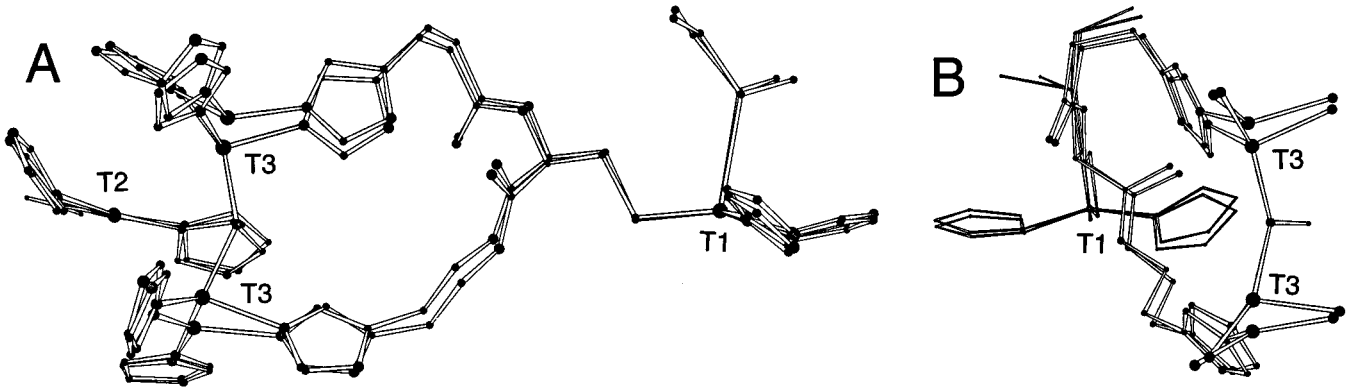

Figure 38. Two views of the T1 to trinuclear cluster electron transfer pathway of AO, showing differences between the reduced and oxidized states: (A) The T1 and T3 coppers are shown all in the same plane; (B) looking along the T1 to trinuclear pathway, from the T3 pair to the T1 copper.

tion of partially reduced enzyme which would not react with oxygen. Also, at the peroxy intermediate stage in the reoxidation cycle, the presence of bound peroxide might make the T1 site easier to oxidize, either by lowering its potential or providing a more efficient pathway for electron transfer.

3. The Role of Additional Coppers in Ceruloplasmin

Cp differs from the other multicopper oxidases in that it has three T1 sites. One of these appear to be permanently reduced by XAS (T1-PR).[292] The other two, redox-active T1 sites show substantial differences in their spectroscopic and kinetic properties and their response to exogenous ligand binding. The T1 sites also differ in their geometric relationship to the trinuclear cluster. As discussed in section III.A, the crystal structure of Cp shows that the trinuclear cluster lies along the border between domains 6 and 1 (see Figure 14). One T1 site is in domain 6 and is connected through a Cys-His pathway to the trinuclear cluster, analogous to the T1 site in AO (T1-Cys-His). Another T1 site is located in domain 2 and lacks an axial methionine, thus making it probable that it is the permanently reduced T1 center. The third is located in domain 4. It has an axial methionine, but lacks the two histidines flanking the cysteine ligated to the T1 copper (T1-Cys-X). The three T1 sites are all about 18 Å from each other.[24] The question arises as to whether both redox-active T1 coppers participate in electron-transfer to the trinuclear cluster, especially since only one is needed for oxidase activity and only one is coupled to the trinuclear cluster through the Cys-His pathway.

As discussed in section III.A.4, Cp exhibits ferroxidase activity. The steady-state oxidation of Fe^{2+} exhibits biphasic kinetics, and Cp is known to have 2−3 binding sites for divalent metal ions.[303] The steady-state kinetics was previously interpreted by Osaki and Walaas as due to two sites where Fe^{2+} may bind and be oxidized.[232−234] This might imply that both redox-active T1 sites are reduced by substrate and transfer electrons to the trinuclear site, thus being catalytically important. Alternatively, Huber and Freiden have interpreted the steady-state kinetics as indicative of substrate activation. In this model, the binding of an Fe^{2+} ion at a regulatory site increases the rate of oxidation of Fe^{2+} ions binding to the substrate binding site.[235] The substrate activation model is also supported by the observation that other divalent metal ions can increase ferroxidase activity. In addition, the transient reoxidation kinetics of fully reduced Cp shows that the two redox-active T1 sites have very different rates of reoxidation.[286,287] One of the T1 sites, the "fast" T1 site, has a first-order reoxidation rate of 439 s^{-1}. The reoxidation rate of the "slow" T1 site is dependent upon the concentration of Fe^{2+}. In the absence of Fe^{2+}, the first-order reoxidation rate of the "slow" T1 site is 0.0009 s^{-1}. Addition of 3.7 equiv of Fe^{2+} greatly increases the reoxidation rate to 0.63 s^{-1}, which is still too slow for catalysis. Further work remains to be done in order to understand the nature of multiple Fe^{2+} binding sites and the cause of biphasic ferroxidase kinetics.

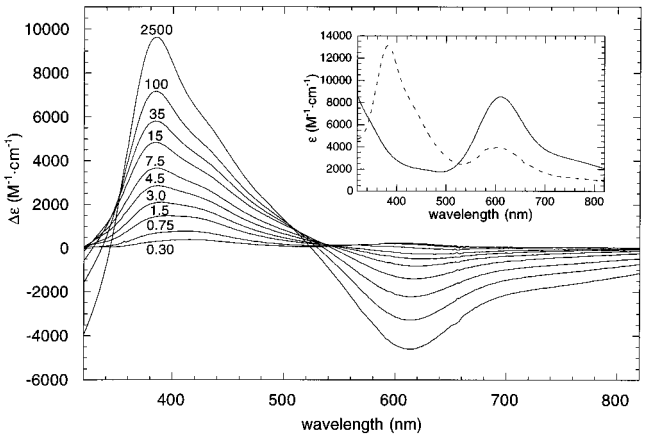

Figure 39. Difference absorption spectra upon the addition of 0−2500 equiv of N_3^- to Cp, showing the partial loss of the 610 nm band and the appearance of intense features at ~400 nm. The inset shows the actual spectra of native fully oxidized Cp (−) and Cp with 2500 equiv of N_3^- (- - -). Spectroscopic changes are reversible upon removal of N_3^-.

The T1 sites of Cp also exhibit unique behavior upon addition of exogenous ligands such as azide and thiocyanate (potent inhibitors of the enzyme).[300−302] Addition of azide causes a dramatic (as much as 50%) decrease in the intensity of the 610 nm band, with the concomitant appearance of intense features in the absorption spectrum at ~400 nm (see Figure 39).[381−384] These changes are reversible upon removal of exogenous ligand. Additional dramatic changes are also observed in the CD[382,384] and resonance Raman spectra.[385] The resonance Raman data indicate that

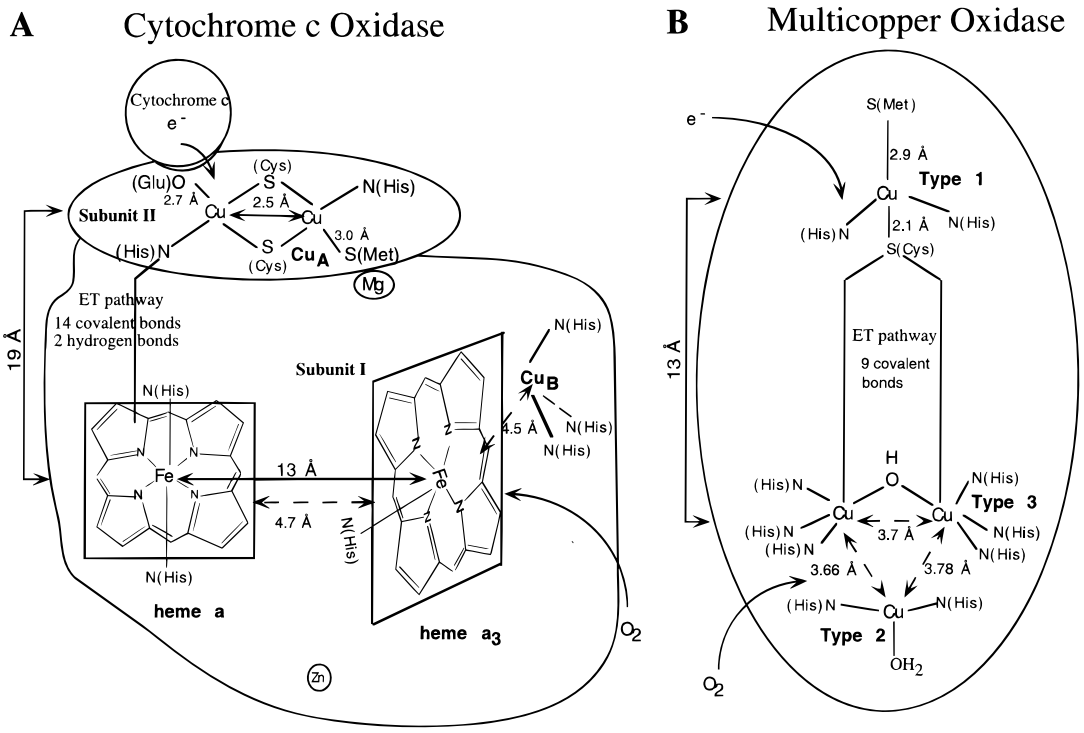

Figure 40. Comparison of the metal configurations and ET pathways in CcO and the multicopper oxidases. (A) CcO: the electron enters at the Cu_A site in subunit II and is transferred across 19 Å to the heme *a* site then to the hetero-binuclear heme a_3−Cu_B oxygen reduction site. The immediate coordination environments of the coppers and heme irons are shown. (B) Multicopper oxidases: the type 1 serves a redox function parallel to Cu_A in CcO and the type 2 correlates with heme *a* and the coupled T3 pair with the binuclear heme a_3−Cu_B pair in CcO. Distances, ET pathways, and dioxygen and redox substrate reaction sites are indicated for both proteins.

the loss of the unique spectroscopic features of the T1 sites may, in fact, be limited to just one of the T1 sites, while the other is only slightly perturbed. Currently, it is not known how many azides bind to Cp nor where they bind. In Lc, azide binds to the trinuclear cluster, and although azide binding to the reduced T3 center in T2D Lc does perturb the spectroscopic features of the T1 copper, no such large perturbations are observed. One possibility in Cp is that azide can bind to one (or both) of the redox-active T1 sites and alter its electronic structure and, thus, spectroscopic features. However, direct ligand-binding to a wild-type blue copper site has not been observed. Alternately, azide may bind to the trinuclear cluster and induce allosteric changes at one or both of the redox-active T1 sites. This could possibly relate to the activity of the enzyme where binding of dioxygen at the trinuclear cluster could induce a conformational change at one or both of the redox-active T1 sites and regulate their rate of electron transfer. The molecular basis for how exogenous ligand-binding induces these dramatic changes in the spectroscopic features of the redox-active T1 site(s) and how this relates to the catalytic function of Cp is a unique feature of this enzyme which remains to be elucidated.

E. Relation to Cytochrome *c* Oxidase

Cytochrome *c* Oxidase (CcO) (ferrocytochrome-*c*:O_2 oxidoreductase, EC 1.9.3.1), which belongs to the family of terminal oxidases found in aerobic organisms, is located in the mitochondrial inner membrane in eukaryotes and in the cytoplasmic membrane in eubacteria. As with the multicopper oxidases, this enzyme catalyzes the four-electron reduction of O_2 to H_2O; it additionally utilizes the energy available from substrate oxidation (~550 mV)[386] to pump protons (from the mitochondrial matrix to the cytoplasm in eukaryotes and from the cytoplasm to the periplasmic space in eubacteria), thus establishing a transmembrane proton potential. This potential then drives the synthesis of ATP from ADP and inorganic phosphate. This enzyme is described in detail in the review by Ferguson-Miller and Babcock in this issue.[387] Here we briefly summarize its structural and functional properties for comparison to the above discussion of the multicopper oxidases.

1. Structure of the Metal Sites

Recently, crystal structures of CcOs from two evolutionarily distant sources were reported.[10−12] The enzyme contains a binuclear Cu_A, a heme *a*, and a binuclear heme a_3−Cu_B site. In addition, the mammalian enzyme contains Mg^{2+} and Zn^{2+} sites. As seen from Figure 40A the Cu_A site is located in subunit II of the protein, which has a substrate (cytochrome *c*) binding pocket; the heme *a* site and the binuclear heme a_3−Cu_B site, where oxygen binding and reduction occurs, are all located in subunit I. The Mg^{2+} ion is located in between subunits I and II, while the Zn^{2+} ion is located much further away in subunit I.

The **Cu_A site** is a binuclear [Cu(1.5) Cu(1.5)] valence delocalized $S_{tot} = {}^1/_2$ center in its oxidized state. The Cu−Cu distance is 2.5−2.7 Å and the site has two bridging cysteines; two histidines, one on each copper; and a methionine on one and a Glu on the second Cu with long bond distances of 3.0 and

2.7 Å, respectively. Each site is thus four-coordinate with distorted tetrahedral structures. As indicated in Figure 40A, Cu_A is the site of primary electron transfer from the substrate[13] and is similar to the type 1 copper center (*vide infra*). However, it has the additional bridged copper and complete electron delocalization. It has been of significant interest to determine the pathway for electron delocalization (a direct Cu−Cu bond *vs* superexchange through the bridging cysteine sulfurs) and the contribution of this valence delocalization to the outer-sphere long-range electron transfer (ET) properties of this center (*vide infra*).

The **heme *a*** site is about 19 Å from the Cu_A site. The Fe is six-coordinate and low-spin, with two axial histidine ligands. The Fe atom of **heme a_3** is five-coordinate and high-spin, the axial ligand being a histidine; the Fe atom is out of the porphyrin plane by ~0.7 Å. The porphyrin planes of heme *a* and heme a_3 are roughly perpendicular to each other (104°) . The **Cu_B site** is located *trans* to the axial His ligand of the heme a_3 center and is coordinated by three histidines in the mammalian[11] and two (or possibly three) in the eubacterial[12] enzyme in a trigonal pyramidal geometry with the open coordination position of the copper oriented toward the open coordination position of the heme a_3 iron center. No other ligand is detected. The metal atoms of the heme a_3 and Cu_B sites are 5.2 Å (eubacterial) and 4.5 Å (mammalian) apart. Early EPR[388] and susceptibility[389] studies had indicated that the metal atoms of the **heme a_3−Cu_B** site were antiferromagnetically coupled, which requires a bridging ligand between the Fe(III) ($S = 5/2$) and Cu(II) ($S = {}^1/_2$), resulting in an $S = 2$ ground state. Based on the crystallographic results,[11] a disordered water-derived ligand is the likely possibility for this bridge (i.e., oxo or hydroxo). Susceptibility studies on bridged binuclear [heme Fe(III) Cu(II)] model systems with $S = 2$ ground states[31,390,391] indicate that an oxo bridge would have an exchange coupling constant J (in $H = -2JS_1 \cdot S_2$) of about -100 cm^{-1}.[392] Recent susceptibility studies on mammalian CcO[393] confirm that the "slow" form (thought to be equivalent to the resting enzyme[394]) has an $S = 2$ ground state with a $-J$ of >100 cm^{-1}. However, this study points out that differences in magnetism are observed between the "fast" and "slow" forms of the enzyme (the "fast" and "slow" forms being interconverted by a change in pH[394]). The results indicate that the "fast" form is a mixture of two species: ~75% with an $S = 1$ [most likely obtained by the antiferromagnetic coupling of an intermediate spin Fe(III) ($S = {}^3/_2$) with the Cu(II) ($S = {}^1/_2$)] ground state and ~25% with an $S = 2$ ground state. The recent crystal structure on the mammalian enzyme appears to have been on the "fast" form of the enzyme (based on its monophasic reactivity with CN^-).[11]

2. Electron Transfer Pathway

The primary site of electron reduction is Cu_A.[395,396] From the crystal structure there is a good "docking site" for cytochrome close to the Cu_A in subunit II (Figure 40A). All intramolecular electron transfers in CcO are fast with rate constants $\geq 10^3$ s^{-1}.[397] The rate of electron transfer from the Cu_A to the heme *a* site is $\sim 2 \times 10^4$ s^{-1} in the fully oxidized enzyme.[398−400] The high rate of this electron transfer despite the low 50 mV driving force is attributed to the availability of a facile ET pathway from Cu_A to heme *a* consisting of 14 covalent bonds and 2 hydrogen bonds.[401] This pathway is proposed to involve a histidine ligand to the Cu_A site, a hydrogen bond to an arginine residue, another hydrogen bond, and ultimately a propionate of the heme *a*. Very similar pathways are proposed for both the eubacterial and mammalian enzymes.[10] Electron transfer then occurs from the heme *a* site to the binuclear heme a_3−Cu_B site, where dioxygen reduction occurs. The closest (edge to edge) distance of the heme *a* and heme a_3 is 4.7 Å, with a center to center distance of ~13 Å. Phe 377 (Phe 412 in eubacterial CcO) is thought to also play a role in the ET between the heme *a* and heme a_3 sites, since it stacks between His 376 (His 411) of heme a_3 and the His 378 (His 413) heme *a* ligand. There are also some notable interactions between heme a_3 and Cu_B that could facilitate electron transfer between these metal centers. In the mammalian enzyme, there is a hydrogen bond between the hydroxyfarnesyl ethyl side chain of the heme a_3 and Tyr 244, which has π−π interactions with His 240, a ligand to Cu_B.[10−12,402]

3. Reactions of CcO with Dioxygen

CcO catalyzes the four-electron reduction of O_2 to H_2O at the hetero-binuclear heme a_3−Cu_B site. Intermediates in this reaction have been obtained and studied using low-temperature[403−405] and time-resolved[406−410] optical absorption and EPR[411−413] methods. Recently, time-resolved resonance Raman spectroscopy (TR^3) has provided significant insight into the nature of these oxygen intermediates.[414−417] At least five intermediates have been observed in the reaction of the fully reduced enzyme with dioxygen. There is general consensus that the first intermediate is a formally Fe(III)−superoxo species, characterized by a ν_{Fe-O_2} at 571 cm^{-1}, and that the last species before decay to the resting form of the enzyme is a hydroxy adduct characterized by a Fe(III)−OH^- stretching mode, ν_{Fe-OH} at 450 cm^{-1}. The assignments of the other intermediates which appear and decay between these initial and final forms are less clear. The superoxo species appeared to decay to a species with a peak at 358 cm^{-1}, which then decays to a species with a peak at 790 cm^{-1}, which subsequently gives the hydroxy form.[414,418] The 358 cm^{-1} peak was assigned to a Fe(III)−O stretch arising from a Fe^{III}−peroxo species, while the 790 cm^{-1} band has been assigned to a Fe^{IV}=O stretch of a ferryl species. Recently, however,[419,420] an additional peak at 804 cm^{-1} which appears before and decays into the 358 cm^{-1} species has been observed. These peaks at 804, 358, and 790 cm^{-1} all show an oxygen isotope effect and are therefore associated with bound oxygen species. The 804 cm^{-1} peak has been considered to be due to the vibration of a Fe^{V}=O species, the 358 cm^{-1} feature a N−Fe=O bending mode, and the 790 cm^{-1} peak is associated with a Fe^{IV}=O species.[420] Since the peak at 804 cm^{-1} appears upon decay of the superoxide species, by reaction of the oxidized enzyme with hydrogen peroxide,[421−423] or by reaction of the mixed valent form[404] (i.e., reduced heme a_3 and

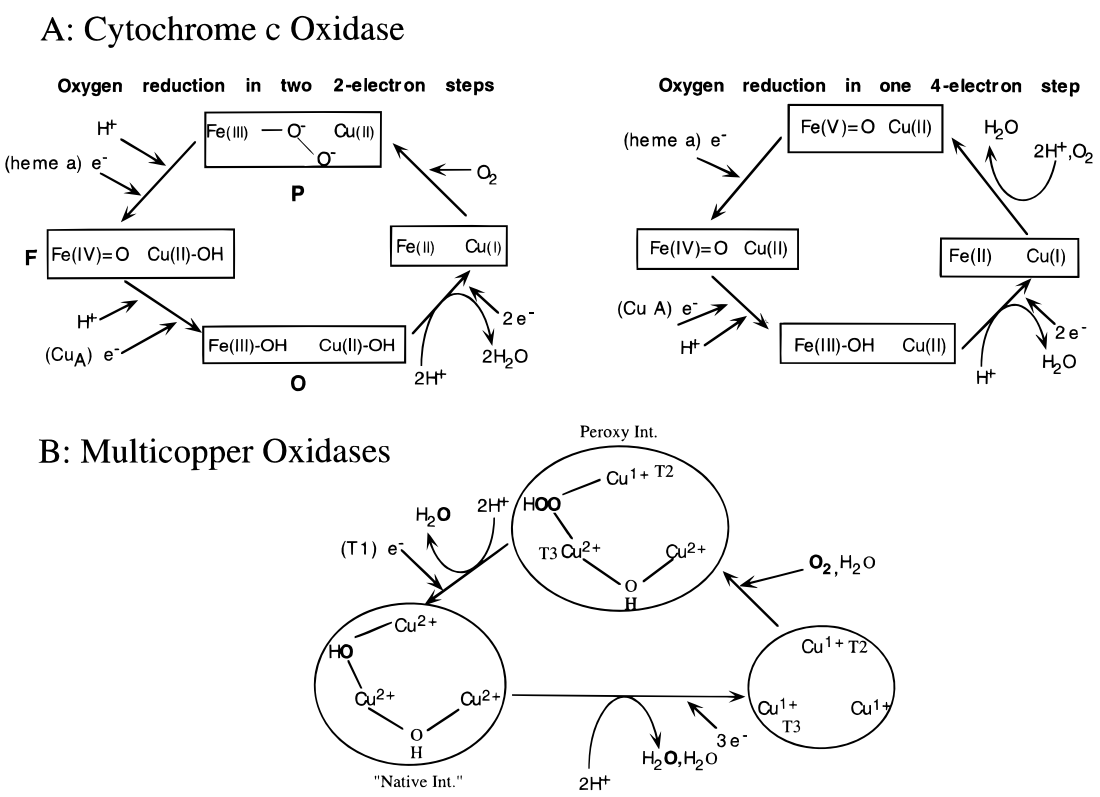

Figure 41. Comparison of dioxygen reduction in CcO and the multicopper oxidases. (A) CcO. (Left) Oxygen reduction to water in two two-electron steps, passing through the peroxo P (two-electron reduced) and the ferryl F (four-electron reduced) stages. (Right) Oxygen reduction by one four-electron step, subsequent steps being electron transfer to rereduce the iron from the 5+ to the 3+ oxidation state. (B) Multicopper oxidases. Oxygen reduction in two two-electron steps, passing through the peroxy intermediate and the fully oxidized OH^- product complex (i.e., the "native intermediate"). Note that, consistent with Figure 35, rereduction is at the "native intermediate" level during turnover catalysis.

Cu_B and oxidized heme *a* and Cu_A) with dioxygen, it is thought to be at the peroxide level. Yet, it is assigned as an Fe^V=O stretch, rather than a O−O vibration, which would be at the same energy position, based on rR data. The rR spectrum of the $^{18}O-^{16}O$ derivative matches that of the average sum of the spectra obtained with the pure isotopes [i.e., ($^{16}O_2$ + $^{18}O_2$)/2], thus indicating that the O−O bond is broken.[419,420]

Thus, the catalytic cycle proposed for dioxygen reduction by CcO has been described by two possible schemes: (1) (Figure 41A, left) Two-electron reduction of O_2 from heme a_3 and Cu_B forms a peroxo species, which passes through a formally superoxo level oxy−heme a_3 species, followed by a second two-electron reduction, one electron coming from heme a_3, which is then oxidized to Fe^{IV}, and the other from the Cu_B site, which had been rereduced by the heme *a* site, resulting in the formation of one water or OH^- and the ferryl (Fe^{IV}=O) species. This then decays to the metal-hydroxide bound form by ET (to reduce the Fe^{IV} center) and protonation; the metal−hydroxide bound species then decays to the resting enzyme by further protonation.[13,424−426] (2) (Figure 41A, right) After the initial formation of the oxy−heme a_3 species (formally Fe(III)−superoxo), all four electrons needed for oxygen reduction to water are transferred directly to dioxygen at the "peroxy" level (three from heme a_3 and one from Cu_B). Subsequent steps in the catalytic cycle then involve the transfer of electrons to reduce the Fe^V back to the ferric oxidation state, with protonation of the oxo ligand to form water.[420] Yet another possibility is for the first intermediate to decay to a Fe^{IV}=O $Cu^{III}B$ species with the peak at 804 cm^{-1} being associated with a Fe^{IV}=O stretch.[427] Cu(III) is found to occur in copper−oxygen model systems;[428] however, its relevance in biological catalytic cycles is yet to be established.

4. Comparison of CcO with the Multicopper Oxidases

The above survey of CcO allows a structure/function comparison with the multicopper oxidases. The Cu_A site in CcO parallels the type 1 site of the multicopper oxidases. They both serve as the primary electron acceptors from substrate and transfer the electron over long distances to the site of dioxygen reduction (Figure 40). The dioxygen reduction site is a trinuclear copper cluster in the multicopper oxidases, while in CcO it is a hetero-binuclear heme a_3-Cu_B moiety with an adjacent heme *a*. In the multicopper oxidases, the long range intramolecular ET occurs from the T1 to the T3 site (Figure 40B), which is ~13 Å away, via a T1-Cys-His-T3 pathway[219] consisting of nine covalent bonds with a rate of 200 s^{-1} for the resting enzyme.[371] In CcO (Figure 40A) a similar rapid long-range ET occurs from the Cu_A site to the heme *a* site, which is 19 Å away, via a pathway which appears to involve a histidine ligand at the Cu_A and includes 14 covalent bonds and 2 hydrogen bonds at a rate of 2×10^4 s^{-1} (*vide supra*). It should be noted that the covalency of the Cu−N bond in Cu_A is much reduced from that of the Cys S−Cu bond in the blue copper site in the multicopper oxidases, and the pathway is longer with more covalent bonds, yet

the ET rate is faster in CcO. This could in part be related to additional geometric and electronic structural contributions to ET associated with the binuclear mixed-valent nature of Cu_A. The possibility of ET through the more covalent Cu−S bond of the Cu_A center should also be considered.

There are striking similarities in the oxygen intermediates between these two enzymes and the structures of the metal sites involved. Both enzymes reduce O_2 to water in two two-electron steps (or the alternative of a four-electron step in CcO, Figure 41A). The two electrons derive from a pair of metal sites, the T3 pair in the multicopper oxidases and the heme a_3−Cu_B pair in CcO, which are antiferromagnetically coupled in the oxidized form through an oxygen atom based bridge. There is a third metal center (the T2 copper in the multicopper oxidases and the heme *a* in CcO) which is required for catalysis, yet this does not directly participate in the initial ET for reduction of dioxygen. Thus both enzymes can be considered to contain a trinuclear metal cluster site with the heme a_3−Cu_B being analogous to the T3 center and the heme *a* playing a parallel role to the T2 center of the multicopper oxidases.

There is also a significant difference in the mechanism of these two enzymes. CcO contains a heme Fe at its coupled binuclear catalytic site which is capable of increasing its oxidation state up to the 5+ level, while for bridged T3 Cu centers even the 3+ oxidation state is considered unlikely. Thus, while in both CcO and Lc the first two electrons derive from the coupled pair to produce a peroxide level intermediate, the second two electrons derive from the T1 and T2 coppers in Lc which directly reduce the peroxide species, while in CcO these derive from further oxidation of the heme a_3 center potentially to the 5+ level. Thus the role of the heme *a* and the Cu_A would be to reduce this highly oxidized heme a_3 center back to the 3+ level, rather than the direct reduction of the peroxide intermediate (Figure 41, part A *vs* B). This would correlate with the different configurations of the trinuclear clusters in the two enzymes, with the T2 copper being positioned close enough for coordination (and electron transfer) to the peroxide intermediate in the multicopper oxidases (Figure 40B), while heme *a* is configured for ET to the highly oxidized heme a_3 center in CcO (Figure 40A). It is possible that this difference in reactivity (full reduction of dioxygen by the heme a_3−Cu_B center versus two-electron reduction by the T3 pair and a second two-electron reduction of the resulting peroxide by the T1 and T2 centers) is necessitated by and correlates with the additional function of translocation of vector protons by CcO for ATP synthesis.

IV. Concluding Comments

Spectroscopy has and continues to play a key role in the field of Cu enzymes in that these exhibit unique spectroscopic features reflecting novel electronic structures that can make major contributions to reactivity. It has also allowed the identification and detailed description of oxygen intermediates in the copper cluster enzymes. It must be emphasized that oxytyrosinase and the peroxy intermediate in Lc are two well-defined oxygen intermediates in Cu enzymes and among the most well-defined intermediates in non-heme bioinorganic chemistry. These are both peroxide-level intermediates which contain the O−O bond. This is in contrast to the heme oxidases and oxygenases (i.e., CcO and P450) where the O−O bond is thought to be broken, which likely reflects the ability of the heme Fe to achieve high oxidation states in the oxo species the form. It should also be noted that these intermediates, oxytyrosinase and the peroxy intermediate in Lc, have different geometric and electronic structures which correlate with their differences in reactivity: hydroxylation of substrate versus further reduction to water. It is now important to understand the role of this different geometric and electronic structure in promoting their associated reactivities.

For tyrosinase, substrate coordination to the oxy site can perturb its electronic structure, and future studies in this field should address whether this increases the peroxide back-bonding to an extent which cleaves the O−O bond and whether this occurs prior to, concerted with, or subsequent to substrate oxidation. In contrast to the well-defined active site in tyrosinase, the nature of the active sites in catechol oxidases and pMMO still need to be determined. For the multicopper oxidases, research has advanced to the stage that a number of timely goals are now accessible: (i) the electronic structure of the hydroperoxide intermediate and its role in promoting further reduction, (ii) the detailed geometric description of the interaction of the peroxide with the trinuclear Cu cluster, (iii) a Marcus theory analysis of the reductive cleavage of the O−O bond in the peroxide intermediate, (iv) the detailed nature of the "native intermediate" (now known to be a hydroxide product) and its high redox reactivity relative to the resting enzyme, and (v) the role of the additional strongly allosterically coupled T1 Cu centers in Cp. These are all of critical importance in understanding the functioning of the Cu cluster enzymes on a molecular level.

List of Abbreviations

$A_{\|\|}$	parallel hyperfine coupling constant in EPR
AMO	ammonia monooxygenase
AO	ascorbate oxidase
ATP	adenosine triphosphate
BO	bilirubin oxidase
CcO	cytochrome *c* oxidase
CD	circular dichroism
Cp	ceruloplasmin
CP	circularly polarized
CT	charge transfer
d → d	ligand field transitions
DHGO	dihydrogeodin oxidase
DMPD	dimethyl-*p*-phenylenediammine
DOPA	dihydroxyphenylalanine
ϵ	molar absorptivity in M^{-1} cm^{-1}
EPR	electron paramagnetic resonance
ET	electron transfer
FET3	gene for iron transport protein 3
Hc	hemocyanin
IRMS	isotope ratio mass spectrometry
Lc	laccase
LT	low temperature
MCD	magnetic circular dichroism
NAD	nicotinamide adenine dinucleotide

NHE	normal hydrogen electrode
PHS	phenoxazinone synthase
pMMO	particulate methane monooxygnase
PQQ	pyrroloquinoline quinone
rR	resonance Raman
RT	room temperature
SO	sulochrin oxidase
TR^3	time resolved resonance Raman
T1	type 1
T1-Cys-His	type 1 cysteine-histidine pathway
T1 Cys-X	type 1 cysteine-no histidine pathway
T1Hg Lc	type 1 mercury substituted laccase
T1-PR	T1-permanently reduced
T2	type 2
T2D Lc	type 2 depleted laccase
T2/T3	type 2/type 3 trinulcear cluster
T3	type 3
Tyr	tyrosinase
XAS	X-ray absorption spectroscopy
XYL	α,α′-bis[*N*,*N*-bis[2-(2-pyridyl)ethyl]amino]-*m*-xylene

Acknowledgments

E.I.S. wishes to thank his past students and collaborators as indicated in the references cited for their outstanding contributions to this field and David Root for allowing his hydroperoxide model studies to be included prior to publication. This research is funded by NIH Grant DK31450. T.E.M. acknowledges the NSF for a predoctoral fellowship.

References

(1) Malkin, R.; Malmström, B. G. *Adv. Enzymol.* **1970**, *33*, 177.
(2) Vänngård, T. In *Biological Applications of Electron Spin Resonance*; Bolton, J. R., Swartz, H. M., Borg, D. C., Eds.; Wiley-Interscience: New York, 1972; pp 411.
(3) Solomon, E. I.; Baldwin, M. J.; Lowery, M. D. *Chem. Rev.* **1992**, *92*, 521.
(4) Reinhammar, B. In *Copper Proteins and Copper Enzymes*; Lontie, R., Ed.; CRC Press: Boca Raton, FL, 1984; Vol. III; pp 1.
(5) Spira-Solomon, D. J.; Allendorf, M. D.; Solomon, E. I. *J. Am. Chem. Soc.* **1986**, *108*, 5318.
(6) Allendorf, M. D.; Spira, D. J.; Solomon, E. I. *Proc. Natl. Acad. Sci. U.S.A.* **1985**, *82*, 3063.
(7) Messerschmidt, A.; Ladenstein, R.; Huber, R.; Bolognesi, M.; Avigliano, L.; Petruzzelli, R.; Rossi, A.; Finazzi-Agro, A. *J. Mol. Biol.* **1992**, *224*, 179. (a) The Protein Data Bank: A computer-based archival file for macromolecular structures.
(8) Antholine, W. E.; Kastrau, D. H. W.; Steffens, G. C. M.; Buse, G.; Zumft, W. G.; Kroneck, P. M. H. *Eur. J. Biochem.* **1992**, *209*, 875.
(9) Kroneck, P. M. H.; Antholine, W. E.; Koteich, H.; Kastrau, D. H. W.; Neese, F.; Zumft, W. G. In *Bioinorganic Chemistry of Copper*; Karlin, K. D., Tyeklar, Z., Eds.; Chapman & Hall: New York, 1993.
(10) Tsukihara, T.; Aoyama, H.; Yamashita, E.; Tomizaki, T.; Yamaguchi, H.; Shinwaza-Itoh, K.; Nakashima, R.; Yaono, R.; Yoshikawa, S. *Science* **1996**, *272*, 1136.
(11) Tsukihara, T.; Aoyama, H.; Yamashita, E.; Tomizaki, T.; Yamaguchi, H.; Shinwaza-Itoh, K.; Nakashima, R.; Yaono, R.; Yoshikawa, S. *Science* **1995**, *269*, 1069.
(12) Iwata, S.; Ostermeier, C.; Ludwig, B.; Michel, H. *Nature* **1995**, *376*, 660.
(13) Malmström, B. G. *Chem. Rev.* **1990**, *90*, 1247.
(14) Farrar, J. A.; Thomson, A. J.; Cheesman, M. R.; Dooley, D. M.; Zumft, W. G. *FEBS Lett.* **1991**, *294*, 11.
(15) Solomon, E. I. *Commun. Inorg. Chem.* **1984**, *3*, 225.
(16) Pantoliano, M. W.; Valentine, J. S.; Nafie, L. A. *J. Am. Chem. Soc.* **1982**, *104*, 6310.
(17) Holm, R. H.; Kennepohl, P.; Solomon, E. I. *Chem. Rev.* **1996**, *96*, 2239 (this issue).
(18) Klinman, J. P.; Brenner, M. In *Oxidases and Related Redox Systems*; Alan Liss: 1988.
(19) Klinman, J. *Chem. Rev.* **1996**, *96*, 2541 (this issue).
(20) Smith, T. D.; Pilbrow, J. R. *Coord. Chem. Rev.* **1974**, *13*, 173.
(21) Wilcox, D. E.; Long, D. E.; Solomon, E. I. *J. Am. Chem. Soc.* **1984**, *106*, 2186.
(22) Spira-Solomon, D. J.; Solomon, E. I. *J. Am. Chem. Soc.* **1987**, *109*, 6421.
(23) Cole, J. L.; Tan, G. O.; Yang, E. K.; Hodgson, K. O.; Solomon, E. I. *J. Am. Chem. Soc.* **1990**, *112*, 2243.
(24) Zaitseva, I.; Zaitsev, V.; Card, G.; Moshov, K.; Bax, B.; Ralph, A.; Lindley, P. *J. Biol. Inorg. Chem.* **1996**, *1*, 15.
(25) Nguyen, H.-H. T.; Shiemke, A. K.; Jacobs, S. J.; Hales, B. J.; Lidstrom, M. E.; Chan, S. I. *J. Biol. Chem.* **1994**, *269*, 14995.
(26) Tang, J.; Albrecht, A. C. In *Raman Spectroscopy*; H. Szmanski, Ed.; Plenum: New York, 1970; Vol. 2; pp 33.
(27) Kau, L. S.; Solomon, E. I.; Hodgson, K. O. *J. Phys.* **1986**, *47*, 289.
(28) Kau, L.-S.; Spira-Solomon, D. J.; Penner-Hahn, J. E.; Hodgson, K. O.; Solomon, E. I. *J. Am. Chem. Soc.* **1987**, *109*, 6433.
(29) Sorrell, T. N. *Tetrahedron* **1989**, *45*, 3.
(30) Kitajima, N.; Moro-Oka, Y. *Chem. Rev.* **1994**, *94*, 737.
(31) Karlin, K. D.; Tyeklar, Z. In *Models in Inorganic Biochemistry*; Eichhorn, G. L., Marzilli, L. G., Eds.; PTR Prentice Hall: Englewood Cliffs, New Jersey, 1994; Vol. 9; pp 123.
(32) Fox, S.; Karlin, K. D. In *Active Oxygen in Biochemistry*; Valentine, J. S., Foote, C. S., Greenberg, A., Liebman, J. F., Eds.; Blacki Academic & Professional: London, 1995; Vol. 3; pp 188.
(33) Solomon, E. I.; Tuczek, F.; Root, D. E.; Brown, C. A. *Chem. Rev.* **1994**, *94*, 827.
(34) Mason, H. S.; Fowlks, W. B.; Peterson, E. W. *J. Am. Chem. Soc.* **1955**, *77*, 2914.
(35) Rodriguez-Lopez, J. N.; Tudela, J.; Varon, R.; Garcia-Carmona, F.; Garcia-Canovas, F. *J. Biol. Chem.* **1992**, *267*, 3801.
(36) Himmelwright, R. S.; Eickman, N. C.; Lubein, C. D.; Lerch, K.; Solomon, E. I. *J. Am. Chem. Soc.* **1980**, *102*, 7339.
(37) Volbeda, A.; Hol, W. G. J. *J. Mol. Biol.* **1989**, *209*, 249.
(38) Magnus, K. A.; Hazes, B.; Ton-That, H.; Bonaventura, C.; Bonaventura, J.; Hol, W. G. J. *Proteins* **1994**, *19*, 302.
(39) Lerch, K.; Ettlinger, L. *Eur. J. Biochem.* **1972**, *31*, 427.
(40) Huber, M.; Hintermann, G.; Lerch, K. *Biochemistry* **1985**, *24*, 6038.
(41) Huber, M.; Lerch, K. *Biochemistry* **1988**, *27*, 5610.
(42) Lerch, K. *FEBS Lett.* **1976**, *69*, 157.
(43) Lerch, K. *J. Biol. Chem.* **1982**, *257*, 6414.
(44) Kupper, U.; Niedermann, D. M.; Travaglini, G.; Lerch, K. *J. Biol. Chem.* **1989**, *264*, 17250.
(45) Lerch, K. *Proc. Natl. Acad. Sci. U.S.A.* **1978**, *75*, 3635.
(46) Nelson, R. M.; Mason, H. S. *Methods Enzymol.* **1970**, *XVIIA*, 626.
(47) Jolley, R. L.; Evans, L. H.; Mason, H. S. *Biochem. Biophys. Res. Commun.* **1972**, *46*, 878.
(48) Jolley, R. L.; Evans, L. H.; Makino, N.; Mason, H. S. *J. Biol. Chem.* **1974**, *249*, 335.
(49) Strothkamp, K. G.; Jolley, R. L.; Mason, H. S. *Biochem. Biophys. Res. Commun.* **1976**, *70*, 519.
(50) Uiterkamp, A. J. M. S.; Evans, L. H.; Jolley, R. L.; Mason, H. S. *Biochim. Biophys. Acta* **1976**, *453*, 200.
(51) Vaughan, P. F. T.; Butt, V. S. *Biochem. J.* **1970**, *119*, 89.
(52) Vaughan, P. F. T.; McIntyre, R. J. *Biochem. J.* **1975**, *151*, 759.
(53) Vaughan, P. F. T.; Eason, R.; Paton, J. Y.; Ritchie, G. A. *Phytochemistry* **1975**, *14*, 2383.
(54) Nishioka, K. *Eur. J. Biochem.* **1978**, *85*, 137.
(55) Kwon, B. S.; Haq, A. K.; Pomerantz, S. H.; Halaban, R. *Proc. Natl. Acad. Sci. U.S.A.* **1987**, *84*, 7473.
(56) Oetting, W. S.; King, R. A. *J. Invest. Dermatol.* **1994**, *103*, 131S.
(57) Mayer, A. M.; Harel, E. *Phytochemistry* **1979**, *18*, 193.
(58) Barrett, F. M. In *Physiology of the Insect Epidermis*; Binnigton, K., Retnakaram, A., Eds.; CISRO: East Melbourne, Australia, 1991; pp 195.
(59) Robb, D. A. In *Copper Proteins and Copper Enzymes*; R. Lontie, Ed.; CRC Press: Boca Raton, FL, 1984; Vol. II; pp 207.
(60) Uiterkamp, A. J. M. S. *FEBS Lett.* **1972**, *20*, 93.
(61) Uiterkamp, A. J. M. S.; Deen, H. v. d.; Berendsen, J.; Boas, J. F. *Biochem. Biophys. Res. Commun.* **1974**, *372*, 407.
(62) Eickman, N. C.; Himmelwright, R. S.; Solomon, E. I. *Proc. Natl. Acad. Sci. U.S.A.* **1979**, *76*, 2094.
(63) Hepp, A. F.; Himmelwright, R. S.; Eickman, N. C.; Solomon, E. I. *Biochem. Biophys. Res. Commun.* **1979**, *89*, 1050.
(64) Himmelwright, R. S.; Eickman, N. C.; Solomon, E. I. *Biochem. Biophys. Res. Commun.* **1978**, *81*, 237.
(65) Himmelwright, R. S.; Eickman, N. C.; Solomon, E. I. *Biochem. Biophys. Res. Commun.* **1978**, *84*, 300.
(66) Himmelwright, R. S.; Eickman, N. C.; Solomon, E. I. *Biochem. Biophys. Res. Commun.* **1979**, *86*, 628.
(67) Himmelwright, R. S.; Eickman, N. C.; Lubein, C. D.; Solomon, E. I. *J. Am. Chem. Soc.* **1980**, *102*, 5378.
(68) Uiterkamp, A. J. M. S.; Mason, H. S. *Proc. Natl. Acad. Sci. U.S.A.* **1973**, *70*, 993.
(69) Eickman, N. C.; Solomon, E. I.; Larrabee, J. A.; Spiro, T. G.; Lerch, K. *J. Am. Chem. Soc.* **1978**, *100*, 6529.
(70) Woolery, G. L.; Powers, L.; Winkler, M.; Solomon, E. I.; Lerch, K.; Spiro, T. G. *Biochim. Biophys. Acta* **1984**, *788*, 155.
(71) Makino, N.; Mason, H. S. *J. Biol. Chem.* **1973**, *248*, 5731.
(72) Wilcox, D. E.; Porras, A. G.; Hwang, Y. T.; Lerch, K.; Winkler, M. E.; Solomon, E. I. *J. Am. Chem. Soc.* **1985**, *107*, 4015.

(73) Freedman, T. B.; Loehr, J. S.; Loehr, T. M. *J. Am. Chem. Soc.* **1976**, *98*, 2809.
(74) Kitajima, N.; Fujisawa, K.; Moro-oka, Y.; Toriumi, K. *J. Am. Chem. Soc.* **1989**, *111*, 8975.
(75) Ross, P. K.; Solomon, E. I. *J. Am. Chem. Soc.* **1990**, *112*, 5871.
(76) Ross, P. K.; Solomon, E. I. *J. Am. Chem. Soc.* **1991**, *113*, 3246.
(77) Baldwin, M. J.; Root, D. E.; Pate, J. E.; Fujisawa, K.; Kitajima, N.; Solomon, E. I. *J. Am. Chem. Soc.* **1992**, *114*, 10421.
(78) Mahapatra, S.; Halfen, J. A.; Wilkinson, E. C.; Pan, G.; Cramer, C. J.; Que, L.; Tolman, W. B. *J. Am. Chem. Soc.* **1995**, *117*, 8865.
(79) Halfen, J. A.; Mahapatra, S.; Wilkinson, E. C.; Kaderli, S.; Que, V. G. Y. L.; Zuberbuhler, A. D.; Tolman, W. B. *Science* **1996**, *271*, 1397.
(80) Langford, C. H.; Gray, H. B. *Ligand Substitution Processes*; Benjamin: Reading MA, 1966.
(81) Lerch, K.; Huber, M. *J. Inorg. Biochem.* **1986**, *26*, 213.
(82) Lerch, K. In *Enzymatic Browning and Its Prevention*; Lee, C. Y., Whitaker, J. R., Eds.; ACS: Washington, DC, 1995.
(83) Lang, W. H.; Holde, K. E. v. *Proc. Natl. Acad. Sci. U.S.A.* **1991**, *88*, 244.
(84) Pfiffner, E.; Lerch, K. *Biochemistry* **1981**, *20*, 6029.
(85) Jackman, M. P.; Hajnal, A.; Lerch, K. *Biochem. J.* **1991**, *274*, 707.
(86) Gielens, C.; Geest, N. D.; Xin, X.-Q.; Préaux, G. *Arch. Int. Physiol. Biochim. Biophys.* **1991**, *102*, B11.
(87) Ito, N.; Phillips, S. E. V.; Stevens, C.; Ogel, Z. B.; McPherson, M. J.; Keen, J. N.; Yadev, K. D. S.; Knowles, P. F. *Nature* **1991**, *350*, 87.
(88) Ito, N.; Phillips, S. E. V.; Yadav, K. D. S.; Knowles, P. F. *J. Mol. Biol.* **1994**, *238*, 794.
(89) Whittaker, M. M.; Whittaker, J. W. *J. Biol. Chem.* **1988**, *263*, 6074.
(90) Winkler, M. E.; Lerch, K.; Solomon, E. I. *J. Am. Chem. Soc.* **1981**, *103*, 7001.
(91) Pomerantz, S. H. *J. Biol. Chem.* **1960**, *241*, 161.
(92) Duckworth, H. W.; Coleman, J. *J. Biol. Chem.* **1970**, *245*, 1613.
(93) García-Carmona, F.; García-Cánovas, F.; Iborra, J. L.; Lozano, J. A. *Biochim. Biophys. Acta* **1982**, *717*, 124.
(94) Cabanes, J.; García-Cásnovas, F.; Lozano, J. A.; García-Carmona, F. *Biochim. Biophys. Acta* **1987**, *923*, 187.
(95) Paul, P. P.; Tyklar, Z.; Jacobson, R. R.; Karlin, K. D. *J. Am. Chem. Soc.* **1991**, *113*, 5322.
(96) Karlin, K. D.; Hayes, J. C.; Gultneh, Y.; Cruse, R. W.; McKown, J. W.; Hutchison, J. P.; Zubieta, J. *J. Am. Chem. Soc.* **1984**, *106*, 2121.
(97) Karlin, K. D.; Cruse, R. W.; Haka, M. S.; Gultneh, Y.; Cohen, B. I. *Inorg. Chim. Acta* **1986**, *125*, L43.
(98) Cruse, R. W.; Kaderli, S.; Karlin, K. D.; Zuberbühler, A. D. *J. Am. Chem. Soc.* **1988**, *110*, 6882.
(99) Zuberbühler, A. D. In *Dioxygen Activation and Homgeneoud Catalytica Oxidation*; Simandi, L. I., Ed.; Elsevier: Amsterdam, 1991; pp 249.
(100) Karlin, K. D.; Tyeklar, Z.; Zuberbühler, A. D. In *Bioinorganic Catalysis*; Reedijk, J., Ed.; Marcel Dekker: New York, 1991.
(101) Nasir, M. S.; Cohen, B. I.; Karlin, K. D. *J. Am. Chem. Soc.* **1992**, *114*, 2482.
(102) Wood, B. J. B.; Ingraham, L. L. *Arch. Biochem. Biophys.* **1962**, *98*, 479.
(103) Cushing, M. L. *J. Am. Chem. Soc.* **1948**, *70*, 1184.
(104) Anthony, C. *The Biochemistry of Methylotrophs*; Academic Press: London, 1982.
(105) Wallar, B. J.; Lipscomb, J. D. *Chem. Rev.* **1996**,
(106) Burrows, K. J.; Cornish, A.; Scott, D.; Higgins, I. J. *J. Gen. Microbiol.* **1984**, *130*, 3327.
(107) Dalton, H.; Prior, S. D.; Leak, D. J.; Stanley, S. H. In *Microbial Growth on C1 Compounds*; Crawford, R. L., Hanson, R. S., Eds.; American Society for Microbiology: Washington, 1984; pp 75.
(108) Prior, S. D.; Dalton, H. *J. Gen. Microbiol.* **1985**, *131*, 155.
(109) Collins, M. L. P.; Buchholz, L. A.; Remsen, C. C. *Appl. Enviorn. Microbiol.* **1991**, *57*, 1261.
(110) Semrau, J. D.; Zolandz, D.; Lidstrom, M. E.; Chan, S. I. *J. Inorg. Biochem.* **1995**, *58*, 235.
(111) Chan, S. I.; Nguyen, H.-H. T.; Shiemke, A. K.; Lidstrom, M. E. In *Microbial Growth on C1 Compounds*; Murrell, J. C., Kelley, D. P., Eds.; Intercept: Andover, Hampshire, U.K., 1993.
(112) DiSpirito, A. A.; Gulledge, J.; Shiemke, A. K.; Murrell, J. C.; Lidstrom, M. E.; Kerma, C. L. *Biodegradation* **1992**, *2*, 151.
(113) Zahn, J. A.; DiSpirito, A. A. *J. Bacteriol.* **1996**, *178*, 1018.
(114) Semrau, J. D.; Chistoserdov, A.; Lebron, J.; Costello, A.; Davagnino, J.; Kenna, E.; Holmes, A. J.; Finch, R.; Murrell, J. C.; Lidstrom, M. E. *J. Bacteriol.* **1995**, *177*, 3071.
(115) Shiemke, A. K.; Cook, S. A.; Miley, T.; Singleton, P. *Arch. Biochem. Biophys.* **1995**, *321*, 421.
(116) Smith, D. D. S.; Dalton, H. *Eur. J. Biochem.* **1989**, *182*, 667.
(117) Priestly, N. D.; Floss, H. G.; Froland, W. A.; Lipscomb, J. D. *J. Am. Chem. Soc.* **1992**, *114*,
(118) Wilkinson, B.; Zhu, M.; Priestley, N. D.; Nguyen, H.-H. T.; Morimoto, H.; Williams, P. G.; Chan, S. I.; Floss, H. G. *J. Am. Chem. Soc.* **1996**, *118*, 921.
(119) Chan, S. I.; Nguyen, H.-H. T.; Shiemke, A. K.; Lidstrom, M. E. In *Bioinorganic Chemistry of Copper*; Karlin, K. D., Tyeklár, Z., Eds.; Chapman and Hall: New York, 1993; pp 184.
(120) Brown, C. A.; Pavlosky, M. A.; Westre, T. E.; Zhang, Y.; Hedman, B.; Hodgson, K. O.; Solomon, E. I. *J. Am. Chem. Soc.* **1995**, *117*, 715.
(121) Wood, P. M. In *Nitrification*; J. I. Prosser, Ed.; IRL Press: Oxford, 1986; Vol. 20; pp 39.
(122) Suzuki, I.; Kwok, S.-C.; Dular, U.; Tang, D. C. Y. *Can. J. Biochem.* **1981**, *59*, 477.
(123) Hyman, M. R.; Murton, I. B.; Arp, D. J. *Appl. Enviorn. Microbiol.* **1988**, *54*, 3187.
(124) Juliette, L. Y.; Hyman, M. R.; Arp, D. J. *Appl. Enviorn. Microbiol.* **1993**, *59*, 3718.
(125) Vannelli, T.; Hooper, A. B. *Biochemistry* **1995**, *34*, 11743.
(126) Hyman, M. R.; Wood, P. M. *Biochem. J.* **1985**, *227*, 719.
(127) Hyman, M. R.; Arp, D. J. *J. Biol. Chem.* **1992**, *267*, 1534.
(128) McTavish, H.; Fuchs, J. A.; Hooper, A. B. *J. Bacteriol.* **1993**, *175*, 2436.
(129) Bergmann, D. J.; Hooper, A. B. *Biochem. Biophys. Res. Commun.* **1994**, *204*, 759.
(130) Ensign, S. A.; Hyman, M. R.; Arp, D. J. *J. Bacteriol.* **1993**, *175*, 1971.
(131) Zahn, J. A.; Arciero, D. M.; Hooper, A. B.; DiSpirito, A. A. *FEBS Lett.*, in press.
(132) Tremolieres, M.; Bieth, J. G. *Phytochemistry* **1984**, *23*, 501.
(133) Rivas, N. d. J.; Whitaker, J. R. *Plant Physiol.* **1973**, *52*, 501.
(134) Matheis, G.; Belitz, H.-D. *Z. Lebensmittel-Untersuchung-Forsch.* **1975**, *157*, 221.
(135) Matheis, G.; Belitz, H.-D. *Z. Lebensmittel-Untersuchung-Forsch.* **1977**, *163*, 279.
(136) Krebs, B. In *Bioinorganic Chemistry: An Inorganic Perspective of Life*; D. P. Kessissoglou, Ed.; Kluwer Academic: Dordrecht, The Netherlands, 1995; pp 371.
(137) Solomon, E. I. *Pure Appl. Chem.* **1983**, *55*, 1069.
(138) Salvato, B.; Jori, G.; Piazzese, A.; Ghiretti, F.; Beltramini, M.; Lerch, K. *Life Chem. Rep.* **1983**, *Supplement 1*, 313.
(139) Nakahara, A.; Suzuki, S.; Kino, J. *Life Chem. Rep.* **1983**, *Supplement 1*, 319.
(140) Reinhammar, B. *Biochim. Biophys. Acta* **1970**, *205*, 35.
(141) Reinhammar, B. R. M. *Biochim. Biophys. Acta* **1972**, *275*, 245.
(142) Omura, T. *J. Biochem.* **1961**, *50*, 264.
(143) Reinhammar, B. R. M.; Vänngård, T. I. *Eur. J. Biochem.* **1971**, *18*, 463.
(144) Morpurgo, L.; Agosinelli, E.; Senepa, M.; Desideri, A. *J. Inorg. Biochem.* **1985**, *24*, 1.
(145) Brändén, R.; Deinum, J. *Biochim. Biophys. Acta* **1978**, *524*, 297.
(146) Bligny, R.; Douce, R. *Biochem. J.* **1983**, *209*, 489.
(147) LaFayette, P. R.; Eriksson, K.-E. L.; Dean, J. F. D. *Plant Physiol.* **1995**, *107*, 667.
(148) Sterjiades, R.; Dean, J. F. D.; Eriksson, K.-E. L. *Plant Physiol.* **1992**, *99*, 1162.
(149) Driouich, A.; Laine, A.-C.; Vian, B.; Faye, L. *Plant J.* **1992**, *2*, 13.
(150) Bao, W.; O'Malley, D. M.; Whetten, R.; Sederoff, R. R. *Science* **1993**, *260*, 672.
(151) Mosbach, R. *Biochim. Biophys. Acta* **1963**, *73*, 204.
(152) Fahraeus, G.; Reinhammer, B. *Acta Chem. Scand.* **1967**, *21*, 2367.
(153) Jonsson, L.; Sjostrom, K.; Haggstrom, I.; Nyman, P. O. *Biochim. Biophys. Acta* **1995**, *1251*, 210.
(154) Taniguchi, V. T.; Malmström, B. G.; Anson, F. C.; Gray, H. B. *Proc. Natl. Acad. Sci. U.S.A.* **1982**, *79*, 3387.
(155) Malmström, B. G.; Reinhammar, B.; Vänngård, T. *Biochim. Biophys. Acta* **1968**, *156*, 67.
(156) Froehner, S. C.; Eriksson, K.-E. *J. Bacteriol.* **1974**, *120*,
(157) Lerch, K.; Deinum, J.; Reinhammar, B. *Biochim. Biophys. Acta* **1978**, *534*, 7.
(158) Germann, U. A.; Muller, G.; Hunziker, P. E.; Lerch, K. *J. Biol. Chem.* **1988**, *263*, 885.
(159) Sannia, G.; Giardina, P.; Luna, M.; Rossi, M.; Buonocore, V. *Biotechnol. Lett.* **1986**, *8*, 797.
(160) Youn, H.-D.; Kim, K.-J.; Maeng, J.-S.; Han, Y.-H.; Jeong, I.-B.; Jeong, G.; Kang, S.-O.; Hah, Y. C. *Microbiology* **1995**, *141*, 393.
(161) Giardina, P.; Cannio, R.; Martirani, L.; Marzullo, L.; Palmieri, G.; Sannia, G. *Appl. Enviorn. Microbiol.* **1995**, *61*, 2408.
(162) Xu, F.; Shin, W.; Brown, S. H.; Wahleithner, J.; Sundaram, U. M.; Solomon, E. I. *Biochim. Biophys. Acta* **1996**,
(163) Yaver, D. S.; Xu, F.; Golightly, E.; Brown, S.; Rey, M.; Scheider, P.; Dalbøge, H. *Gen. Tech. Rep. NC* **1994**, *175*, 115.
(164) Yaver, D. S.; Xu, F.; Dalbøge, H.; Schneider, P.; Aaslyng, D. International Patent Application PCT/US95/07536, 1996.
(165) Wahleithner, J. A.; Xu, F.; Brown, K. M.; Brown, S. H.; Golightly, E. J.; Halkier, T.; Kauppinen, S.; Pederson, A.; Schneider, P. *Curr. Genet.* **1996**, *29*, 395.
(166) Berka, R. M.; Xu, F.; Thompson, S. A. International Patent Application PCT/US95/06816, 1995.
(167) Vaitkyavichyus, R. K.; Bel'zhite, V. A.; Chenas, N. K.; Banis, R. G.; Kulis, Y. Y. *Biokhimiya (Moscow)* **1984**, *49*, 1000.

(168) Karhunen, E.; Niku-Paavola, M.-L.; Viikari, L.; Haltia, T.; Meer, R. A. v. d.; Duine, J. *FEBS Lett.* **1990**, *267*, 6.
(169) Saloheimo, M.; Niku-Paavola, M.-L.; Knowles, J. K. C. *J. Gen. Microbiol.* **1991**, *137*, 1537.
(170) Molitoris, H. P.; Esser, K. *Arch. Mikrobiol.* **1970**, *72*, 267.
(171) Minuth, W.; Klischies, M.; Esser, K. *Eur. J. Biochem.* **1978**, *90*, 73.
(172) Molitoris, H. P.; Reinhammar, B. *Biochim. Biophys. Acta* **1975**, *386*, 493.
(173) Marchesini, A.; Kroneck, P. M. N. *Eur. J. Biochem.* **1979**, *101*, 65.
(174) Deinum, J.; Reinhammar, B. *FEBS Lett.* **1974**, *42*, 241.
(175) Avigliano, L.; Vecchini, P.; Sirianni, P.; Marcozzi, G.; Marchesini, A.; Mondovi, B. *Mol. Cell. Biochem.* **1983**, *56*, 107.
(176) Mondovi, B.; Avigliano, L. In *Copper Proteins and Copper Enzymes*; Lontie, R., Ed.; CRC Press: Boca Raton, FL, 1984; Vol. 3; pp 101.
(177) Nakamura, T.; Makino, N.; Ogura, Y. *J. Biochem.* **1968**, *64*, 189.
(178) Kawahara, K.; Suzuki, S.; Sakurai, T.; Nakahara, A. *Arch. Biochem. Biophys.* **1985**, *241*, 179.
(179) Ohkawa, J.; Okada, N.; Shinmyo, A.; Takano, M. *Proc. Natl. Acad. Sci. U.S.A.* **1989**, *86*, 1239.
(180) Hirose, J.; Sakurai, T.; Imamura, K.; Watanabe, H.; Iwamoto, H.; Hiromi, K.; Itoh, H.; Shin, T.; Murao, S. *J. Biochem.* **1994**, *115*, 811.
(181) Itoh, H.; Hirota, A.; Hirayama, K.; Shin, T.; Murao, S. *Biosci. Biotech. Biochem.* **1995**, *59*, 1052.
(182) Ryden, L.; Björk, I. *Biochemistry* **1976**, *15*, 3411.
(183) Musci, G.; Patti, M. C. B. d.; Fagiolo, U.; Calabrese, L. *J. Biol. Chem.* **1993**, *268*, 13388.
(184) Musci, G.; Patti, M. C. B. d.; Calabrese, L. *Arch. Biochem. Biophys.* **1993**, *306*, 111.
(185) Takahashi, N.; Ortel, T. L.; Putnam, F. W. *Proc. Natl. Acad. Sci. U.S.A.* **1984**, *81*, 390.
(186) Koschinsky, M. L.; Funk, W. D.; Oost, B. A. v.; MacGillivray, R. T. A. *Proc. Natl. Acad. Sci. U.S.A.* **1986**, *83*, 5086.
(187) Magdoff-Fairchild, B.; Lovell, F. M.; Low, B. W. *J. Biol. Chem.* **1969**, *244*, 3497.
(188) Deinum, J.; Vänngård, T. *Biochim. Biophys. Acta* **1973**, *310*, 321.
(189) Gunnarsson, P.-O.; Nylen, U.; Pettersson, G. *Eur. J. Biochem.* **1973**, *37*, 47.
(190) Disilvestro, R. A.; Harris, E. D. *Arch. Biochem. Biophys.* **1985**, *241*, 438.
(191) Calabrese, L.; Carbonaro, M.; Musci, G. *J. Biol. Chem.* **1988**, *263*, 6480.
(192) Musci, G.; Carbonaro, M.; Adriani, A.; Lania, A.; Galtieri, A.; Calabrese, L. *Arch. Biochem. Biophys.* **1990**, *279*, 8.
(193) Calabrese, L.; Malatesta, F.; Barra, D. *Biochem. J.* **1981**, *199*, 667.
(194) Sakurai, T.; Nakahara, A. *Inorg. Chim. Acta* **1986**, *123*, 217.
(195) Calabrese, L.; Capuozzo, E.; Galtieri, A.; Bellocco, E. *Mol. Cell. Biochem.* **1983**, *51*, 129.
(196) Calabrese, L.; Carbonaro, M. *Biochem. J.* **1986**, *238*, 291.
(197) Patti, M. C. B. d.; Galtieri, A.; Giartosio, A.; Musci, G.; Calabrese, L. *Comp. Biochem. Physiol.* **1992**, *103B*, 183.
(198) Hilewicz-Grabska, M.; Zgirski, A.; Krajewski, T.; Plonka, A. *Arch. Biochem. Biophys.* **1988**, *260*, 18.
(199) Choy, H. A.; Jones, G. H. *Arch. Biochem. Biophys.* **1981**, *211*, 55.
(200) Barry, C. E.; Nayar, P. G.; Begley, T. P. *Biochemistry* **1989**, *28*, 6323.
(201) Freeman, J. C.; Nayar, P. G.; Begley, T. P.; Villafranca, J. J. *Biochemistry* **1993**, *32*, 4826.
(202) Hsieh, C.-J.; Jones, G. H. *J. Bacteriol.* **1995**, *177*, 5740.
(203) Murao, S.; Tanaka, N. *Agric. Biol. Chem.* **1981**, *45*, 2383.
(204) Tanaka, N.; Murao, S. *Agric. Biol. Chem.* **1982**, *46*, 2499.
(205) Gotoh, Y.; Kondo, Y.; Kaji, H.; Takeda, A.; Samejima, T. *J. Biochem.* **1989**, *106*, 621.
(206) Koikeda, S.; Ando, K.; Kaji, H.; Inoue, T.; Murao, S.; Takeuchi, K.; Samejima, T. *J. Biol. Chem.* **1993**, *268*, 18801.
(207) Hiromi, K.; Yamaguchi, Y.; Sugiura, Y.; Iwamoto, H.; Hirose, J. *Biosci. Biotechnol. Biochem.* **1992**, *56*, 1349.
(208) Nordlöv, H.; Gatenbeck, S. *Arch. Microbiol.* **1982**, *131*, 208.
(209) Fujii, I.; Iijima, H.; Tsukita, S.; Ebizuka, Y.; Sankawa, U. *J. Biochem.* **1987**, *101*, 11.
(210) Huang, K.-X.; Fujii, I.; Ebizuka, Y.; Gomi, K.; Sankawa, U. *J. Biol. Chem.* **1995**, *270*, 21495.
(211) Askwith, C.; Eide, D.; Ho, A. V.; Bernard, P. S.; Li, L.; Davis-Kaplan, S.; Sipe, D. M.; Kaplan, J. *Cell* **1994**, *76*, 403.
(212) Silva, D. M. D.; Askwidth, C.; Eide, D.; Kaplan, J. *J. Biol. Chem.* **1995**, *270*, 1098.
(213) Aramayo, R.; Timberlake, W. E. *Nucleic Acids Res.* **1990**, *18*, 3415.
(214) Guckert, J. A.; Lowery, M. D.; Solomon, E. I. *J. Am. Chem. Soc.* **1995**,
(215) Blair, D. F.; Campbell, G. W.; Schoonover, J. R.; Chan, S. I.; Gray, H. B.; Malmström, B. G.; Pecht, I.; Swanson, B. I.; Woodruff, W. H.; Cho, W. K.; English, A. M.; Fry, H. A.; Lum, V.; Norton, K. A. *J. Am. Chem. Soc.* **1985**, *107*, 5755.
(216) Pascher, T.; Karlsson, B. G.; Nordling, M.; Malmström, B. G.; Vänngård, T. *Eur. J. Biochem.* **1993**, *212*, 289.
(217) Langen, R.; Jensen, G. M.; Jacob, U.; Stephens, P. J.; Warshel, A. *J. Biol. Chem.* **1992**, *267*, 25625.
(218) Stephens, P. J.; Jollie, D. R.; Warshel, A. *Chem. Rev.* **1996**, *96*, 2491 (in this issue).
(219) Lowery, M. D.; Guckert, J. A.; Gebhard, M. S.; Solomon, E. I. *J. Am. Chem. Soc.* **1993**, *115*, 3012.
(220) Malkin, R.; Malmström, B. G.; Vänngård, T. *FEBS Lett.* **1968**, *1*, 50.
(221) Brändén, R.; Malmström, B. G.; Vänngård, T. *Eur. J. Biochem.* **1973**, *36*, 195.
(222) Dawson, J. H.; Dooley, D. M.; Gray, H. B. *Proc. Natl. Acad. Sci. U.S.A.* **1978**, *75*, 4078.
(223) Aikazyan, V. T.; Nalbandyan, R. M. *Biokhimiya* **1977**, *42*, 2027.
(224) Messerschimdt, A.; Huber, R. *Eur. J. Biochem.* **1990**, *187*, 341.
(225) Ryden, L. G.; Hunt, L. T. *J. Mol. Evol.* **1993**, *36*, 41.
(226) Peisach, J.; Levine, W. G. *J. Biol. Chem.* **1965**, *240*, 2284.
(227) Xu, F. *Biochemistry* **1996**, *35*, 7608.
(228) Marcus, R. A.; Sutin, N. *Biochim. Biophys. Acta* **1985**, *811*, 265.
(229) Dodds, M. L. *Arch. Biochem.* **1948**, *18*, 51.
(230) Wimalasena, K.; Dharmasena, S. *Biochem. Biophys. Res. Commun.* **1994**, *203*, 1471.
(231) Osaki, S.; Johnson, D. A.; Frieden, E. *J. Biol. Chem.* **1966**, *241*, 2746.
(232) Osaki, S. *J. Biol. Chem.* **1966**, *241*, 5053.
(233) Osaki, S.; Walaas, O. *J. Biol. Chem.* **1967**, *242*, 2653.
(234) Osaki, S.; Walaas, O. *Arch. Biochem. Biophys.* **1968**, *125*, 918.
(235) Huber, C. T.; Frieden, E. *J. Biol. Chem.* **1970**, *245*, 3973.
(236) Barrett, F. M.; Anderson, S. O. *Insect Biochem.* **1981**, *11*, 17.
(237) Thomas, B. R.; Yonekura, M.; Morgan, T. D.; Czapla, T. H.; Hopkins, T. L.; Kramer, K. J. *Insect Biochem.* **1989**, *19*, 611.
(238) Givaudan, A.; Effosse, A.; Faure, D.; Potier, P.; Bouillant, M.-L. *FEMS Microbiol. Lett.* **1993**, *1993*, 205.
(239) Dean, J. F. D.; Eriksson, K.-E. L. *Holzforschung* **1994**, *48*, 21.
(240) Thurston, C. F. *Microbiology* **1994**, *140*, 19.
(241) Savidge, R.; Udagama-Randeniya, P. *Phytochemistry* **1992**, *31*, 2959.
(242) McDougall, G. J.; Stewart, D.; Morrison, I. M. *Phytochemistry* **1994**, *37*, 683.
(243) O'Malley, D. M.; Whetten, R.; Bao, W.; Chen, C.-L.; Sederoff, R. R. *Plant J.* **1993**, *4*, 751.
(244) Liu, L.; Dean, J. F. D.; Friedman, W. E.; Eriksson, K.-E. L. *Plant J.* **1994**, *6*, 213.
(245) Siegel, S. M. *Physiol. Plantarum* **1953**, *6*, 134.
(246) Higuchi, T. *Physiol. Plantarum* **1957**, *10*, 356.
(247) Higuchi, T.; Ito, Y. *J. Biochem.* **1958**, *45*, 575.
(248) Nakamura, W. *J. Biochem.* **1967**, *62*, 54.
(249) Harkin, J. M.; Obst, J. R. *Science* **1973**, *180*, 296.
(250) Sterjiades, R.; Dean, J. F. D.; Gamble, G.; Himmelsbach, D. S.; Eriksson, K.-E. L. *Planta* **1993**, *190*, 75.
(251) Higuchi, T. In *Biosynthesis and Biodegradation of Wood Components*; Higuchi, T., Ed.; Academic Press: Orlando, FL, 1985; pp 141.
(252) Kumanotani, J. *Makromol. Chem.* **1978**, *179*, 47.
(253) Oshima, R.; Yamauchi, Y.; Watanabe, C.; Kumanotani, J. *J. Org. Chem.* **1985**, *50*, 2613.
(254) Malmström, B. G.; Andreasson, L.-E.; Reinhammar, B. In *The Enzymes*; Boyer, P. D., Ed.; Academic Press: New York, 1975; Vol. 12; pp 507.
(255) Clutterbuck, A. J. *J. Gen. Microbiol.* **1972**, *70*, 423.
(256) Esser, K.; Minuth, W. *Genetics* **1970**, *64*, 441.
(257) Tanaka, C.; Tajima, S.; Furusawa, I.; Tsuda, M. *Mycol. Res.* **1992**, *96*, 959.
(258) Ander, P.; Eriksson, K.-E. *Arch. Microbiol.* **1976**, *109*, 1.
(259) Leonowicz, A.; Szklarz, G.; Wojtas-Wasilewska, M. *Phytochemistry* **1985**, *24*, 393.
(260) Kirk, T. K.; Harkin, J. M.; Cowling, E. B. *Biochim. Biophys. Acta* **1968**, *165*, 145.
(261) Kawai, S.; Umezawa, T.; Higuchi, T. *Arch. Biochem. Biophys.* **1988**, *262*, 99.
(262) Gierer, J.; Opara, A. E. *Acta Chem. Scand.* **1973**, *27*, 2909.
(263) Bourbonnais, R.; Paice, M. G. *FEBS Lett.* **1990**, *267*, 99.
(264) Szklarz, G.; Leonowicz, A. *Phytochemistry* **1986**, *25*, 2537.
(265) Galliano, H.; Gas, G.; Seris, J. L.; Boudet, A. M. *Enzyme Microb. Technol.* **1991**, *13*, 478.
(266) Marzullo, L.; Cannio, R.; Giardina, P.; Santini, M. T.; Sannia, G. *J. Biol. Chem.* **1995**, *270*, 3823.
(267) Bollag, J.-M.; Shuttleworth, K. L.; Anderson, D. H. *Appl. Enviorn. Microbiol.* **1988**, *54*, 3086.
(268) White, N. A.; Boddy, L. *FEMS Microbiol. Lett.* **1992**, *98*, 75.
(269) Pezet, R.; Pont, V.; Hoang-Van, K. *Physiolog. Mol. Plant Pathol.* **1991**, *39*, 441.
(270) Brown, D. W.; Hauser, F. M.; Tommasi, R.; Corlett, S. *Tetrahedron Lett.* **1993**, *34*, 419.
(271) Dawson, C. R. In *The Biochemistry of Copper*; Peisach, J., Aisen, P., Blumberg, W., Eds.; Academic Press: New York, 1966; pp 305.
(272) Volk, W. A.; Larsen, J. L. *Biochim. Biophys. Acta* **1963**, *67*, 576.

(273) White, G. A.; Krupka, R. M. *Arch. Biochem. Biophys.* **1965**, *110*, 448.
(274) Reid, M. E. *Am. J. Bot.* **1941**, *28*, 410.
(275) Newcomb, E. H. *Proc. Soc. Exp. Biol. Med.* **1951**, *76*, 504.
(276) Honda, S. I. *Plant Physiol.* **1955**, *30*, 174.
(277) Jensen, W. A.; Kavaljian, L. G. *J. Biophys. Biochem. Cytol.* **1956**, *2*, 87.
(278) Mertz, D. *Am. J. Bot.* **1961**, *48*, 405.
(279) Hallaway, M.; Phethean, P. D.; Taggart, J. *Phytochemistry* **1970**, *9*, 935.
(280) Lin, L.-S.; Varner, J. E. *Plant Physiol.* **1990**, *96*, 159.
(281) Esaka, M.; Fujisawa, K.; Gota, M.; Kisu, Y. *Plant Physiol.* **1992**, *100*, 231.
(282) Takahama, U.; Oniki, T. *Plant Cell Physiol.* **1994**, *35*, 257.
(283) Broman, L. *Nature* **1958**, *182*, 1655.
(284) Yamashita, K.; Liang, C.-J.; Funakoshi, S.; Kobata, A. *J. Biol. Chem.* **1981**, *265*, 1283.
(285) Ryden, L. In *Copper Proteins and Copper Enzymes*; Lontie, R., Ed.; CRC Press: Boca Raton, FL, 1984; Vol. III; pp 37.
(286) Carrico, R. J.; Malmström, B. G.; Vänngard, T. *Eur. J. Biochem.* **1971**, *22*, 127.
(287) Ley, M. d.; Osaki, S. *Biochem. J.* **1975**, *151*, 561.
(288) Kasper, C. B.; Deutsch, H. F.; Beinert, H. *J. Biol. Chem.* **1963**, *238*, 2338.
(289) Andréasson, L.-E.; Vänngård, T. *Biochim. Biophys. Acta* **1970**, *200*, 247.
(290) Aisen, P.; Koenig, S. H.; Lilienthal, H. R. *J. Mol. Biol.* **1967**, *28*, 225.
(291) Ortel, T. L.; Takashi, N.; Putnam, F. W. *Proc. Natl. Acad. Sci. U.S.A.* **1984**, *81*, 4761.
(292) Machonkin, T. E.; Solomon, E. I.; Zhang, H. H.; Hodgson, K. O., unpublished data.
(293) Lahey, M. E.; Gubler, C. J.; Chase, M. S.; Cartwright, G. E.; Wintrobe, M. M. *Blood* **1952**, *7*, 1053.
(294) Roeser, H. P.; Lee, G. R.; Cartwright, G. E. *J. Clin. Invest.* **1970**, *49*, 2408.
(295) Ragan, H. A.; Nacht, S.; Lee, G. R.; Bishop, C. R.; Cartwright, G. E. *Am. J. Physiol.* **1969**, *217*, 1320.
(296) Osaki, S.; Johnson, D. A. *J. Biol. Chem.* **1969**, *244*, 5757.
(297) Huber, C. T.; Frieden, E. *J. Biol. Chem.* **1970**, *245*, 3979.
(298) Carver, F. J.; Farb, D. L.; Frieden, E. *Biol. Trace Elem. Res.* **1982**, *4*, 1.
(299) Chidambaram, M. V.; Barnes, G.; Frieden, E. *FEBS Lett.* **1983**, *159*, 137.
(300) Curzon, G. *Biochem. J.* **1966**, *100*, 295.
(301) Curzon, G.; Speyer, B. E. *Biochem. J.* **1967**, *105*, 243.
(302) Gunnarsson, P.-O.; Nylen, U.; Pettersson, G. *Eur. J. Biochem.* **1972**, *27*, 572.
(303) McKee, D. J.; Frieden, E. *Biochemistry* **1971**, *10*, 3880.
(304) See also: Kaplan, J.; O'Halloran, T. V. *Science* **1996**, *271*, 1510.
(305) Lane, E. E.; Walker, J. F. *Clinical Arterial Blood Gas Analysis*; C. V. Mosby: St. Louis, 1987.
(306) Henry, J. B. *Clinical Diagnosis and Management by Laboratory Methods*, 7th ed.; W. B. Saunders: Philadelphia, PA, 1984.
(307) Weinberg, E. D. *Microbiol. Rev.* **1978**, *42*, 45.
(308) Letendre, E. D.; Holbein, B. E. *Infect. Immun.* **1984**, *45*, 133.
(309) Beaumier, D. L.; Caldwell, M. A.; Holbein, B. E. *Infect. Immun.* **1984**, *46*, 489.
(310) Gutteridge, J. M. C. *Biochem. Biophys. Res. Commun.* **1977**, *77*, 379.
(311) Gutteridge, J. M. C.; Richmond, R.; Halliwell, B. *FEBS Lett.* **1980**, *112*, 269.
(312) Gutteridge, J. M. C. *FEBS Lett.* **1982**, *150*, 454.
(313) Gutteridge, J. M. C. *FEBS Lett.* **1983**, *157*, 37.
(314) Gutteridge, J. M. C. *Chem.-Biol. Interactions* **1985**, *56*, 113.
(315) Gutteridge, J. M. C. *Clin. Sci.* **1991**, *81*, 413.
(316) Gutteridge, J. M. C.; Quinlan, G. J. *Biochim. Biophys. Acta* **1993**, *1156*, 144.
(317) Owen, C. A. *Am. J. Physiol.* **1965**, *209*, 900.
(318) Marceau, N.; Aspin, N. *Biochim. Biophys. Acta* **1973**, *293*, 338.
(319) Marceau, N.; Aspin, N. *Biochim. Biophys. Acta* **1973**, *328*, 351.
(320) Hsieh, H. S.; Frieden, E. *Biochem. Biophys. Res. Commun.* **1975**, *67*, 1326.
(321) Stevens, M. D.; DiSilvestro, R. A.; Harris, E. D. *Biochemistry* **1984**, *23*, 261.
(322) Barnes, G.; Frieden, E. *Biochem. Biophys. Res. Commun.* **1984**, *125*, 157.
(323) Kataoka, M.; Tavassoli, M. *Exp. Hematol.* **1985**, *13*, 806.
(324) Orena, S. J.; Goode, C. A.; Linder, M. C. *Biochem. Biophys. Res. Commun.* **1986**, *139*, 822.
(325) Percival, S. S.; Harris, E. D. *Am. J. Physiol.* **1990**, *258*, C140.
(326) Omoto, E.; Tavassoli, M. *Arch. Biochem. Biophys.* **1990**, *282*, 34.
(327) Katz, E.; Weissbach, H. *J. Biol. Chem.* **1962**, *237*, 882.
(328) Golub, E. E.; Nishimura, J. S. *J. Bacteriol.* **1972**, *112*, 1353.
(329) Barry, C. E.; Nayar, P. G.; Begley, T. P. *J. Am. Chem. Soc.* **1988**, *110*, 3333.
(330) Salzman, L.; Weissbach, H.; Katz, E. *Arch. Biochem. Biophys.* **1969**, *130*, 536.
(331) Dancis, A.; Klausner, R. D.; Hinnebusch, A. G.; Barriocanal, J. G. *Mol. Cell. Biol.* **1990**, *10*, 2294.
(332) Eide, D.; Davis-Kaplan, S.; Jordan, I.; Sipe, D.; Kaplan, J. *J. Biol. Chem.* **1992**, *267*, 20774.
(333) Stearman, R.; Yuan, D. S.; Yamaguchi-Iwai, Y.; Klausner, R. D.; Dancis, A. *Science* **1996**, *271*, 1552.
(334) Graziani, M. T.; Morpurgo, L.; Rotilio, G.; Mondoví, B. *FEBS Lett.* **1976**, *70*, 87.
(335) Morie-Bebel, M. M.; Morris, M. C.; Menzie, J. L.; McMillin, D. R. *J. Am. Chem. Soc.* **1984**, *106*, 3677.
(336) Morie-Bebel, M. M.; Menzie, J. L.; McMillin, D. R. In *Biological and Inorganic Copper Chemistry, Proceedings of the Conference on Copper Coordination Chemistry, 2nd, 1984*; Karlin, K. D., Zubieta, J., Eds.; Adenine Press: Guilderland, NY, 1986; Vol. 1; pp 89.
(337) Severns, J. C.; McMillin, D. R. *Biochemistry* **1990**, *29*, 8592.
(338) LuBien, C. D.; Winkler, M. E.; Thamann, T. J.; Scott, R. A.; Co, M. S.; Hodgson, K. O.; Solomon, E. I. *J. Am. Chem. Soc.* **1981**, *103*, 7014.
(339) Reinhammar, B.; Oda, Y. *J. Inorg. Biochem.* **1979**, *11*, 115.
(340) Messerschmidt, A.; Rossi, A.; Ladenstein, R.; Huber, R.; Bolognesi, M.; Guiseppina, G.; Marchesini, A.; Petruzzelli, R.; Finazzi-Agro, A. *J. Mol. Biol.* **1989**, *206*, 513.
(341) Messerschmidt, A.; Luecke, H.; Huber, R. *J. Mol. Biol.* **1993**, 997.
(342) Hazes, B.; Magnus, K. A.; Bonaventura, C.; Bonaventura, J.; Dauter, Z.; Kalk, K. H.; Hol, W. G. J. *Prot. Sci.* **1993**, *2*, 597.
(343) Kitajima, N.; Fujisawa, K.; Fujimoto, C.; Moro-oka, Y.; Hashimoto, S.; Kitagawa, T.; Toriumi, K.; Tatsumi, K.; Nakamura, A. *J. Am. Chem. Soc.* **1992**, *114*, 1277.
(344) Morie-Bebel, M. M.; McMillin, D. R. *Biochem. J.* **1986**, *235*, 415.
(345) Brändén, R.; Reinhammar, B. *Biochim. Biophys. Acta* **1975**, *405*, 236.
(346) Tamilarasan, R.; McMillin, D. R. *Biochem. J.* **1989**, *263*, 425.
(347) Cole, J. L.; Clark, P. A.; Solomon, E. I. *J. Am. Chem. Soc.* **1990**, *112*, 9534.
(348) Companion, A. L.; Komarynsky, M. A. *J. Chem. Educ.* **1964**, *41*, 257.
(349) Sundaram, U. M.; Zhang, H. H.; Hedman, B.; Hodgson, K.; Solomon, E. I., manuscript in preparation.
(350) Clark, P. A.; Solomon, E. I., unpublished results.
(351) Miller, C.; McMillin, D. R. *Biophys. Chem.* **1995**, *53*, 189.
(352) Li, J. B.; McMillin, D. R.; Antholine, W. E. *J. Am. Chem. Soc.* **1992**, *114*, 725.
(353) Andréasson, L.-E.; Brändén, R.; Malmström, B. G.; Vänngård, T. *FEBS Lett.* **1973**, *32*, 187.
(354) Cole, J. L.; Ballou, D. P.; Solomon, E. I. *J. Am. Chem. Soc.* **1991**, *113*, 8544.
(355) Shin, W.; Sundaram, U. M.; Cole, J. L.; Zhang, H. H.; Hedman, B.; Hodgson, K.; Solomon, E. I. *J. Am. Chem. Soc.* **1996**, *118*, 3202.
(356) Karlin, K. D.; Cruse, R. W.; Gultneh, Y.; Farooq, A.; Hayes, J. C.; Zubieta, J. *J. Am. Chem. Soc.* **1987**, *109*, 2668.
(357) Karlin, K. D.; Ghosh, P.; Cruse, R. W.; Farooq, A.; Gultneh, Y.; Jacobson, R. R.; Blackburn, N. J.; Strange, R. W.; Zubieta, J. *J. Am. Chem. Soc.* **1988**, *110*, 6769.
(358) Ghosh, P.; Tyeklar, Z.; Karlin, K. D.; Jacobson, R. R.; Zubieta, J. *J. Am. Chem. Soc.* **1987**, *109*, 6889.
(359) Farver, O.; Goldberg, M.; Lancet, D.; Pecht, I. *Biochem. Biophys. Res. Commun.* **1976**, *73*, 494.
(360) Frank, P.; Farver, O.; Pecht, I. *Inorg. Chim. Acta* **1984**, *91*, 81.
(361) Root, D.; Karlin, K.; Solomon, E. I., manuscript in preparation.
(362) Aasa, R.; Brändén, R.; Deinum, J.; Malmström, B. G.; Reinhammar, B.; Vänngård, T. *FEBS Lett.* **1976**, *61*, 115.
(363) Aasa, R.; Brändén, R.; Deinum, J.; Malmström, B. G.; Reinhammar, B.; Vänngård, T. *Biochem. Biophys. Res. Commun.* **1976**, *70*, 1204.
(364) Reinhammar, B. In *Gas Enzymology, Proceedings of the Symposium*; Degn, H., Cox, R. P., Toftlund, H., Eds.; Reidel, Dordrecht, Netherlands: 1985; pp 79.
(365) Clark, P. A.; Solomon, E. I. *J. Am. Chem. Soc.* **1992**, *114*, 1108.
(366) Petersen, L. C.; Degn, H. *Biochim. Biophys. Acta* **1978**, *526*, 85.
(367) Andréasson, L.-E.; Reinhammar, B. *Biochim. Biophys. Acta* **1976**, *445*, 579.
(368) Brändén, R.; Deinum, J. *FEBS Lett.* **1977**, *73*, 144.
(369) Andréasson, L.-E.; Reinhammar, B. *Biochim. Biophys. Acta* **1979**, *568*, 145.
(370) Meyer, T. E.; Marchesini, A.; Cusanovich, M. S.; Tollin, G. *Biochemistry* **1991**, *30*, 4619.
(371) Farver, O.; Pecht, I. *Proc. Natl. Acad. Sci. U.S.A.* **1992**, *89*, 8283.
(372) Kyritsis, P.; Messerschmidt, A.; Huber, R.; Salmon, G. A.; Sykes, A. G. *J. Chem. Soc. Dalton Trans.* **1993**, *5*, 731.
(373) Hansen, F. B.; Koudelka, G. B.; Noble, R. W.; Ettinger, M. J. *Biochemistry* **1984**, *23*, 2057.
(374) Reinhammar, B. *J. Inorg. Biochem.* **1981**, *15*, 27.
(375) Farver, O.; Pecht, I. *Mol. Cryst. Liq. Cryst.* **1991**, *194*, 215.
(376) Penfield, K. W.; Gewirth, A. A.; Solomon, E. I. *J. Am. Chem. Soc.* **1985**, *107*, 4519.
(377) Gewirth, A. A.; Solomon, E. I. *J. Am. Chem. Soc.* **1988**, *110*, 3811.
(378) George, S. J.; Lowery, M. D.; Cramer, S. P.; Solomon, E. I. *J. Am. Chem. Soc.* **1993**, *115*, 2968.

(379) Shadle, S. E.; Penner-Hahn, J. E.; Schugar, H.; Hedman, B.; Hodgson, K. O.; Solomon, E. I. *J. Am. Chem. Soc.* **1993**, *115*, 767.
(380) Spira, D. J. Ph.D. Thesis, Massachusetts Institute of Technology, 1984.
(381) Kasper, C. B. *J. Biol. Chem.* **1968**, *243*, 3218.
(382) Falk, K.-E.; Reinhammar, B. *Biochim. Biophys. Acta* **1972**, *285*, 84.
(383) Byers, W.; Curzon, G.; Garbett, K.; Speyer, B. E.; Young, S. N.; Williams, R. J. P. *Biochim. Biophys. Acta* **1973**, *310*, 38.
(384) Herve, M.; Garnier, A.; Tosi, L.; Steinbuch, M. *Biochim. Biophys. Acta* **1976**, *439*, 432.
(385) Tosi, L.; Garnier, A.; Herve, M.; Steinbuch, M. *Biochem. Biophys. Res. Commun.* **1975**, *65*, 100.
(386) Beinert, H. *Curr. Biol.* **1995**, *2*, 781.
(387) Fergusson-Miller, S.; Babcock, G. T. *Chem. Rev.* **1996**, *96*, 2889 (in this issue).
(388) Van Gelder, B. F.; Beinert, H. *Biochim. Biophys. Acta* **1969**, *189*, 1.
(389) Tweedle, M. F.; Wilson, L. J.; García-Iniguez, L.; Babcock, G. T.; Palmer, G. *J. Biol. Chem.* **1978**, *253*, 8065.
(390) Lee, S. C.; Holm, R. H. *J. Am. Chem. Soc.* **1993**, *115*, 5833.
(391) Holm, R. H. *Pure Appl. Chem.* **1995**, *67*, 217.
(392) Karlin, K. D.; Nanthakumar, A.; Fox, S.; Murthy, N. N.; Ravi, N.; Huynh, B. H.; Orosz, R. D.; Day, E. P. *J. Am. Chem. Soc.* **1994**, *116*, 4753.
(393) Day, E. P.; Peterson, J.; Sendova, M. S.; Schoonover, J.; Palmer, G. *Biochemistry* **1993**, *32*, 7855.
(394) Moody, J. A.; Cooper, C. E.; Rich, P. R. *Biochim. Biophys. Acta* **1991**, *1059*, 189.
(395) Hill, B. C. *J. Biol. Chem.* **1991**, *266*, 2219.
(396) Babcock, G. T. In *Encyclopedia of Inorganic Chemistry*; King, R. B., Ed.; Wiley: Chichester, U.K., 1994; pp 950.
(397) Malmström, B. G. *Acc. Chem. Res.* **1993**, *26*, 332.
(398) Winkler, J. R.; Malmström, B. G.; Gray, H. B. *Biophys. Chem.* **1995**, *54*, 199.
(399) Kobayashi, K.; Une, H.; Hayashi, K. *J. Biol. Chem.* **1989**, *264*, 7976.
(400) Morgan, J. E.; Li, P. M.; Jang, D.-E.; El-Sayed, M. A.; Chan, S. I. *Biochemistry* **1989**, *28*, 6975.
(401) Ramirez, B. E.; Malmström, B. G.; Winkler, J. R.; Gray, H. B. *Proc. Natl. Acad. Sci. U.S.A.* **1995**, *92*, 11949.
(402) Scott, D.; Brannan, J.; Higgins, I. J. *J. Gen. Microbiol.* **1981**, *125*, 63.
(403) Chance, B.; Saronio, C.; Leigh JR., J. S. *J. Biol. Chem.* **1975**, *250*, 9226.
(404) Chance, B.; Saronio, C.; Leigh JR., J. S. *Proc. Natl. Acad. Sci. U.S.A.* **1975**, *72*, 1635.
(405) Clore, G. M.; Andreasson, L. E.; Karlsson, B.; Aasa, R.; Malmström, B. G. *Biochem. J.* **1980**, *185*, 155.
(406) Gibson, Q. H.; Greenwood, C. *Biochem. J.* **1963**, *86*, 541.
(407) Hill, B. C.; Greenwoon, C. *Biochem. J.* **1984**, *218*, 913.
(408) Orii, Y. *Ann. N. Y. Acad. Sci.* **1988**, *550*, 105.
(409) Oliveberg, M.; Brzezinski, P.; Malmström, B. G. *Biochim. Biophys. Acta* **1989**, *977*, 322.
(410) Verkhovsky, M. I.; Morgan, J. E.; Wikström, M. *Biochemistry* **1994**, *33*, 3079.
(411) Hansson, O.; Karlsson, B.; Aasa, R.; Vanngård, T.; Malmström, B. G. *EMBO J.* **1982**, *1*, 1295.
(412) Blair, D. F.; Witt, S. N.; Chan, S. I. *J. Am. Chem. Soc.* **1985**, *107*, 7389.
(413) Witt, S. N.; Chan, S. I. *J. Biol. Chem.* **1987**, *262*, 1446.
(414) Han, S.; Ching, Y.-c.; Rousseau, D. L. *Nature* **1990**, *348*, 89.
(415) Varotsis, C.; Woodruff, W. H.; Babcock, G. T. *J. Am. Chem. Soc.* **1989**, *111*, 6439.
(416) Varotsis, C.; Woodruff, W. H.; Babcock, G. T. *J. Am. Chem. Soc.* **1990**, *112*, 1297.
(417) Ogura, T.; Takahashi, S.; Shinwaza-Itoh, K.; Yoshikawa, S.; Kitagawa, T. *J. Am. Chem. Soc.* **1990**, *112*, 5630.
(418) Varotsis, C.; Zhang, Y.; Appleman, E. H.; Babcock, G. T. *Proc. Natl. Acad. Sci. U.S.A.* **1993**, *90*, 237.
(419) Ogura, T.; Takahashi, S.; Hirota, S.; Shinwaza-Itoh, K.; Yoshikawa, S.; Appleman, E. H.; Kitagawa, T. *J. Am. Chem. Soc.* **1993**, *115*, 8527.
(420) Ogura, T.; Hirota, S.; Proshlyakov, D. A.; Shinwaza-Itoh, K.; Yoshikawa, S.; Kitagawa, T. *J. Am. Chem. Soc.* **1996**, *118*, 5443.
(421) Proshlyakov, D. A.; Ogura, T.; Shinwaza-Itoh, K.; Yoshikawa, S.; Appleman, E. H.; Kitagawa, T. *J. Biol. Chem.* **1994**, *269*, 29385.
(422) Proshlyakov, D. A.; Ogura, T.; Shinwaza-Itoh, K.; Yoshikawa, S.; Kitagawa, T. *Biochemistry* **1996**, *35*, 8580.
(423) Proshlyakov, D. A.; Ogura, T.; Shinwaza-Itoh, K.; Yoshikawa, S.; Kitagawa, T. *Biochemistry* **1996**, *35*, 76.
(424) Wikström, M. *Chem. Scripta* **1988**, *28A*, 71.
(425) Babcock, G. T.; Wikström, M. *Nature* **1992**, *356*, 301.
(426) Musser, S. M.; Stowell, M. H. B.; Chan, S. I. In *Advances in Enzymology and Related Areas of Molecular Biology*; Meister, A., Ed.; John Wiley and Sons, Inc: New York, 1995; Vol. 71; pp 79.
(427) Fabian, M.; Palmer, G. *Biochemistry* **1995**, *34*, 13802.
(428) Cole, A. P.; Root, D. E.; Mukherjee, P.; Solomon, E. I.; Stack, T. D. P. *Science*, in press.

CR950046O